Final Report

ESTCP Project 200101

Demonstration of Airborne Electromagnetic Systems for Detection and Characterization of Unexploded Ordnance at the Badlands Bombing Range, South Dakota

Revision 3

August 2004

Prepared by
Oak Ridge National Laboratory
for the
Environmental Security Technology Certification Program (ESTCP)

Environmental Security
Technology Certification
Program

CLEARANCE REQUEST FOR PUBLIC RELEASE OF DEPARTMENT OF DEFENSE INFORMATION

(See Instructions on back.)

(This form is to be used in requesting review and clearance of DoD information proposed for public release in accordance with DoDD 5230.9.)

TO: Director, Freedom of Information & Security Review, Rm. 2C757, Pentagon

1. DOCUMENT DESCRIPTION

a. TYPE Final Report	b. TITLE Dem of Airborne Electromagnetic Systems for Detection & Characterization of Unexploded Ordnance at the Badlands Bombing Range, SD (UX-0101)
c. PAGE COUNT 110	d. SUBJECT AREA Environmental Security Technology Certification Program (ESTCP)

2. AUTHOR/SPEAKER

a. NAME *(Last, First, Middle Initial)* Doll, William	b. RANK	c. TITLE
d. OFFICE Battelle Memorial Institute		e. AGENCY Battelle Memorial Institute

3. PRESENTATION/PUBLICATION DATA *(Date, Place, Event)*

Posting on the ESTCP web site.

CLEARED
For Open Publication

JUL 11 2005 3

Office of Freedom of Information
and Security Review
Department of Defense

4. POINT OF CONTACT

a. NAME *(Last, First, Middle Initial)* Rusk, Jennifer	b. TELEPHONE NO. *(Include Area Code)*

5. PRIOR COORDINATION

a. NAME *(Last, First, Middle Initial)*	b. OFFICE/AGENCY	c. TELEPHONE NO. *(Include Area Code)*
Marqusee, Jeffrey Andrews, Anne	ESTCP Director ESTCP Unexploded Ordnance Program Manager	

6. REMARKS

THE INFORMATION CONTAINED IN THIS REPORT FALLS UNDER THE PURVIEW OF THIS OFFICE.

WHEN CLEARED, PLEASE FAX DD-1910 TO 703-478-0526. ATTN: Jennifer Rusk (phor

if mailed: ATTN: Jennifer Rusk, 1155 Herndon Parkway, Suite 900, Herndon, VA 20170

7. RECOMMENDATION OF SUBMITTING OFFICE/AGENCY

a. THE ATTACHED MATERIAL HAS DEPARTMENT/OFFICE/AGENCY APPROVAL FOR PUBLIC RELEASE *(qualifications, if any, are indicated in Remarks section)* AND CLEARANCE FOR OPEN PUBLICATION IS RECOMMENDED UNDER PROVISIONS OF DODD 5320.9. I AM AUTHORIZED TO MAKE THIS RECOMMENDATION FOR RELEASE ON BEHALF OF:

Environmental Security Technology Certification Program

b. CLEARANCE IS REQUESTED BY 20050706 *(YYYYMMDD)*.

c. NAME *(Last, First, Middle Initial)* Smith, Bradley P.	d. TITLE Deputy Director, Environ. Security Technology Certification Progr
e. OFFICE OUSD(I&E)	f. AGENCY OUSD (A&T)
g. SIGNATURE	h. DATE SIGNED *(YYYYMMDD)* 20050620

This report was prepared under contract to the Department of Defense Strategic Environmental Research and Development Program (SERDP). The publication of this report does not indicate endorsement by the Department of Defense, nor should the contents be construed as reflecting the official policy or position of the Department of Defense. Reference herein to any specific commercial product, process, or service by trade name, trademark, manufacturer, or otherwise, does not necessarily constitute or imply its endorsement, recommendation, or favoring by the Department of Defense.

Table of Contents

Table of Contents……..i
Acronym List iv
List of Figures v
List of Tables viii
Acknowledgments..... ix
Summary x
1. Introduction..... 1
1.1 Background 1
1.2 Objectives of the Demonstration 2
1.3 Regulatory Drivers..... 3
1.4 Stakeholder/End-User Issues 3
2. Technology Description..... 3
2.1 Technology Development and Application 3
2.2 Previous Testing of the Technology 6
2.2.1 First Shakedown Test: Toronto, Ontario, December 2001 7
2.2.1.1 Airworthiness Tests 7
2.2.1.2 Noise Tests..... 9
2.2.1.3 Test Grid Profiles..... 11
2.2.1.4 Summary of EM System Status Following the Toronto Shakedown Test 13
2.2.2 Second Shakedown Test, Hyannis, MA, March 22-24, 2002..... 14
2.2.2.1 Test Attributes..... 14
2.2.2.2 Summary of Massachusetts Test..... 15
2.2.3 Results of the Third Shakedown Test, Pueblo of Laguna, NM 19
2.3 Factors Affecting Cost and Performance 20
2.4 Advantages and Limitations of the Technology 21
3. Demonstration Design 22
3.1 Performance Objectives 22
3.2 Selecting Test Sites 22
3.3 Test site History / Characteristics 22
3.3.1 BBR Test Site 23

3.3.2 Bombing Target 1 24
3.4 Present Operations 27
3.5 Pre-Demonstration Testing and Analysis 27
3.6 Testing and Evaluation Plan 27
3.6.1 Demonstration Set-Up and Start-Up 27
3.6.2 Period of Operation 27
3.6.3 Area Characterized 28
3.6.4 Residuals Handling 28
3.6.5 Operating Parameters for the Technology 28
3.6.6 Experimental Design 29
3.6.6.1 Quality Control 33
3.6.6.2 Positioning 33
3.6.6.3 Electromagnetic Data Processing 33
3.6.7 Sampling Plan 34
3.6.8 Demobilization 35
4. Performance Assessment 36
4.1 Performance Criteria 36
4.2 Performance Confirmation Methods 39
4.3 Data Analysis, Interpretation, and Evaluation 39
4.3.1 Results from BBR Test Site 40
4.3.1.1 Comparison of Gridded Data at the BBR Test Site 40
4.3.1.2 Signal/Noise Comparison to Other Systems from BBR Test Site Data 54
4.3.1.3 Altitude and Signal/Noise Assessment for Specific Ordnance Types 58
4.3.1.3.1 Signal/Noise Ratio Estimation Method 58
4.3.1.3.2 SNR Variation with Height 62
4.3.1.4 Summary of Data Analysis from BBR Test Site 65
4.3.2 Comparison of gridded data at Bombing Target 1 67
4.3.2.1 Comparison of EM and Magnetic Anomaly Picks, Bombing Target 1 73
4.3.2.2 Advantages of Processing Schemes that use the Full Transient Response 77
5.0 Conclusions 84
6.0 Cost Assessment 86
7.0 Implementation Issues 92
7.1 Environmental Checklist 92
7.2 Other Regulatory Issues 92

7.3 End-User Issues 92
8.0 References 92
9.0 Points of Contact 95
Appendix A: Data Storage and Archiving Procedures 96

Acronym List

AGL	Above Ground Level
ALASA	As Low As Safely Achievable
ASCII	American Standard Code for Information Interchange
BBR	Badlands Bombing Range
CERCLA	Comprehensive Environmental Response, Compensation, and Liability Act
DoD	Department of Defense
EM	Electromagnetic
EPA	Environmental Protection Agency
ERDC	Engineer Research and Development Center
ESTCP	Environmental Security Technology Certification Program
FAA	Federal Aviation Administration
FUDS	Formerly Used Defense Sites
GPS, DGPS, RT-DGPS	(Real Time- (Differential)) Global Positioning System
LASI	Laboratory for Advanced Subsurface Investigations
MTADS	Multisensor Towed Array Detection System
NRL	Naval Research Laboratory
ORAGS	Oak Ridge Airborne Geophysical System
ORAGS-EMP	Oak Ridge Airborne Geophysical System – Electromagnetic Prototype
ORAGS-TEM	Oak Ridge Airborne Geophysical System – Time-domain Electromagnetic
ORNL	Oak Ridge National Laboratory
SAGEEP	Symposium on the Application of Geophysics to Environmental and Engineering Problems
SERDP	Strategic Environmental Research & Development Program
SNR	Signal-to-Noise Ratio
TEM	Time-domain Electromagnetic
USAESCH	United States Army Engineering and Support Center -- Huntsville
UXO	Unexploded Ordnance

List of Figures

Figure Number	Caption	Page
1	ORAGS-TEM system in flight at BBR. The red square line shows the large receiver coil position, and the black line represents the anti-symmetric transmitter coil layout.	2
2	ORAGS-TEM console, AgNav navigation system, and Novatel GPS unit as installed in the helicopter.	5
3	ORAGS-TEM waveform and receiver sampling for 90 Hz base frequency.	6
4	Prototype ORAGS-EM system during testing in Toronto.	9
5	Influence of the helicopter on receiver noise as a function of distance from the helicopter.	9
6	Amplitude spectrum in dB for the inner receiver coil at 4m from the helicopter centerline as a function of frequency for the ORAGS-TEM system with the transmitter off (top panel) and on (bottom panel).	10
7	Test results for the first four time gates, using a Z-directed dipole receiver.	12
8	Response vs. time gate response for the five most frequently detected objects in the Toronto test line.	12
9	Crossbeams added to the ORAGS-TEM system for the Massachusetts test.	15
10	Noise spectra shown at a series of time steps, during approach, landing, cool down, and shutdown of the helicopter for the inner (top image) and outer (bottom image) receiving coils.	17
11	EM response of test items at Toronto shakedown test site. The base frequency is 135 Hz.	18
12	Schematic map of BBR Test Site.	23
13	Bombing Target 1 at BBR.	24
14	ORAGS-TEM large receiver loop configuration.	28
15	ORAGS-EM small receiver coil configuration.	29
16	Lobed 3 m X 3 m transmitter configuration. Note the transmitter cable does not extend across a portion of the front boom.	30
17	ORAGS-TEM results from BBR Test Grid, vibration-isolated lower small loop receiver, configuration IS-Rect-270. Data acquired at 270 Hz base frequency and 1.0-1.5 m altitude.	42
18	Results from ORAGS-TEM, BBR Test Grid, lower large loop receiver. Data acquired at 270 Hz base frequency and 1.0-1.5 m altitude with configuration L-Rect-270.	43

Figure Number	Caption	Page
19	Results from ground-based EM61, bottom coil, BBR Test Grid, for comparison with airborne results.	44
20	Results from EM-61AB-based airborne proof-of-concept system, BBR Test Grid, outer coil receiver.	45
21	Results from EM-61AB-based airborne proof-of-concept system, BBR Test Grid, horizontal difference (outer coil minus scaled inner coil).	46
22	Analytic signal derived from ground-based magnetometer bottom sensor (G858), BBR Test Grid.	47
23	Analytic signal map derived from airborne (ORAGS-Arrowhead) magnetic data, BBR Test Site, September 2002, for comparison with EM results.	48
24	ORAGS-TEM results for 90 Hz base frequency small coil data, BBR Test Site. Data acquired at 1.0-1.5 m altitude.	49
25	Results for ORAGS-TEM small coil vertical gradient configuration, BBR Test Site. Data acquired at 270 Hz base frequency and 1.0-1.5 m altitude.	50
26	Results for ORAGS-TEM, lobed symmetric transmitter configuration, large loop receivers, BBR Test Site. Data acquired at 270 Hz base frequency and 1.0-1.5 m altitude.	51
27	Results for anti-symmetric lobed transmitter configuration with large loop receivers, BBR Test Site. Data acquired at 270 Hz base frequency and 1.0-1.5 m altitude.	52
28	Results for large loop receiver, 270 Hz base frequency, and standard rectangular transmitter at 3 m nominal altitude.	53
29	Profiles for selected configurations and acquisition systems over Line C of the BBR Test Grid. a) Configurations S-Rect-270 and S-Rect-270-Diff; b) Configurations IS-Rect-270 and IS-Rect-270-Diff; c) Configurations L-Rect-270 and L-Rect-270-Diff; d) Configuration L-Alob-270. Profiles for selected configurations and acquisition systems over Line C of the BBR Test Grid. d) Configuration S-Rect-90; e) Ground-based EM-61, top minus bottom coil; f) Total magnetic field data acquired with the ORAGS-Arrowhead system.	56
30	Signal/Noise estimates vs. sensor-to-target height for the 250 lb bombs (inert and simulants) located on the BBR Test Grid during the 2002 field trials for Bin 1 responses of the 270 Hz, isolation-mounted standard receiver coil configuration (IS-Rect-270).	60
31	ORAGS-TEM results for Bombing Target 1 – large loop, time gate 1 (ending at 93 μs).	68
32	Results from Bombing Target 1 for the ORAGS-TEM system, large loop receiver, time gate 2 (93-186 μs).	69

Figure Number	Caption	Page
33	Analytic signal map of Bombing Target 1, derived from ORAGS-Arrowhead airborne magnetic data.	70
34	ORAGS-TEM results for BBR Bombing Target 1 small coil receiver, first time gate.	71
35	90 Hz base frequency small coil receiver output (dash-dot lines, proportional to dB/dt) and integrated coil output (solid lines, proportional to B) over scrap (red), M38 (blue) and 250 lb bombs (cyan and green). Items listed in legend (C5 etc.) correlate with those listed in Table 1.	72
36	Comparison of anomaly picks from ORAGS-TEM system and ORAGS-Arrowhead system, Bombing Target 1, BBR.	73
37	Bar graph showing the number of EM anomalies in a given class that have corresponding magnetic anomalies.	75
38	Scatter plot of EM and magnetic anomalies at Bombing Target 1.	76
39	Scatter and mean of analytic signal anomalies according to EM anomaly class, arranged by EM anomaly amplitude.	76
40	Log-linear plot of plate model response in mV (+) and nT (x), with corresponding approximate responses estimated by during MPM exponential decomposition fitting process (solid and dashed lines). Two time constants were estimated by the Matrix Pencil Method for this example.	79
41	B-field transients and estimated dominant time constants for M-38 scrap pits.	80
42	B-field transients and time constant estimates for 250 lb simulants and 100 lb practice bomb.	81
43	B-field transient response for 155 mm projectile, yielding a time constant estimate of 8 ms.	82
44	Time constants and SNR values for selected objects on BBR test grid. Left axis represents observed Signal/Noise Ratio (blue bars), while right axis represents estimated time constant.	82

List of Tables

Table Number	Description	Page
1	Peer Review Panel Members	2
2	ORAGS-TEM Specifications	4
3	Incremental improvements during the shakedown phase of development	8
4	Test grid target description for Toronto Shakedown test	11
5	Description of Massachusetts EM test grid items	16
6	Performance Objectives of ORAGS-TEM Airborne Electromagnetic System	22
7	Description of BBR Test Grid Items	25
8	Sequence of ORAGS-TEM tests conducted at BBR	31
9	Performance Criteria for this Demonstration	37
10	Calculated SNR for Items in Line C of the BBR Test Site	55
11	Signal/Noise Descriptors for Various ORAGS-EM Configurations at BBR02 Test Grid	61
12	Signal-to-Noise Estimates for 1.5 and 4m Sensor-Target Distance	64
13	Cost Assessment Table	87

Acknowledgments

This project was funded by the Environmental Security Technology Certification Program (ESTCP) with ancillary support from the United States Army Engineering Support Center – Huntsville (USAESCH). We would like to thank those who supported ORNL and Geosensors personnel in this project. In particular, Dr. Jonathan Nyquist and Dr. Dwain Butler provided valuable guidance as co-investigators during the design and review phase of this project. Mr. James Mewett worked with our team in designing and constructing a safe and effective boom structure for our application. Dr. Alex Becker, Mr. Miro Bosnar, Dr. Pieter Hoekstra, Dr. Ben Sternberg, Dr. Vic Labson, and Dr. Richard Wold committed time and experience to reviewing and guiding this project as part of the Advisory Panel that met three times during the course of the project. We thank Dan Munro, Chris Keller, Marcus Watson, Dan Henderson, and Andrew Dunt of National Helicopters for safe helicopter support throughout the shakedown and demonstration phases of the project

Summary

This report describes a set of field tests conducted at Badlands Bombing Range (BBR) in South Dakota in September 2002. The primary goal of the field tests was to evaluate parameters critical to the design of an airborne electromagnetic system capable of detecting a variety of buried ordnance. The resulting system, called ORAGS-TEM, was patterned after the low-flying helicopter magnetic systems under development at ORNL through separate SERDP/ESTCP programs. Thus, the ORAGS-TEM has a frame mounted, multiple sensor design that permits helicopter surveys at altitudes as low as one meter over UXO-contaminated terrain. As with the magnetic systems, GPS and laser altimetry provide precise positioning to within a few tens of centimeters.

The BBR tests followed three shakedown tests and included evaluation of design parameters suggested by results of the shakedown flights, as well as additional design aspects. The major design considerations were the identification of base frequencies that produced the highest signal-to-noise ratios for ordnance, determination of whether vibration isolation reduced noise in small coil receivers, selection of optimal transmitter cables to improve flightworthiness, and evaluation of transmitter/receiver configurations to produce best signal-to-noise. We tested two receiver types—small multi-turn coils and a large single turn loop, both in single coil and vertical gradient modes—and three transmitter configurations: a 12 m X 3 m rectangular loop, and two variants of a double-lobed loop.

We found that under favorable field conditions the ORAGS-TEM was able to detect ordnance items as small as were detectable with the more mature helicopter total magnetic field system, i.e. 60 mm rounds. The best ORAGS-TEM test grid results were considerably better than the results from the proof-of-concept ORAGS-EMP; in fact, some of the ORAGS-TEM configurations tested yielded higher signal-to-noise ratios than ground EM survey data. At survey altitudes below 1.5 m, the small multiple turn receiver coils in the vertical gradient configuration produced the highest signal-to-noise over most ordnance, but the advantage of the gradient configuration was lost at higher survey heights because gradient fields decay more rapidly than single coil responses. Furthermore, the large 3 m X 3 m receiver loop produced equivalent or higher signal-to-noise than the small coils at a 3 m survey altitude. EM fields decayed at spatial rates between R^{-2} and R^{-6} according to the height of the survey, the transmitter-receiver configuration used, and whether or not gradient data were considered. Responses from ordnance measured at 3 m survey altitude decayed to background for most mid- and small sized ordnance, irrespective of transmitter-receiver configuration.

The objective of small ordnance detection is best achieved with a high base frequency, whereas ordnance discrimination is best realized with lower base frequencies. Examination of 270 Hz base frequency data show that smaller ordnance items appear more clearly than at a 90 Hz base,

but estimates of time constants are more reliable with the 90 Hz base frequency data. Using the 90 Hz data, estimates of time constants from thick walled ordnance such as 155 mm artillery shells are noticeably longer than from thin-walled ordnance.

In its current configurations, the ORAGS-TEM is a two-channel system. This was adequate for comparing one configuration with another, but is inefficient for "production" surveys because the swath width is small and requires interleaving and precise positioning in order to fully survey a site. Similar magnetic system tests have demonstrated that interleaving and variations from one flight pass to the next results in a degrading of data quality. The cost for expanding from a two-channel to an eight-channel system is quite small, as it will only require construction of more amplifiers in the existing console, along with new coils and preamplifiers. The BBR demonstration provided a thorough evaluation of several system configurations and a comparison with previous airborne magnetic and electromagnetic systems. It showed that the ORAGS-TEM system can serve as a flexible platform in which the configuration, base frequency, and acquisition procedure can be adjusted for optimal performance at each site. It did not exploit the strengths of electromagnetic systems in environments where magnetic systems fall short. Therefore, it is appropriate to follow this project with a demonstration of a "production" 8-channel system at a site where geologic conditions are unsuitable for magnetometer-based systems, in conjunction with targets that are also unsuitable for magnetic systems, as a demonstration of the value of the ORAGS-TEM system in future UXO remediation efforts

1.0 Introduction

1.1 Background

Portions of lands belonging to the Lakota Nation, known as the Badlands Bombing Range (BBR), in South Dakota have been contaminated with unexploded ordnance (UXO) through Department of Defense (DoD) activities, e.g. during training exercises or during weapons tests. Several sites in the BBR have been surveyed as part of ESTCP projects, including three previous airborne surveys conducted by Oak Ridge National Laboratory (ORNL) and ground surveys performed by the Naval Research Laboratory (NRL). The airborne technology offers an approach for rapid reconnaissance of large UXO-contaminated sites which are common at DoD sites, particularly in the western United States.

All previous airborne surveys have deployed magnetometer sensors, with the exception of a proof-of-concept test conducted in association with a magnetometer survey in September 2000. The proof-of-concept system, known as the ORAGS-Electromagnetic Prototype System (ORAGS-EMP) deployed a specially modified EM61 on a frame attached to the existing ORNL Airborne Geophysical System (ORAGS) booms (Doll et al., in press). Development of an airborne electromagnetic system is desirable for conditions that are also encountered during ground-based surveys for UXO: 1) where the background geology is dominated by basalt or other rock types which have a high magnetic mineral content, rendering magnetometer-based systems ineffective; 2) where the UXO to be detected is non-ferrous, and thus undetectable with magnetometer-based systems; or 3) where more parameters must be measured to allow improved discrimination between ordnance and non-ordnance , or between one type of ordnance and another. Thus airborne electromagnetic systems are appropriate to complement or supplement magnetometer-based surveys.

In 2001, ORNL initiated a project for ESTCP to demonstrate an airborne electromagnetic system for detection of unexploded ordnance. Several attributes of the new system were selected through preliminary analysis and field testing of the ORAGS-EMP proof-of-concept system. Following analysis, design, and construction phases of the project, shakedown tests of prototypes began in Toronto in December 2001. The shakedown phase proved to be more demanding than anticipated, requiring two additional shakedown tests, conducted in association with other ORNL airborne projects to minimize costs. These tests were conducted near Hyannis, Massachusetts in March 2002 and near Albuquerque, New Mexico in May 2002.

The shakedown testing culminated in a series of tests with the new system that were conducted at the preexisting ORNL/USAESCH UXO test site and Bombing Target 1 from September 9 to October 6, 2002. The survey was carried out in conjunction with a demonstration of the ORAGS-Arrowhead magnetometer system, outlined in a separate ESTCP report (ORNL, 2004). The ORAGS-TEM tests proved very successful and demonstrate the capabilities of airborne EM mapping for UXO. Such a system could prove effective as a supplement to airborne magnetic mapping (to aid in anomaly selection), to detect non-ferrous ordnance, or for use where magnetic systems are inadequate because of geologic or other interference.

Figure 1. ORAGS-TEM system in flight at BBR. The red square line shows the large receiver coil position, and the black line represents the anti-symmetric transmitter coil layout.

An advisory panel composed of airborne and electromagnetic geophysical experts was formed to provide guidance to the project as it progressed. The panel met annually at the SAGEEP conference in 2001, 2002, and 2003. Panel members, listed in Table 1, participated voluntarily and provided guidance to the project as it progressed that contributed to the success of the project. We are very grateful for their assistance and encouragement.

Table 1. Peer Review Panel Members

Dr. Alex Becker	Professor, Dept. of Mineral Engineering, Univ. Calif. – Berkeley
Mr. Miro Bosnar	President, Geonics Ltd.
Dr. Pieter Hoekstra	Distinguished Visiting Scientist, Colorado School of Mines
Dr. Ben Sternberg	Professor and Director LASI, Dept. Mining and Geol. Eng., Univ. Arizona
Dr. Vic Labson	Associate Chief Scientist, U.S. Geological Survey, Denver, CO
Dr. Richard Wold	President, Blackhawk Geometrics

1.2 Objectives of the Demonstration

The objectives of the demonstration survey were:

- To expand on the results of the ORAGS-EMP prototype test by evaluating design attributes for a more effective airborne electromagnetic system for detection of UXO;
- To provide a means of comparing the performance of an airborne electromagnetic system with the ORAGS total field helicopter-borne magnetometry systems;
- To assess the capabilities of the system at a site representing conditions and ordnance types typically found on former DoD ranges;
- To detect and map UXO and UXO-related items for subsequent clearance actions.

1.3 Regulatory Drivers

UXO clearance is generally conducted under CERCLA authority. A draft EPA policy is in review. Attempts to establish a "Range Rule" have been abandoned. Irrespective of lack of specific regulatory drivers, many DoD sites and installations are pursuing innovative technologies to address a variety of issues associated with ordnance and ordnance-related artifacts (e.g. buried waste sites or ordnance caches) that resulted from weapons testing and/or training activities. These issues include footprint reduction and site characterization, areas of particular focus for the application of technologies in advance of future regulatory drivers and mandates.

1.4 Stakeholder/End-User Issues

The BBR site is a formerly used defense site (FUDS) and as such it is important that concentrations of ordnance and locations of possibly live ordnance be mapped so that actions can be taken toward removal of UXO or safeguards can be established where there is the possibility that live ordnance is still in place. It is also important that a permanent record be maintained to document all measurements that are made to support clearance activities. Advanced technology is expected to contribute to the performance of these activities in terms of effectiveness as well as cost.

2.0 Technology Description

2.1 Technology Development and Application

The Oak Ridge Airborne Geophysical System – Time-domain Electromagnetic (ORAGS-TEM) system is a boom-mounted electromagnetic induction system that was designed for mounting on rigid Kevlar and carbon fiber booms attached to the underside of a Bell 206L Long Ranger helicopter (Figure 1). Rigid booms allow the helicopter to fly closer to the ground, thus increasing system resolution, and also permit precise control of receiver positions, allowing more accurate determination of UXO locations.

Specifications for the ORAGS-TEM system are listed in Table 2. The system was designed primarily for evaluation of the transient EM method. Several parameters are adjustable, as we will describe more fully in Section 2.3. As shown in Figure 1, the transmitter coil may be arranged in a rectangular geometry, or in a two-lobed configuration. As with most transient EM systems, a current is established in the loop, then rapidly switched off, inducing a secondary magnetic field in the earth, the decay of which is measured in the receiver coils. In the rectangular transmitter configuration, a transmitter cable is wrapped around a 12 m x 3 m rectangular, composite frame. The turnoff time for the 12 m x 3 m rectangular transmitter is about 230 μs, and for the lobed configuration about 160 μs. At BBR we tested two different receiver types—single turn receiver loops having dimensions of about 2.7 m x 2.7 m, and also smaller loops. The small loop receiver configuration consisted of two 23 cm x 60 cm multiple turn loops vertically offset by 34 cm. This allowed us to make vertical gradient measurements

Table 2. ORAGS-TEM Specifications

Console:			
	Power Supply	28V DC 30A or 110V 8A	
	Control	K6-IIIE+ 550	
		User interface device	
		User interface device	
		Pilot's laser altimeter display	
		Auxiliary keyboard and monitor, trackball	
	Transmitter		
		Peak Current	30A
		Turnoff ramp length	110-230 μs (Tx loop dependent)
		Waveform	Programmable; normally castle (Figure 3)
		Base Frequencies	30, 45, 75, 90, 135, 270 Hz
		Coil configurations	13.0m X 3.0m rectangular
			Symmetric lobed 3.0 m X 3.0 m
			Anti-symmetric lobed 3.0 m X 3.0 m
		Coil material	No. 2 aluminum
		Number of turns	4
	Receiver	A/D board	24-bit 4V p-p, 2 channels
		A/D Dynamic Range	120 dB
		Operating sample rate	10.8 kHz (0.003 m @ 60 knots airspeed)
		First Sample Window	0-93 μs after end of transmitter turnoff ramp
		Number of channels	Currently 2; boards can be added to increase to 8
		Time gates	Depends on base frequency, e.g. at 90 Hz, 5 time gates are calculated real time and stored in data base
		Coil configurations	2.7 m X 2.7 m large loop
			23 cm X 60 cm multi-turn small coil (can be placed inside tube or as a gradient pair external to the tube)
Altimeter	Optech ADM-3A Geophysical Rangefinder		
Positioning System	Novatel DL-4 GPS receiver, post-processed with base station		
Attitude Measurement	Ashtech ADU-2		
	Bartington MAG03ML7ONT 3-axis fluxgate magnetometer,		
Navigation	Picodas PNAV100 Model P141-E Real Time Navigation System with GPS/DGPS I/O ports		
	Racal Landstar differential GPS corrections satellite receiver Type 90952/3/1		
Booms	Kevlar/fiberglass/graphite composite		

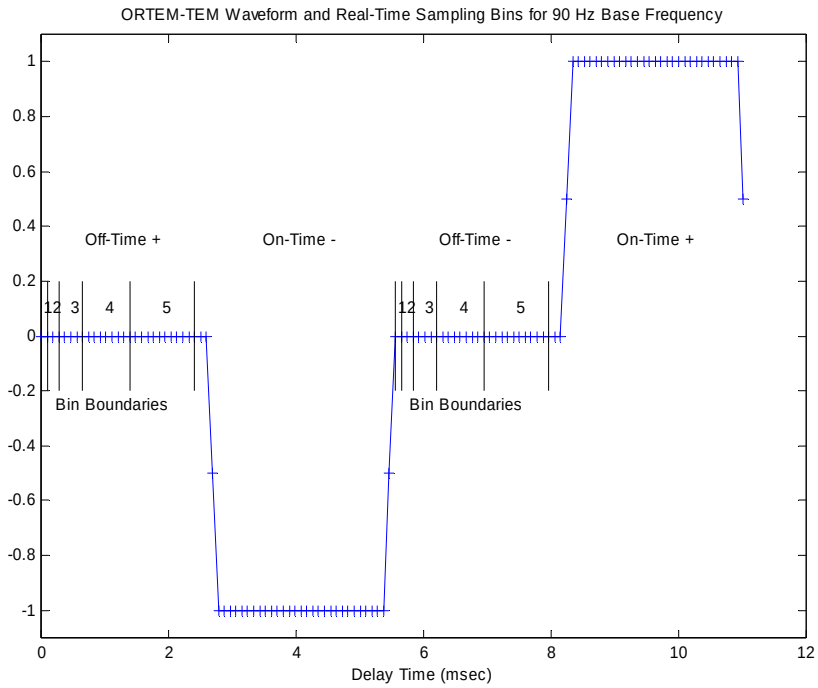

Figure 2. ORAGS-TEM console, AgNav navigation system, and Novatel GPS unit as installed in the helicopter.

as well as single loop measurements. The small loop receivers were mounted at the center of a crossbeam connecting the forward and aft booms, and the distance from the centerline of the helicopter to the receiver center was 4 m. A laser altimeter was mounted on the underside of the helicopter, and position information was gathered using differential GPS.

The transmitter, receivers, and laser altimeter are integrated via a console containing Pentium-3 based computer, the transmitter power supply, the transmitter driver board, and a digital system control and acquisition board that governs all system timing and performs digitization for EM receiver coil outputs and auxiliary analog signals (Figure 2). The data from the acquisition board, from GPS positioning, and from altitude and attitude instrumentation are stored on a 60-gigabyte hard drive. These data can be quickly copied to an external drive for transport to a base computer for processing and analysis.

The ORAGS-TEM transmitter waveform is of the alternating "castle" type, as indicated in Figure 3. Alternating positive and negative "on-time" current pulses with linear on- and off-ramps are separated by "off-time" periods during which the transient measurements are made. During the waveform's on-time, the transmitted magnetic field polarizes nearby conductive objects, with the eddy currents set up during the on-ramp decaying toward the end of the on-time. When the transmitted field is brought rapidly to zero, "early time" eddy currents are generated at the surface of the objects, which migrate into the object and attenuate in amplitude as the off-time progresses. At "late time", the eddy current density becomes constant throughout

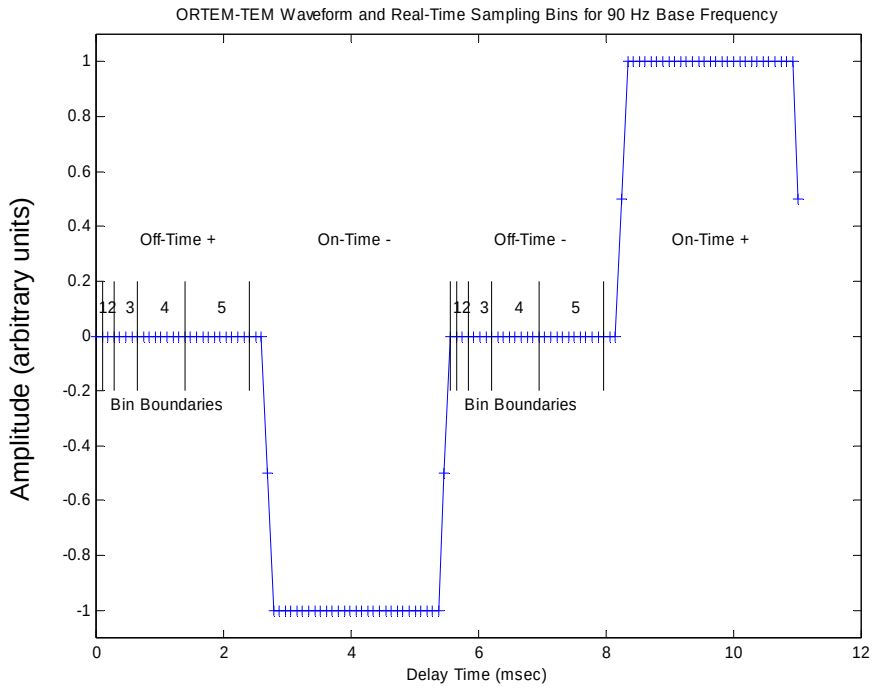

Figure 3. ORAGS-TEM waveform and receiver sampling for 90 Hz base frequency. Cross symbols (+) indicate 10.8 kHz sample locations, and real-time output data bins are indicated by the vertical lines and bin labels during the off times.

the conductor and the secondary field due to the eddy currents decays with a single time constant.

2.2 Previous Testing of the Technology

The development of the ORAGS-TEM system involved an evaluation of design options before initiating system construction. This review phase included reanalysis of the results from the 2000 ORAGS-EMP prototype data from BBR, a literature search, an analysis of system configuration options, consideration of flight safety constraints, modeling, ground testing, and review by a peer panel (Table 1).

Pre-design ground testing included acquisition of electromagnetic data with a Geonics EM63 around a stationary helicopter with and without the engine running, in order to map the noise field in the vicinity of the helicopter. These data were acquired by Jose Llopis at the U. S. Army Engineer Research and Development Center (ERDC). Additional helicopter noise measurements were subsequently acquired by ORNL. In both cases, data were also acquired over the test area with the helicopter absent.

As a result of the review phase, design attributes were selected for the demonstration system. A time-domain architecture was chosen as the primary focus, with the intent of making a system which could also acquire data to assess probable frequency domain performance. Transmitter structure and electronics, waveform, receiver configuration and electronics, and interfaces with other instruments that provide positioning data were selected. Initial ground-testing was done at a convenient outdoor location to test sensitivity to UXO-like items in anticipation of subsequent measurements in the presence of a helicopter.

Three shakedown tests were performed with ORAGS-TEM prototypes before the 2002 BBR test. These shakedown tests were conducted near Toronto, Ontario in December 2001, near Hyannis, Massachusetts in March 2002 and near Albuquerque, New Mexico in May 2002. Several incremental improvements were made to the system during the course of these tests, as summarized in Table 3 and discussed later in this section.

2.2.1 First Shakedown Test: Toronto, Ontario, December 2001

The system that was deployed for the first time in the December 2001 shakedown test was entirely new in concept, design, and hardware. Because of this, testing of the system was more fundamental in nature than that of the magnetic systems, which were essentially modifications of preexisting systems. More extensive data analysis was required, as it was necessary to confirm proper performance of several components and explore unanticipated issues. The first shakedown test consisted of three categories of evaluation: airworthiness tests, noise tests, and field trials. The airworthiness tests consisted of on-ground checking of load distribution and overall system weight, followed by hover tests and then a full test flight. Noise tests included high and low altitude noise tests with the transmitter on and off, and on-ground assessment of the response of the helicopter when energized by the transmitting coil. The field trials were used to measure variations in response to targets with increasing altitude, and target response to receiving coils oriented horizontally (vertical dipole) and vertically (horizontal dipoles). All EM system tests were carried out using various base frequencies in order to evaluate which was optimal.

2.2.1.1 Airworthiness Tests

Before any airborne testing of the EM system could be carried out, the boom structure and other system components were mounted on a Long Ranger helicopter and balance-tested on the ground at the National Helicopters hangar. As anticipated, the system required no ballast for stable operation. The test flight consisted of a hover test, then a full flight of several minutes duration. Upon completion of these tests the aerodynamic performance of the system was deemed satisfactory by the aeronautical engineer and pilot, and we were permitted to carry out airborne field tests of the EM system. It was noted that the maneuverability with the system mounted was lower than that of the ORAGS magnetic systems, presumably because of the distribution of mass in the side booms.

Table 3. Incremental improvements during the shakedown phase of development

Modification	Reason for change	First Airborne Test	Effect
Reduce receiver preamplifier gain	Apparent clipping at first shakedown test	Shakedown Test #2 (Massachusetts)	Overall improvement negligible.
Modify transmitter to lobed configuration	To reduce broadband noise due to signal induced in helicopter	Shakedown Test #2 (Massachusetts)	< 5 dB improvement vis late times for tested configuration.
Build internal receiver coils	To reduce noise due to wind vibration	Shakedown Test #2 (Massachusetts)	5-10 dB noise improvement
Construct vertical gradient configuration	To improve signal by allowing subtraction of coherent noise	Shakedown Test #3 (New Mexico)	8-10 dB noise improvement at low base frequencies.
Evaluate large loop receiver coils	To reduce vibration effects and improve depth sensitivity	Shakedown Test #3 (New Mexico)	7-8 dB improvement observed for 2m target-sensor height.
Isolation mounts	To reduce vibration	BBR Demonstration (South Dakota)	2-5 dB noise improvement
Improve transmitter precision/jitter, reduce dead time	To allow acquisition of earlier time response for improved overall SNR	BBR Demonstration (South Dakota)	Improved early-time data by ~10 dB
Central-loop small-coil receiver location	To reduce off-time transmitter-receiver noise	BBR Demonstration (South Dakota)	2-5 dB noise improvement

Figure 4. Prototype ORAGS-EM system during testing in Toronto.

2.2.1.2 Noise Tests

We conducted several noise tests, both on the ground and airborne, and with the transmitter on and off. In one on-ground test we varied the position of one of the two receiving coils, moving it from a position adjacent to the helicopter to a position at the far end of the boom. The second coil remained stationary for reference. The purpose of these tests was to determine whether

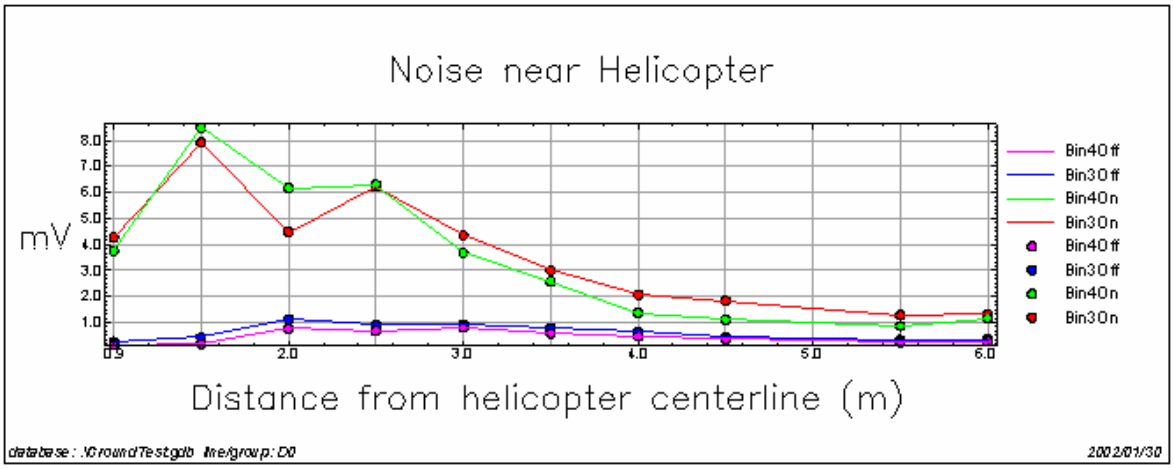

Figure 5. Influence of the helicopter on receiver noise as a function of distance from the helicopter. The forward boom (green line) is generally less noisy than the rear boom (red) when the helicopter is energized. The rear boom is less noisy near the aircraft where both are unacceptably high. Bottom lines represent noise with the helicopter turned off.

alternative coil positions would be preferred over those selected in advance. Figure 4 shows the Toronto test receivers in their standard positions, 4m and 5m from the centerline of the helicopter. Figure 5 shows the responses of a receiver coil in mV plotted as a function of distance from the centerline of the helicopter. The data show the front boom to be slightly less noisy than the rear boom, and also show that at a distance of about 4.5 m from the centerline of the helicopter the influence of the energized helicopter on the receiving coil drops to near background levels.

Figure 6 is a power spectrum for the inner receiver coil, located at 4m from the helicopter centerline, from a high altitude flight (200 m AGL) with the transmitter turned off (top panel) and the transmitter on (lower panel). Two types of noise are present, narrowband and broadband. With the transmitter on, narrowband noise peaks appear at frequencies near 1, 4, 5, 8, 9 and 13 Hz. The 13 Hz peak is caused by induction in the helicopter blades. The 4 and 9 Hz noise peaks were hypothesized to be artifacts caused by signal clipping, a result of our setting the gains too high on this shakedown test. Other noise peaks were not attributed to a particular source, but they almost certainly are some combination of torsional motion of the boom assembly, and EM fields induced on or inside the helicopter. We associated much of the broadband noise, exhibited over most of the frequency range of interest, to EM fields induced in the helicopter due to the portion of the transmitter coil that is directly beneath the body of the aircraft.

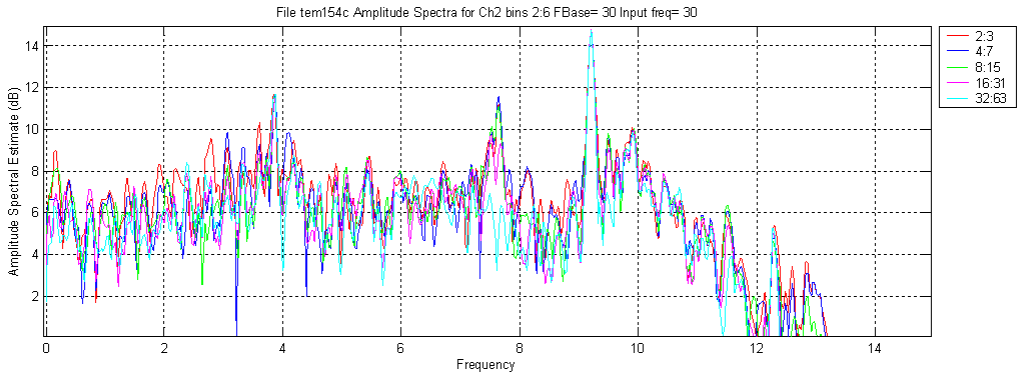

Figure 6. Amplitude spectrum in dB for the inner receiver coil at 4m from the helicopter centerline as a function of frequency for the ORAGS-TEM system with the transmitter off (top panel) and on (bottom panel). Each color represents a different time gate, and the numbers in the legend refer to which samples are included in each time gate. For example, the green line corresponds to the third time gate, comprised of an average of samples 8 through 15.

2.2.1.3 Test Grid Profiles

Objects in the test grid were chosen to emulate the previous tests with the ORAGS EMP proof-of-principle system, which was based on the Geonics EM-61AB. The target objects were placed along a line spaced at 25 m intervals. The list of targets is given in Table 4. The longest dimension of each test object was oriented so that it was perpendicular to the profile line (flight direction).

Table 4. Test grid target description for Toronto Shakedown test

Position along profile (m)	Description of targets
0	200 liter steel fuel drum, empty
25	5 kg steel barbell weight
50	1.5 m long steel pry bar, approximate weight 10 kg
75	1 m long thin-walled steel stovepipe, diameter approximately 20 cm.
100	Heavy duty steel chain, approximately 5-10 kg
125	Aluminum ladder, 2 m long, 0.5 m wide, laid flat on ground
150	Unknown buried feature, probably human-made and metallic, highly magnetic
175	4 kg steel cube
200	4 kg steel pipe, 1 m long
225	Rectangular steel frame, 2 m x 1 m
250	200 liter steel fuel drum, empty

Several base frequencies and nominal sensor heights of 2, 4, and 6 m AGL were examined while over the test grid. We also varied the receiver coil orientation. Most flights were with receiver coils parallel to the earth's surface (i.e., Z-directed dipoles), but a few test profiles were flown with receiver coils oriented parallel to the helicopter's direction of flight (X-directed dipoles). Using Z-directed receiver dipoles, four targets were clearly detected on every test profile: the two drums, the ladder, and the rectangular frame. The stovepipe produced a small but distinct anomaly on most profiles. The other items showed small but discernable anomalies on one or more profiles, but did not produce clear anomalies in all profiles. None of these can be discerned in Figure 7, which shows a sample profile from the first four time gates (0.2 ms to 2 ms) using the Z-directed dipole receiver (coil parallel with the earth's surface). The four largest objects produce distinctive anomalies, but smaller anomalies can be discerned from some of the other objects as well.

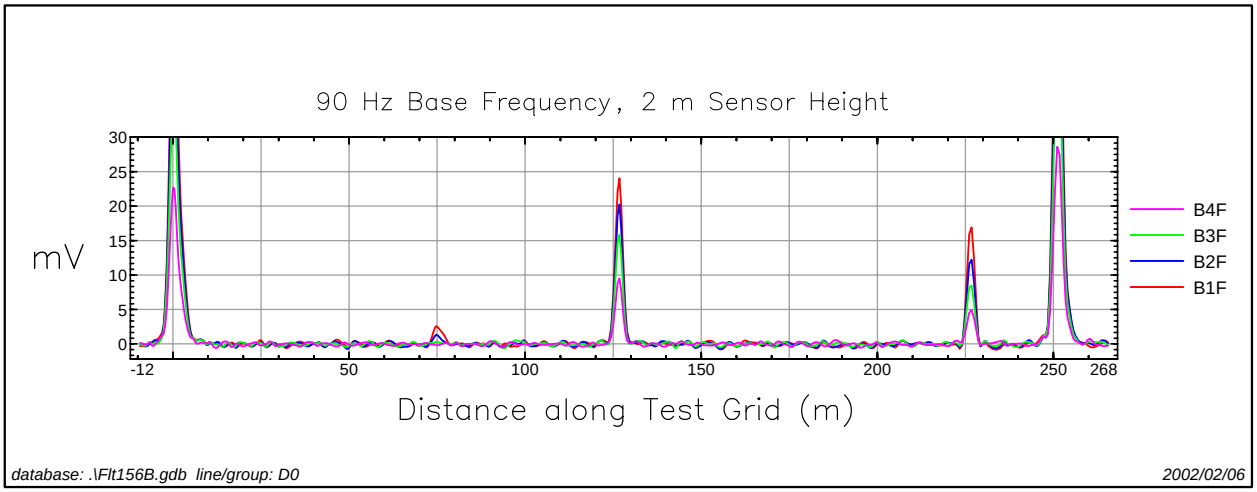

Figure 7. Test results for the first four time gates, using a Z-directed dipole receiver. The large anomalies are associated with 55-gallon drums (at each end of the profile), an aluminum ladder (125 m) and a rectangular steel frame (225 m).

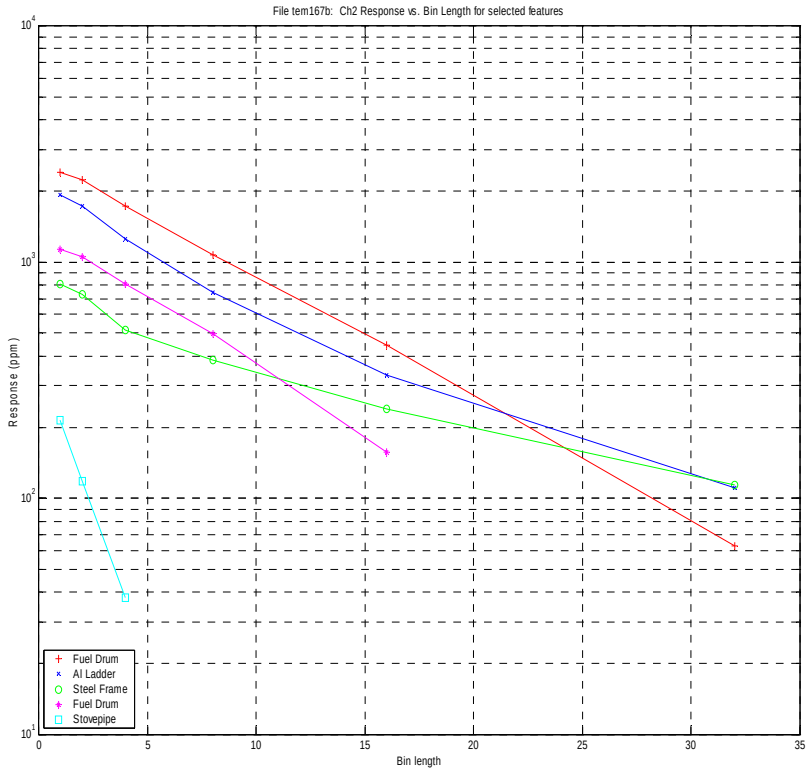

Figure 8. Response vs. time gate response for the five most frequently detected objects in the Toronto test line. This suggested the possibility of exploiting the airborne EM system for some level of discrimination.

The X-directed coil test demonstrated about an order of magnitude more noise than the Z-directed test. Further, the magnitude of anomalies was notably different with the X-directed coil, as might be expected by their shape and orientation relative to the coil.

2.2.1.4 Summary of EM System Status Following the Toronto Shakedown Test

The results of the Toronto shakedown test as a first evaluation of the performance of this new system were very encouraging. It indicated that the geometry of the system is well-suited for addressing the UXO problem, with minor modifications. It also demonstrated clear and reproducible differences in the transient response properties of different targets. Figure 8 shows decay curves plotted for the five most frequently detected objects. It shows the rapid decay of the stovepipe relative to the other objects, as would be expected from a thin-walled, open-geometry metallic object. This "discrimination" attribute would not be available in instruments that have one or two time gates. Performance of the system approached, but did not exceed, that of the predecessor system which was a modification of a thoroughly tested ground-based instrument.

The Toronto shakedown test indicated five important issues that needed to be addressed and could yield major benefits in system performance. As a result, we decided to perform a second shakedown test. The issues and related modifications were:

1) We were unable to use differences in amplitude between the two receiving coils as a means of removing noise because the output of one of the receivers was more frequently clipped than the other, and subtraction generated false peaks. The system should therefore operate at lower receiver gain, seeking to eliminate some of the narrowband noise.
2) Broadband noise is more difficult to remove by processing than narrowband noise. We anticipated that a significant reduction in broadband noise could be accomplished by reducing the field induced in the helicopter. Calculations supported this view. We decided to test this concept by building two "bridges" on which the transmitter loop would be mounted, extending from the front boom to the back boom, one to two meters from the centerline of the helicopter. This would segment the transmitter into two rectangular loops measuring 3m X 4m or 3m X 5m on each side of the helicopter. If the test with wooden bridges proved effective, we anticipated construction of composite bridges in the final version of the system.
3) Some of the noise peaks were associated with "microphonic noise" (using the term in the broad sense) where the transmitting field is variable or a voltage is produced in vibrating receiving coils due to their movement through the transmitted or secondary fields. This was thought to be due in part to turbulence effects associated with the external placement of the receiving coil. We chose to test this concept by using internal receiving coils in the second shakedown test.

4) In addition to relocating the coils to reduce "microphonic noise", we wanted to monitor this vibration by placing accelerometers on the booms during the second shakedown test, and if vibrational frequencies were identified, we would attempt to construct fairings for the booms before the field test at BBR.
5) Some EM noise during the Toronto test was thought to be associated in a primary or secondary sense to the high rotor noise that was observed in corresponding magnetic data that were acquired immediately after the EM data. The second shakedown test would be conducted with a properly demagnetized rotor and would provide a basis for determining whether any such noise exists.

2.2.2 Second Shakedown Test, Hyannis, MA, March 22-24, 2002

The second shakedown test was conducted in association with a magnetic survey at Camp Wellfleet, MA that was being conducted for the U. S. Army Corps of Engineers in March 2001.

2.2.2.1 Test Attributes

With the exception of accelerometers, all of the concerns described in Section 2.2.1.4 were addressed in the second shakedown test. To reduce clipping, we reduced the gain of the receiver preamplifier for each channel. Wooden bridges were constructed as shown in Figure 9 to allow testing of a new transmitter coil geometry to reduce the signal induced in the helicopter. The resulting coil loops on each side of the helicopter measured 3 m X 4 m. Receiver coils were constructed and installed inside the booms. Proper FAA paperwork was approved for these modifications in advance of the test. The helicopter rotor was thoroughly demagnetized in advance of deployment to Massachusetts, and this was verified by direct measurement. A significant reduction in rotor noise was observed in the magnetic data that were acquired in Massachusetts in advance of EM testing.

Instead of installing accelerometers, we acquired data with the EM system operating during the time when the helicopter was approaching, landing, cooling off, and shutting down. By plotting the spectra of these data as a function of time, we obtained a plot showing dynamic changes in the noise harmonics, making it possible to distinguish between vibrational noise sources and electronic noise sources.

Survey activities were impacted by bad weather, which caused the testing period to be extended from one to three days. Most of the second set of shakedown tests was conducted at a test site in a relatively flat portion of the sand dunes a few hundred meters inland from the beach at Camp Wellfleet. The test array consisted of galvanized garbage cans (about 40 gal), iron pipes, stovepipes, an aluminum ladder, and a steel bedspring platform. Details are shown in Table 5. All items lying horizontally were oriented with long dimensions perpendicular to the flight line direction.

Figure 9. Crossbeams added to the ORAGS-TEM system for the Massachusetts test.

EM tests that were conducted in Massachusetts included:

- High altitude noise measurements with transmitter on and off at four different flight speeds
- Low altitude speed tests over the airport runway to help identify noise that might vary as a function of flight speed.
- Base frequency comparisons at the Massachusetts test site at a constant flight speed of 30 knots
- Altitude tests at the Massachusetts test site with coils passing directly over the test objects (ALASA[1], 3 m, 5 m, 8 m)
- Velocity test at the Massachusetts test site
- Offset test at the Massachusetts test site (coils pass 6m and 12 m outboard of test items)

2.2.2.2 Summary of Massachusetts Test

Noise

The noise level was reduced 10-20% from that observed in the Toronto test, presumably due primarily to the revised transmitter coil geometry and gain adjustment. The noise during approach, landing, cool down, and shutdown (Figure 10) indicates that the dominant noise frequencies are at about 4, 9, and 13 Hz. Note that some of the dominant frequencies are observed to bifurcate and/or vary in flight, presumably due to variations in throttle, wind conditions, velocity, or some other movement of the aircraft.

Further reductions in noise were desired, and might be accomplished with a coil differencing

[1] ALASA is the flight altitude which is 'as low as safely achievable'

approach. In this design, two coils would be placed in a "vertical gradient" configuration and the response to ordnance would be determined by subtracting the two signals, as is done with an EM61. The differences could be acquired electronically by wiring the two coils together before pre-amplification, or they could be recorded separately to allow maximum opportunities for processing, at the expense of doubling file size and electronics. A simple test flight that determines the viability of a differencing scheme was to be conducted in advance of deployment to BBR.

Table 5. Description of Massachusetts EM test grid items

Item	Position in m from S to N	Description
1	0 (Southernmost item)	Galvanized steel trash can, upright, no top. Ht: 68 cm. D: 52 cm. Wall thickness: 1 mm. Wt: 13 kg.
2	25	Horizontal steel stove pipe. L: 60 cm. D: 18 cm. Wall thickness: 0.05 cm. Wt: 1 kg.
3	50	Vertical steel stove pipe. Same dimensions as item 2.
4	75	Two large diameter horizontal steel pipes, laying side-by-side in contact. Each pipe: L: 91 cm. D: 6 cm. Wall thickness: 5 mm. Wt: 4.5 kg.
5	100	Aluminum culvert. L: 172 cm. D: 25 cm. Wall thickness: 2 mm. Wt: 7 kg.
6	125	Aluminum ladder. L: 184 cm. Max. Width: 53 cm. Top W: 33 cm. Thickness: 11 cm. Wt: 6 kg.
7	150	One large diameter horizontal steel pipe. Same dimensions as item 4.
8	175	Steel bed frame with wire grid. L: 200 cm. W: 90 cm. Wt: 24 kg.
9	200	One medium diameter horizontal steel pipe. L: 91 cm. D: 4.8 cm. Wall thickness: 4 mm. Wt: 3.25kg.
10	225 (Northernmost item)	Galvanized steel trash can, upright, no top. Same dimensions as item 1.

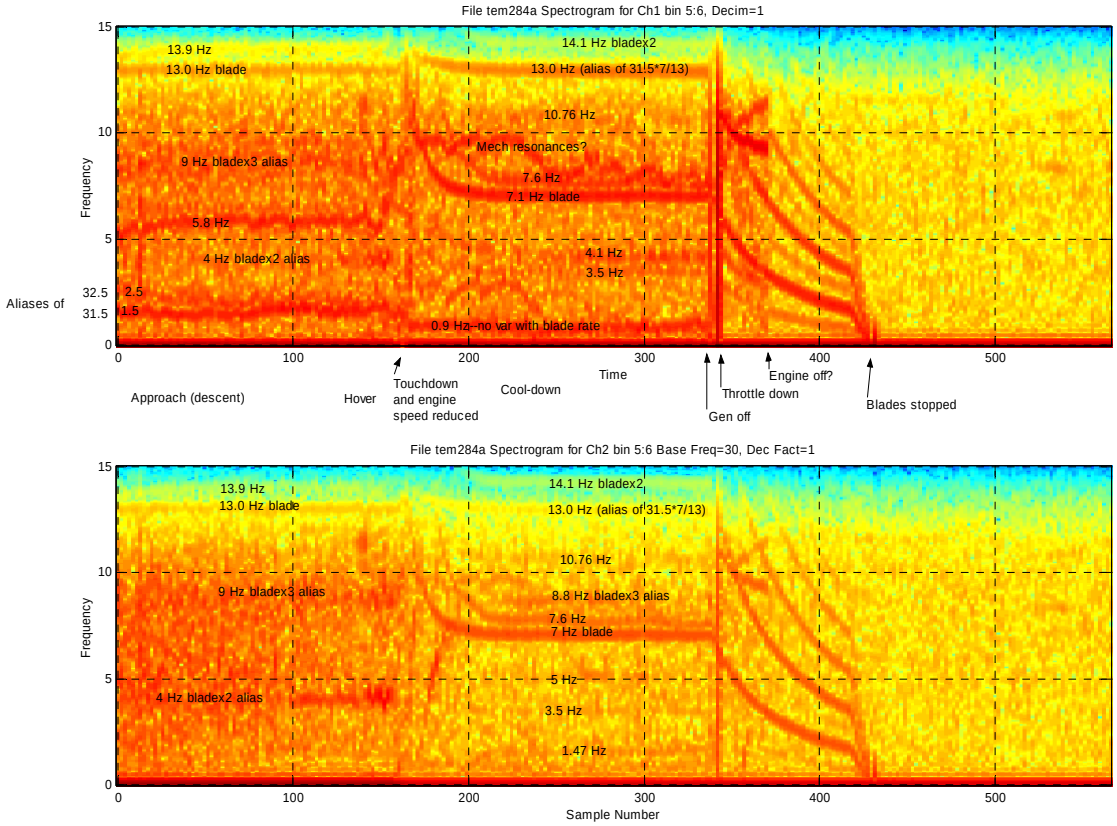

Figure 10. Noise spectra shown at a series of time steps, during approach, landing, cool down, and shutdown of the helicopter for the inner (top image) and outer (bottom image) receiving coils.

Overall sensitivity

The test results indicate that our design improvements have raised the sensitivity of the system beyond that which was observed in the Toronto shakedown test. Of the frequencies tested, the 135 Hz base frequency provided the greatest sensitivity to all targets. This is shown in Figure 11, where all of the targets that were emplaced were detected.

Base frequency

The base frequency selection depends on whether detection or discrimination is of primary concern. For best detection, the higher base frequency, 135 Hz performed best. This is because more repetitions of the transmitter can be stacked when a higher base frequency is used. On the other hand, the best opportunity to use the data for discrimination (determining target attributes)

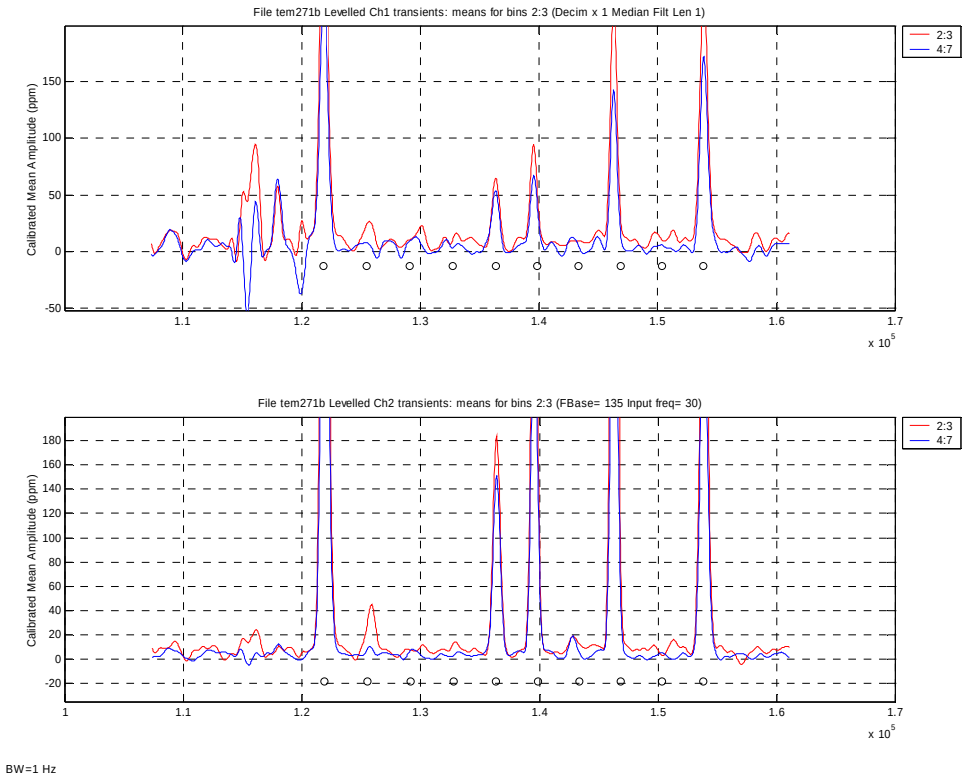

Figure 11. EM response of test items at Toronto shakedown test site. The base frequency is 135 Hz. Time gates 2 (red) and 3 (blue) are shown for upper receiver coil (top panel) and lower receiver coil (bottom panel).

occurs when a lower base frequency is used, e.g. 45 Hz. This is because the decay rate of the response is more characteristic of the target when more of the decay is captured. Our primary goal is to optimize detection. We therefore favor the higher base frequency, but note that the system will remain capable of acquiring data at lower base frequencies so that its use in discrimination can be exploited in future projects if appropriate.

Velocity

Noteworthy increases in noise were observed in the outboard (Channel 2) coil when aircraft velocities were increased (a few dB per 20 knots was observed). The noise at hover speed was similar to that at 20 knots, but at 60 knots, the noise level was significantly higher. Vibrational energy is present and this is aliased into the passband. For low base frequencies (30 and 45 Hz), the 26 and 39 Hz blade harmonics are problematic. Higher vibrational harmonics are important at higher base frequencies. For channel 1 (receiver closest to helicopter), the variation in noise as a function of velocity was less predictable than for channel 2.

Offset
Data were acquired with coils offset laterally to provide initial indications of the footprint of the system. It was observed that the response fell off dramatically when the coils were shifted 2 m from the target. This is a combined effect associated with the size of the area that is energized by the transmitter coil (slightly less than the area for the system that was deployed in the Toronto shakedown test) and the footprint of the receivers. The result speaks to the number and separation of coils that will be required to be used in the final system in order to have full coverage of the area of interest. A separation of about 1.0-1.5 m is anticipated. Of course, a similar result would likely be determined simply by examining the sensitivity along a flight line, but the system is not symmetric, so both dimensions should be reviewed.

2.2.3 Results of the Third Shakedown Test, Pueblo of Laguna, NM

The third shakedown test had a narrower scope than previous tests. It was designed to provide guidance on two key design attributes: 1) the relative effectiveness of vertical gradient receiver configuration vs. single loop configurations; and 2) the strengths and weaknesses of a large (~3 m X 4 m) single turn receiver loop, compared to a smaller multi-turn coil, as used in the previous shakedown tests. At the Pueblo of Laguna site, we were also able to deploy some true ordnance items, rather than the miscellaneous metal objects that had been used in previous tests. Preliminary Signal/Noise Ratio (SNR) estimates prepared from this dataset confirmed that (1) vertical gradient measurements could be used to suppress some vibrational noise, particularly at low base frequencies and for targets at shallow depths below the sensor, and (2) that large-loop receiver coils are more resistant to vibrational noise than rigidly-mounted small receiver coils, that their SNR decays more slowly with respect to height than the SNR for small-coil receivers, and that their broader anomaly footprint can improve target detection when only two receiver channels are available.

Several improvements (and one reduction) in SNR arose from configuration changes performed during these tests. These were:

1. An increase of 1.35 times (at 2.5 m sensor-target distance) through the use of vertical differencing. Despite the short vertical separation imposed by the boom geometry and aerodynamic considerations, this boost is interesting because it could lead to more flexibility in base frequency for areas where very low survey altitudes are practical.
2. An increase of 5.5 to 7 times (at 2.5 m sensor-target distance) in SNR is seen through the use of a large-loop receiver strung around the inside perimeter of the transmitter lobe, relative to the small in-boom receiver coils.
3. An estimated increase of 2.8 times was calculated to be possible through the use of earlier time bins. This large benefit is most visible in differential data; single-coil noise levels increase at very early times, this noise is strongly correlated between the differential inputs.
4. A decrease of 2 times was seen for the standard receiver coil mounted externally (at New Mexico) rather than inside the booms (Massachusetts) and analyzed individually rather than as differential pairs. This comparison was made only at 135 Hz, and the coil mounting

structure was mounted on the booms broadside to the wind stream, so that relatively large buffeting forces were being applied to it.

At 75 Hz, the large loop receiver yielded SNR's approaching those of the EM-61AB Ch1 levels at 2.5 m sensor-target distance.

A brief ground study was conducted after the shakedown test and before the BBR demonstration to establish the power law exponents for various configurations for the height range that can be reasonably achieved with such tests. These were used as a benchmark to measure improvements achieved by adjustment of gain, coil area and vertical differencing for the large-loop configuration.

Weight and balance analysis conducted prior to the BBR demonstration indicated that improved aeronautical performance should be obtained by reducing the system's moment of inertia as computed about the flight direction vector, as well as by reducing drag. These objectives were addressed by:

1. Reducing the transmitter cable weight by switching to electrically equivalent aluminum cable
2. Eliminating (for large-loop measurements) or minimizing (for standard-coil measurements) the mass and turbulence-generating effects of receiver coil mounts.
3. Using a lighter "bridge" between the forward and rear booms to carry the transmitter and/or receiver cables or coils.

2.3 Factors Affecting Cost and Performance

The cost of an airborne survey depends on several factors, including:

- Helicopter service costs, which depend on the cost of ferrying the aircraft to the site and fuel costs, among other factors.
- The total size of the blocks to be surveyed
- The length of flight lines
- The extent of topographic irregularities or vegetation that can influence flight variations and performance
- Ordnance objectives which dictate survey altitude and number of flight lines
- The temperature and season, which can control the number of hours that can be flown each day
- The location of the site, which can influence the cost of logistics
- The number of sensors and their spacing; systems with too few sensors may require more flying if they require interleaving of flight lines

- Survey type (survey objectives), specifically high density for individual ordnance detection versus transects for target/impact area delineation and footprint reduction
- System swath width, and any interleaving of flight lines that may be required

2.4 Advantages and Limitations of the Technology

Airborne surveys for UXO are capable of providing data for characterizing potential UXO contamination at a site at considerably lower cost than ground-based systems. Current indications are that the ORAGS-Arrowhead magnetic survey cost may approach $60 per acre under *optimal* conditions. An optimized EM system under favorable conditions will still require interleaving, and therefore will have higher cost, most likely about $100 per acre. Airborne systems are particularly effective for sites characterized by low-growth vegetation and minimal topographic relief. They can also be used where heavy brush, mud, or swampy conditions makes it difficult to conduct ground-based surveys.

Experience with airborne magnetic and EM surveys to date indicate that with existing hardware, the smallest objects that can be routinely detected have a nominal mass of about 2 kg when surveys are flown at approximately 1-2 m above ground level (AGL). The 2 kg threshold is larger than the threshold value for ground surveys (e.g. towed array surveys using MTADS), which can operate with sensors at less than 0.5 m AGL.

Both airborne and ground magnetometer systems are susceptible to interference from magnetic rocks and magnetic soils. Airborne electromagnetic systems are less vulnerable to these natural conditions, as proven by numerous ground-based surveys. Rough topography and tall vegetation limits the utility of helicopter systems, necessitating survey heights too high to be of practical benefit.

3.0 Demonstration Design

3.1 Performance Objectives

Table 6 is a listing of the various performance objectives for this survey.

Table 6. Performance Objectives of ORAGS-TEM Airborne Electromagnetic System

Type of Performance Objective	Primary Performance Criteria	Expected Performance (Metric)	Actual Performance Objective Met?
Qualitative	ORAGS-TEM system aerodynamically stable	Pilot report	Yes
Qualitative/ Quantitative	ORAGS-TEM data can be used for discrimination	Processing of selected data sets shows different response from some types of UXO and scrap.	Yes
Quantitative	Reduced system noise levels	Comparison to previous noise levels	Yes
Quantitative	Improved sensitivity	Comparison to previous detection thresholds over calibrated test grid	Yes
Quantitative	Minimize coupling to active helicopter noise source	Compare noise levels from various orientations of EM receiver	Yes

3.2 Selecting Test Sites

Two sites were selected for data acquisition during the 2002 tests: The ORNL-established airborne system Calibration Site, and Bombing Target 1, both on Cuny Table at BBR. We had planned to acquire data at Stronghold Table as well, but this was not possible because of Native American protests unrelated to the helicopter survey. These sites were chosen to enable, where possible, direct comparison of results from the new generation airborne systems with results of previous airborne and ground-based geophysical systems for UXO detection and mapping. These include airborne surveys with the Aerodat HM-3 system, the ORAGS-Hammerhead system, the ORAGS-EMP system, the ORAGS-Arrowhead system, and the ORAGS-VG system, and ground-based surveys at the Calibration Site with a Geometrics G-858 magnetometer system and a Geonics EM-61 TEM system.

3.3 Test Site History/Characteristics

3.3.1 BBR Test Site

In 1999-2000, ORNL and USAESCH established a test grid at BBR to support evaluation of airborne magnetometer systems. The test grid was constructed in an area of relatively flat rangeland on Cuny Table, a mesa bounded by steep escarpments bordering Badlands National Park. The soil is unconsolidated and thick, consisting mainly of layers of sand and silt. The geological background of the site is thus relatively clean, producing few sizeable short wavelength EM anomalies.

Ordnance and non-ordnance items were buried at a total of 53 different locations, distributed along eight rows spaced 15 m apart, in a four-acre area, about 150 m x 105 m. Buried items were as small as 8 inch nails and as large as an inert 250 lb bomb. Along the rows, many items are evenly spaced 20 m apart, but some items are as close as 10 m and as far apart as 75 m. This is shown schematically in Figure 12 and the buried items are more fully described in Table 7. The accuracy of the locations of the buried items is generally good, but varies because the items were not all buried at the same time and varying quality GPS systems were used to determine their locations. Airborne systems that have acquired data at the BBR test grid at one time or another include the HM-3, ORAGS-Hammerhead, ORAGS-EMP, ORAGS-Arrowhead, and ORAGS-TEM systems.

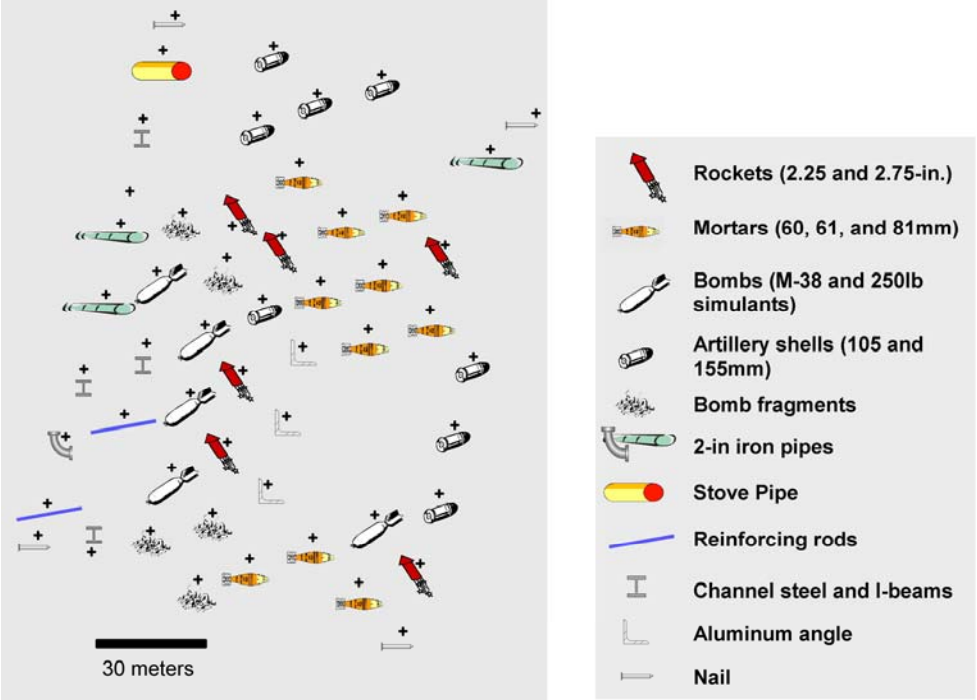

Figure 12. Schematic map of BBR Test Site.

3.3.2 Bombing Target 1

Bombing Target 1 (Figure 13) was used for training missions in World War II. As a result, most of the ordnance at the site are M-38 100 lb sand-filled practice bombs. These contain approximately 10-15 kg of steel, but much smaller fragments are also found at the site as well as smaller ordnance items. The target is marked with a circular berm and crosshairs (Figure 13) that is 1.0-1.5 m in height. A barbed wire fence passes through the center of the target with an east-west orientation. Some of the ordnance items have been removed from the northern side of the fence during evaluation of previous mapping projects. To our knowledge, the area south of the fence has not been excavated for UXO, although it is part of a field and is routinely plowed. The site was previously surveyed with the NRL MTADS system in 1997 (McDonald et al., 1998), and subsequently by the ORNL with the HM-3 magnetometer-based system in 1999. Some excavation of UXO was conducted for validation of the 1997 MTADS survey in the area north of the fence (Andrews et al., 2001). In the same 2002 deployment described in this report, we acquired data over Bombing Target 1 with the ORAGS-VG Vertical Gradient system. These results will be discussed in a separate report to ESTCP.

Figure 13. Bombing Target 1 at BBR.

Table 7. Description of BBR Test Grid Items

Item ID	Description	Weight (kg)	Long dimension (m)	Orientation	Depth of burial (m)
Row A					
A1	8 in nail+2 in galv pipe	2.7	0.3	E-W	0.5
A2	3 rebar rods	5.5	0.8	random	0.6
A3	2 in galv pipe elbow	4.5	0.6	random	0.7
A4	steel channel	6.8	0.5	random	0.6
A5	2 in galv pipe	2.7	0.3	E-W	0.3
A6	2 in galv pipe with flanges	4.5	0.4	E-W	0.4
A7	unknown				
A8	box beam	4.5	0.7	E-W	0.6
A9	galv stove pipe	1.8	0.8	E-W	1.0
A10	8 in nail	0	0.2	vertical	0
Row B					
B1	I beam	13.2	0.4	E-W	0.4
B2	4 rebar rods	4.1	0.8	random	0.5
B3	I beam	4.5	0.2	random	0.6
B4	250 lb bomb	52	0.6	vertical	1.0
B5	100 lb bomb fragments	unknown	unknown	unknown	0.1
Row C					
C1	100 lb bomb fragments	8.6	unknown	unknown	0.4
C2	250 lb bomb simulant	22.7	1.6	N-S	1.3
C3	250 lb bomb simulant	29	1.6	E-W	0.7
C4	100 lb bomb intact	22.7	1.2	N-S	0.9
C5	100 lb bomb fragments	14.5	0.7	N-S	0.4
C6	2.75 in rocket nose section	4.1	0.3	E-W	0.5
C7	155 mm round	24	0.6	vertical	0.7
C8	105 mm round	8.6	0.4	vertical	0.7
Row D					
D1	100 lb bomb fragments	unknown	unknown	random	0.1
D2	100 lb bomb fragments	unknown	unknown	random	0.1

D3	2.75 in rocket cylinder	4.1	0.1	E-W	0.6
D4	2.75 in rocket	2.3	0.7	N-S	0.6
D5	105 mm round	8.6	0.4	vertical	0.8
D6	2 2.75 in rocket simulants	5.4	0.2	N-S and E-W	0.4
D7	61 mm illumination round	0.9	0.2	vertical	0.4
D8	105 mm round	8.6	0.4	vertical	0.8
Row E					
E1	81 mm round	4.1	0.4	vertical	0.4
E2	aluminum rod	0.5	0.9	E-W	0.3
E3	aluminum rod	0.5	0.9	E-W	0.5
E4	aluminum rod	0.5	0.9	E-W	0.8
E5	81 mm round	3.6	0.4	N-S	0.7
E6	81 mm round	3.6	0.4	N-S	0.8
E7	105 mm round	8.2	0.4	E-W	0.3
Row F					
F1	81 mm round	3.2	0.4	N-S	0.6
F2	60 mm illumination round	1.8	0.4	E-W	0.1
F3	60 mm illumination round	1.8	0.4	N-S	0.1
F4	60 mm illumination round	0.9	0.4	vertical	0.1
Row G					
G1	81 mm round	3.2	0.4	E-W	0.5
G2	100 lb bomb	2.7	0.8	vertical	0.5
G3	60 mm mortar round	1.4	0.2	vertical	0.4
G4	2.25 in rocket	4.5	0.7	N-S	0.5
G5	steel pipe	4.1	0.5	E-W	0.6
Row H					
H1	8 in nail	0	0.2	vertical	0
H2	2.75 in rocket	3.2	0.3	N-S	0.9
H3	155 mm round	25.5	0.5	E-W	0.9
H4	155 mm round	25.5	0.6	N-S	0.7
H5	155 mm round	25.5	0.6	vertical	0.6
H6	8 in nail	0	0.2	vertical	0

3.4 Present Operations

Bombing Target 1 at BBR had been previously surveyed by the NRL MTADS magnetometer array (McDonald, et. al. 1998) under the guidance of the ESTCP Program Office. Selected anomalies were excavated as part of the analysis of those data, before the data described in this report were acquired. The site was subsequently surveyed with the HM-3 system in 1999. From the two data sets (MTADS and HM-3), 146 items were excavated north of the fence at Bombing Target 1, including 17 targets selected from the airborne data. These results were assessed by Andrews et al., 2001. It is possible that surficial objects have moved by frost-heaving or domestic animals between the earlier surveys and the 2002 ORAGS-Arrowhead survey, and that buried objects south of the fence have been moved due to plowing, but these effects are assumed to have a minimal impact.

3.5 Pre-Demonstration Testing and Analysis

In addition to the shakedown tests described in Section 2.2, adjustments were made to the console between the completion of the third shakedown test (New Mexico) and the initiation of data acquisition for the BBR Demonstration. These included improvements to the transmitter to reduce early time jitter (to enable acquisition at earlier decay times) and testing of vibration mounts.

3.6 Testing and Evaluation Plan

3.6.1 Demonstration Set-Up and Start-Up

Mobilization involved transporting all system components by trailer to Rapid City and installing them on a Bell 206L Long Ranger helicopter. All system components, including the transmitter/ data recording console, GPS receivers, and laser altimeter were tested to ensure proper operation and performance. The Mission Plan was read and signed by all project participants to assure safe operation of all systems.

3.6.2 Period of Operation

Mobilization of the geophysical crew from Oak Ridge, Tennessee and the flight crew from Toronto, Canada began on September 8, 2002. This required two and a half days travel to Rapid City with the geophysical equipment trailer. The helicopter crew departed Toronto on September 9 and both the geophysical crew and the helicopter crew arrived on September 10. The project involved acquisition of both magnetometer and electromagnetic (EM) data. Initial measurements were made with the EM system on September 14-16. Helicopter repairs and repair of the attitude measurement unit resulted in a delay in acquisition of EM data until September 25. EM acquisition was completed on September 28. Magnetic data acquisition was initiated after acquisition of EM data was complete, and ended on October 7. De-installation

Figure 14. ORAGS-TEM large receiver loop configuration. Single loops of wire are attached to the top and bottom of the 3 m X 3 m outer portion of the booms.

was completed on October 8, and the geophysical and air crews departed for another project in Arizona.

3.6.3 Area Characterized

Two sites were surveyed, as described previously. Several configurations of the system were tested at the BBR test site. At Bombing Target 1, approximately 14 hectares were surveyed with the large-loop receiver configuration, and a smaller area, approximately 2.4 hectares, was covered with a small coil system.

3.6.4 Residuals Handling

This section does not apply to this project.

3.6.5 Operating Parameters for the Technology

The ORAGS -TEM system is designed for daylight operations only. Lines were flown in a generally north-south pattern. Data were sampled at a rate of 10.8 kHz. Survey speeds at the BBR sites ranged from 10-14m/s. These speeds were required to minimize positional errors with a two-receiver system. Higher speeds, perhaps 30m/s or 100 km/hr, are anticipated with a production system where a wider swath will allow coarser line spacing. Survey altitude is 1-3 m above ground level (AGL) were safely achievable. Data were acquired at higher altitudes at the test site to guide performance assessments. Line spacing was dependent upon the receiving coils used, and the altitude of the test. In general data were acquired in a “vertical difference” configuration with one coil mounted above the other. With small receiver coils at 1.0-1.5 m

altitude AGL, a line spacing of 1m was used. Large loop receivers at this altitude required 3 m line spacing. Large loop data acquired at Bombing Target 1 did not use a "vertical difference" configuration, but operated with one large loop coil on each side of the aircraft to maximize efficiency in 2-channel production mode.

3.6.6 Experimental Design

Data were acquired to compare several system parameters. The system parameters were selected on the basis of previous shakedown tests, but it was determined that some parameters could not be adequately assessed without acquiring data over a documented test site where only one parameter was changed at a time. The tests conducted with the ORAGS-TEM Time-Domain Electromagnetic System are summarized in Table 8. The parameters that were assessed at BBR through data acquisition at the test site were:

1) Flight performance. Previous shakedowns had shown in-flight sensitivity associated with the mass distribution of the system. We reduced overall mass by replacing a copper transmitter cable with an aluminum transmitter cable, and by replacing plywood crossbeams with fiberglass tubes. These improvements could only be assessed by flight-testing.

2) Large/small loop receiving coils: previous shakedown tests had shown mixed results with coils that were either small (~30 cm X 50 cm multi-turn) or large (single turn 3 m X 3 m). We acquired data with both configurations. The large loop receiver coil configuration is shown in Figure 14 and the small loop receiver coil configuration is shown in Figure 15.

Figure 15. ORAGS-EM small receiver coil configuration. Inset shows enlarged view of coils.

3) "Vertical difference" configurations (subtract upper loop response from a lower loop response with ~30 cm separation) vs. vertical field (single loop) configurations. These data were acquired simultaneously with data from the single receiving coils by recording from upper and lower loops separately. Gradient coils for the small loop system are positioned at the top and bottom of the frames shown in Figure 15, and for the large loop system are at the top and bottom of the boom tubes in Figure 14.

4) Transmitter configuration comparison. We had previously acquired data with two different transmitter configurations: a simple rectangular loop that measured 3 m X 12 m, and a lobed transmitter in which the central portion of the transmitter was eliminated to reduce induction in the helicopter, and thus reduce noise. A sketch of the anti-symmetric lobed transmitter is superimposed as a black line in Figure 1. A photograph showing the black transmitter cable on the boom tubes with a lobed configuration is shown in Figure 16. The lobed configuration was deployed in two formats – symmetric and anti-symmetric current directions in the transmitter lobes.

5) Base frequency tests. Although we had compared base frequency tests in previous shakedowns, modifications to the weight distribution (see item 1 above) would affect vibrational harmonics of the system, and fine tuning of the system console would allow testing of higher base frequencies than in previous shakedown tests.

6) Vibration-isolated mounts. Previous tests had been conducted with receiver coils mounted rigidly to the support structure. Most major noise sources had been identified and eliminated prior to the BBR deployment, so that a test with the small coil receivers coupled to the support structure through isolation mounts was called for to assess the potential for further reduction of vibration induced noise.

Figure 16. Lobed 3 m X 3 m transmitter configuration. Note the transmitter cable does not extend across a portion of the front boom.

Table 8. Sequence of ORAGS-TEM tests conducted at BBR

ID	Configuration Name(s)‡	Description	Base Freq.	Receiver Coil Type	Receiver Geometry	Transmitter Configuration	Altitude	Site(s)
1.	L-Rect-270, L-Rect-270-Diff	Large loop at one base frequency (270 Hz).	270Hz	Large loops, vertical field component	Z, centered at 4.5m	Rectangular	ALASA*, 2.0,3.0	Test Site; full coverage†
2a.	S-Rect-270, S-Rect-270-Diff	Small coil at high base frequency (270 Hz) at 1 m alt.	270Hz	External, small coils, total field and vertical difference.	Z, @4.5m from CL (on bridge)	Rectangular	ALASA*, 2.0, 3.0	Test Site; full coverage†
2b.	IS-Rect-270 IS-Rect-270-Diff	Isolation-mounted small coils at high base frequency (270 Hz) at ALASA	270Hz	***Isolation-mounted*** external, small coils,	Z, @4.5m from CL (on bridge)	Rectangular	ALASA*	Test Site; full coverage†
2c	S-Rect-90 S-Rect-90-Diff	Collect survey data at ***low base frequency (90Hz)*** at ALASA	***90 Hz***	External, small coils, total field and vertical difference	Z, @4.5m from CL (on bridge)	Rectangular	ALASA*	Test Site; Two passes with sensors over rows of targets only.
3.	L-Slob-270 L-Slob-270-Diff	Lobed symmetric data at high base frequency (270 Hz) at ALASA	270Hz	Large loops, vertical field component	Z, centered at 4.5m	***Lobed symmetric***	ALASA*	Test Site; full coverage†
4.	L-Alob-270 L-Alob-270-Diff	Lobed anti-symmetric data at high base frequency (270 Hz) at ALASA	270Hz	Large loops, vertical field component	Z, centered at 4.5m	***Lobed anti-symmetric***	ALASA*	Test Site; full coverage†
5.	S-Rect-270-3m S-Rect-270-3mdiff	Place external (standard and vertical gradient) coils, mounted on bridge, closer to helicopter to determine noise effects	270 Hz	External, small coils, total field and vertical difference	***Z, @3m from CL (on bridge)***	Rectangular	ALASA*	Test Site; Two passes with sensors over rows of targets only.
6.	S-Rect-270-dual	Place coils on opposite sides of helicopter to ascertain symmetry in noise	270 Hz	Large loops	Z, 4.5m from centerline ***on both sides of***	Rectangular	ALASA*	Test Site; Two passes with sensors over

					aircraft			rows of targets only.
7a.	L-Rect-270 L-Rect-270-Diff	Large loop coils at a bombing target	90 or 270 Hz	Large loops	Z @ 4.5m from centerline	Rectangular	ALASA*	Bombing Target 1
7a.	S-Rect-270 S-Rect-270-Diff	Small coils at a bombing target	90 or 270 Hz	External small coil vertical component with vertical gradient	Z @ 4.5m from centerline	Rectangular	ALASA*	Bombing Target 1

‡ Basic configuration notations follow the format 'Receiver type'-'Transmitter type' – 'Base Frequency' – 'Special'.
# Z is used to compactly denote the vertical (up) direction for the receiver coils—coil orientation being specified as the direction of the vector normal to the plane of the coil.
* ALASA = As Low as Safely Achievable
† Full coverage is considered 3m line spacing at 1m altitude, and 5m line spacing at higher altitudes.

Data quality objectives to be used for this technology demonstration focused on prior generation airborne results as the baseline performance condition, as well as previous MTADS demonstration data.

Given the various considerations associated with both the interpretation of airborne geophysical survey data and the calculations of the various performance parameters, DQOs for the demonstration of the ORAGS-TEM system should be expected to meet or exceed the current performance parameters.

3.6.6.1 Quality Control

All data were examined in the field to ensure sufficient data quality for final processing. Each of the items discussed in the previous sections were considered and tested. During survey operations, flight lines were plotted to verify full coverage of the area. Missing lines or areas where data were not captured were reacquired. Data were also examined for high noise levels, data drop outs, or other unacceptable conditions. Lines flown, but deemed to be unacceptable for quality reasons, were re-flown.

3.6.6.2 Positioning

During flight, the pilot was guided by an on-board navigation system that used real-time satellite-based DGPS positions. This provided sufficient accuracy for data collection (approximately 1 m), but was inadequate for final data positioning. To increase the accuracy of the final data positioning, a GPS base station, CT-1 on Cuny Table near the field sites was used. This site was established in 1999 during ongoing EE/CA investigations by Parsons Engineering Science. Its location is WGS-84 43.5204408, 102.6983032, 3307.86 m.

Raw data in the aircraft and on the ground were collected. Differential corrections were post-processed to provide approximately 20 cm accuracy for the airborne GPS antenna in the final data positioning, as specified by the manufacturer. Additional positioning errors will be introduced by any pitch, roll, or yaw of the aircraft. The final latitude and longitude data were projected onto an orthogonal grid using the North American Datum 1983 (NAD 83) South Dakota CS 83 South Zone. Vertical positioning was monitored by laser altimeter with an accuracy of 2 cm. No filtering was required of this data, although occasional drop-outs were removed.

3.6.6.3 Electromagnetic Data Processing

The electromagnetic data were subjected to several stages of geophysical processing. The processing flow has not been finalized to the extent that it has in the ORAGS total magnetic field system, but follows some of the same steps.

The 10,800 Hz raw data were desampled in the signal processing stage to a 120 Hz recording rate. All other raw data were recorded at a 60 Hz sample rate. Data were converted to an ASCII format. Using the MATLAB software package, the data were “baselined” using the following procedure:

(i) Remove high frequency anomalies, sensor dropouts, and data spikes from an entire flight of data, and interpolate between the points where data has been excised.

(ii) Smooth the remaining low frequency data.

(iii) Subtract the smoothed low frequency data from the original data set to extract short wavelength anomalies associated with compact sources.

After baselining was completed, we imported the modified ASCII data into a Geosoft format database for processing. With the exception of the differential GPS post-processing, all further data processing was conducted using the Geosoft software suite and proprietary ORNL algorithms and filters. The quality control, positioning, and electromagnetic magnetic data processing procedures (steps 1-4) are described below.

(1) Data were inspected according to the quality control procedure described above in section 3.6.6.1.

(2) Time Lag Correction
There is a lag between the time the sensor makes a measurement and the time it is time stamped and recorded. This applies to both the EM receiver and the GPS antenna. Accurate positioning requires a correction for this lag. Time lags between the EM receivers and GPS signals were measured by a proprietary ORAGS firmware utility. This utility sends a single pulse that is visible in the data streams of the instruments. This lag was corrected in all data streams before processing.

(3) Sensor positions were corrected according to the procedure described in section 3.6.6.2.

(4) Filtering/Differencing
Other filters, usually high- or low-pass filters, were applied as needed to individual channels we chose to focus on. For vertical gradient measurements, we differenced the upper and lower receivers for each channel.

Data were rarely broken up from flights to individual lines as gridding and analysis could as easily be done on full flights of data.

3.6.7 Sampling Plan

This section does not apply to this report.

3.6.8 Demobilization

EM acquisition was completed on September 28. Magnetic data acquisition was initiated after acquisition of EM data, and ended on October 7. De-installation and demobilization were completed on October 8.

4.0 Performance Assessment

4.1 Performance Criteria

Demonstration effectiveness was determined directly from comparisons of the processed/analyzed results from the demonstration survey and the results of previous airborne and ground-based surveys. These comparisons include both the quantitative and qualitative items described here. Demonstration success was determined as the successful acquisition of airborne geophysical data (without any aviation incident or airborne system failure) and meeting the baseline requirements for system performance as established previously in this document (Section 3.1). Methods utilized by ORNL on both current and past airborne acquisitions to ensure airborne survey success include daily QA/QC checks on all system parameters (e.g. GPS, transmitter operation, data recording, system compensation measurements, etc.) in the acquired data sets, continual inspections of all system hardware and software ensuring optimal performance during the data acquisition phase, and review of data upon completion of each processing phase.

Several factors associated with data acquisition cannot be strictly controlled, such as aircraft altitude and attitude. Altitude is recorded and enters into the data analysis and comparisons with previous results. The aircraft attitude measuring system provides a documented database that cannot be directly compared with previous surveys when this system was not available. The consistent and scientific evaluation of performance are accomplished by using identical or parallel (where parameters are dataset dependent) processing methods with identical software to produce a final map, and following consistent procedures in interpretation when comparing new and existing datasets from the test sites.

Data processing involves several steps, as described in Section 3.6.6.3. Each step will be performed in the same manner on data acquired with sequential generations of the system at the same sites, to provide a basis for comparing the performance of the systems. The processing procedures have been selected and developed from experience with similar data over a span of more than five years for optimal sensitivity to UXO.

Data quality objectives, as described in Section 3.6.6 (Experimental Design), were used for this demonstration. Surveys over the previously described test areas are conducted as described in Section 3.6. Data were acquired with a variety of configurations and at a variety of flight altitudes over the test areas and configurations as described in Section 3.6.6. Data confirmation is in accordance with the processes previously described in this section.

Table 9 identifies the expected performance criteria for this demonstration, complete with expected/desired values (quantitative) and/or definitions and descriptions (qualitative).

Table 9. Performance Criteria for this Demonstration

Performance Criteria	Expected Performance Metric (Pre-demo)	Performance Confirmation Method	Actual Performance (Post-demo)
Primary Criteria (Performance Objectives) – Quantitative			
System Performance	Detection threshold (sensitivity) Anomaly positional accuracy	Comparison to prior collected ground-based geophysical data	SNR assessments show similar performance (e.g. Table 10)
Primary Criteria (Performance Objectives) – Qualitative			
Process Waste	None	Observations	None
Factors Affecting Technology Performance	Helicopter geophysical noise GPS satellite constellations Cultural artifacts	Comparison to expected noise levels based on prior geophysical measurements around the helicopter Record constellation changes and use during positioning accuracy determination Compare fence line and post anomalies at Bombing Target 1 against previous survey results	Noise similar to previous surveys Recorded ORAGS-TEM shows two peaks at fence, where magnetic data have one peak
Reliability	False positives – less than or equal to 6%	Comparison to prior collected ground-based data and excavations (as needed)	No estimate of false positives[2]

2 Validation, i.e. assessment of ordnance detection and false positives, could not be done because no post-survey excavation was conducted.

Secondary Criteria (Performance Objectives) – Quantitative			
Hazardous Materials	None expected, other than spotting charges in M-38 practice ordnance	Observations and documentation during excavations	No hazardous materials encountered
Secondary Criteria (Performance Objectives) – Qualitative			
Reliability	No system or component failures	Observations and documentation	Some transmitter overheating if current too high.
Ease of Use	Pilot "comfort" when flying with the system installed No ballast required	Observations and documentation Observations and documentation	The pilot reported no issues with maneuverability, and similar positive performance when compared to the ORAGS-Arrowhead magnetic system. No ballast required.
Safety	Conformance with all FAA requirements and requirements as documented in the Mission Plan	Observations and documentation	System met all FAA requirements
Versatility	Cultural feature detection and mapping	Comparison of anomaly count, strength, and position to previously collected data at Bombing Target 1 regarding barbwire fence crossing the middle of the targets	Cultural features clearly distinguished from ordnance

Maintenance	System mount points, hardware, and component inspection	Observations and documentation	Minimal wear and tear
Scale-up Constraints	None	Observations and documentation	Test site data provide guidance on positioning and spacing of additional receiving coils.

4.2 Performance Confirmation Methods

Estimation of two of the system performance criteria was to be based on comparisons of system performance at the BBR Test Site and qualitative analysis of data acquired at Bombing Target 1. Validation, i.e. assessment of ordnance detection and false positives, could not be done because no post-survey excavation was conducted.

4.3 Data Analysis, Interpretation, and Evaluation

The ORAGS-TEM data does not in itself distinguish the numerous features mapped as UXO or ferrous scrap without interpretation. The analytic signal maps provided in this report depict bombing targets (areas of high ordnance density), infrastructure (larger items or areas of ferrous debris associated with human activity), and potential UXO items (discrete sources). Those responses, interpreted as potential UXO, will likely also include smaller pieces of ferrous debris.

A Test Site or Calibration Grid was established to verify the system response to expected UXO items under local geologic conditions. Before and after seeding target items in 1999 (other than the iron stakes), the area was surveyed with a Geometrics G858 magnetic gradiometer and real-time DGPS navigation system. Before testing in 2000, areas north and east of the original test site were magnetically surveyed, then seeded with additional ordnance items. After seeding, it was surveyed with the G858 magnetometer and an EM61 ground-based electromagnetic system.

The pre-seeding results showed occasional anomalies associated with ferrous objects or magnetic soils. Every attempt was made to place targets at a sufficient distance from these anomalies to create a distinct anomaly. The list of seeded items (including iron stakes) is presented in Table 7.

4.3.1 Results from BBR Test Site

4.3.1.1 Comparison of Gridded Data at the BBR Test Site

Figures 17 through 28 show maps derived from data acquired during the 2002 test and previous tests at the BBR test site. With the exception of the 3 m altitude result in Figure 28, and ground-based measurements in Figures 19 and 22, all data were acquired at a nominal altitude of 1.0-1.5 m AGL at an average air speed of 12 m/s. These are lower speeds than commonly used in airborne magnetometer surveys, and are required in order to maintain adequate positional control for the two-receiver system. A TEM system with more channels could be flown at velocities approximately equal to those of the magnetometer system. The results from previous tests are provided to allow comparison of the new prototypes with ground-based EM61 data, the earlier ORAGS-EMP airborne prototype, ground-based magnetometer data, and ORAGS-Hammerhead airborne magnetometer data. Table 7 is keyed to the columns and rows of the test site, using the notation shown in Figures 17 through 28. Two receiving channels were available for the current system, and these were generally placed on one side of the aircraft, leaving the other side with ballast to maintain aircraft stability. Two base frequencies were selected for these tests, 90 Hz and 270 Hz. The 90 Hz base frequency allowed more of the decay to be recorded, thus opening the door for advanced processing aimed at discrimination. The 270 Hz base frequency had slightly better SNR over most targets because of more signal stacking. The ORAGS-TEM results are for 270 Hz base frequency except where noted (Figure 24). The entire rectangle was used as a transmitter for most tests, except for one test series when a lobed transmitter was tested.

In general terms, the "swath" of an EM sensor may be defined as the zone at the ground surface that is illuminated by the transmitter and scanned by its multiple-receiver array. In the context of the two-channel ORAGS-TEM prototype and for the purposes of this report, the term "footprint" will be used as an abbreviation for the "receiver footprint," defined as the diameter of the region on the ground beneath the receiving coil within which a typical target can be detected. It is assumed that the transmitted field is approximately uniform on the ground in the vicinity of the receivers, which is valid when the vertical distance between the ground surface and the transmitter plane is less than the smallest horizontal dimension of the transmitter.

At low altitudes, the small coils have a footprint of about 1.5 m. For flights at ~1 m laser altitude at the BBR test site, small coil data were acquired along three lines at 1m nominal separation for each row of targets. Additional lines were flown midway between each row of targets. Full coverage was not practical with a single small receiving coil, but will be appropriate for a final production system, which will have more receiving coils.

Figure 17 shows data acquired at the test site with the small vibration-isolated coil configuration, IS-Rect-270 (Table 8). The small receiving coils were placed above and below the boom tubes to allow direct comparison of vertical component and "vertical gradient" results. Only the response from the first time sample ending at 93 μs is plotted in Figure 17.

Figure 18 shows data acquired at the test site with the large loop configuration, L-Rect-270. This configuration had single wire loops affixed to the top and bottom of the 3 m X 3 m outer

segment of the boom tubes. At low altitudes, the large loop receiving coils average the response over a larger area of the ground surface than do the small receiving coils, so full coverage of the test site can be accomplished with a larger line spacing. As with Figure 17, only the response from the first time sample ending at 93 μs is shown here.

Figures 19 through 23 show results from previous magnetic and electromagnetic surveys of the BBR test site for comparison with Figures 17 and 18. Figure 19 shows results from a ground-based EM61 survey of the site. Figures 20 and 21 show results from the first prototype survey that was conducted at the test site in September 2000 with the ORAGS-EMP (EM-61AB sensor) system. Figures 22 and 23 show ground-based and airborne magnetic surveys of the site for comparison with the magnetic data.

Figure 24 shows the result for a 90 Hz base frequency, configuration S-Rect-90, while Figure 25 shows the vertical gradient small coil, configuration IS-Rect-270-Diff. In Figures 26 and 27, we show results for symmetric and anti-symmetric lobed configurations, L-Slob-270 and L-Alob-270. The effect of altitude is demonstrated in Figure 28, which shows the system response at a nominal 3m survey altitude with a small coil configuration, L-Rect-270.

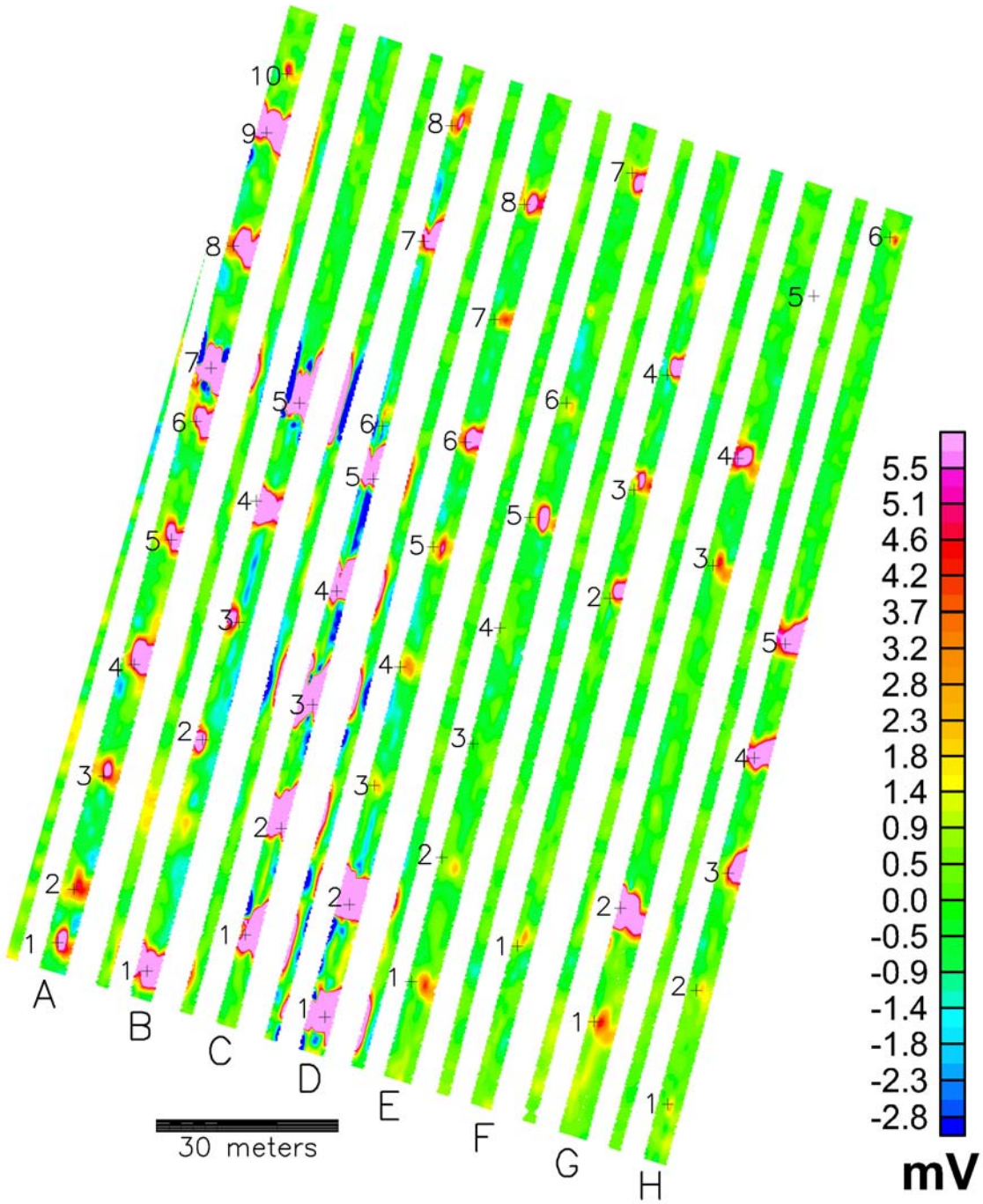

Figure 17. ORAGS-TEM results from BBR Test Grid, vibration-isolated lower small loop receiver, configuration IS-Rect-270. Data acquired at 270 Hz base frequency and 1.0-1.5 m altitude.

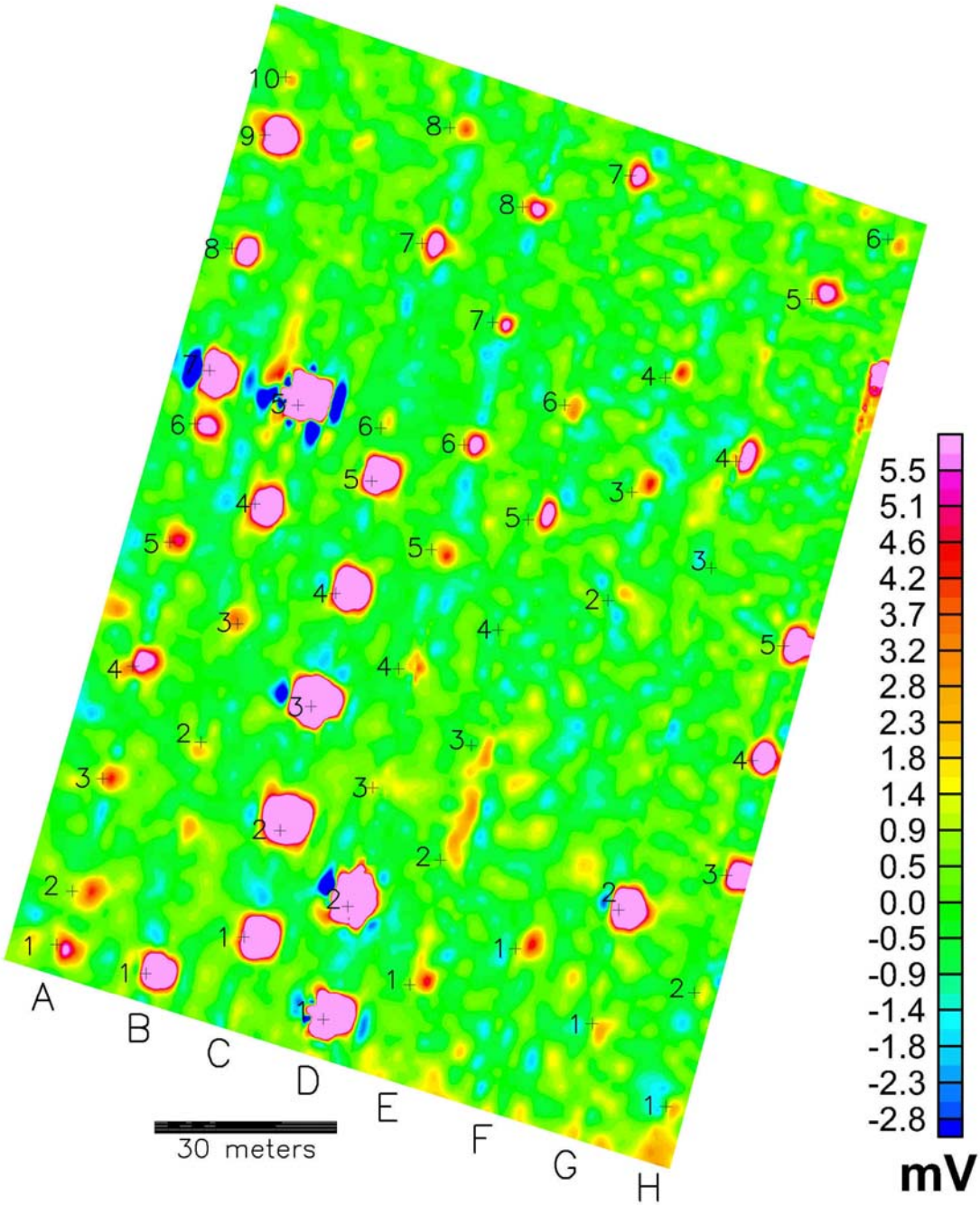

Figure 18. Results from ORAGS-TEM, BBR Test Grid, lower large loop receiver. Data acquired at 270 Hz base frequency and 1.0-1.5 m altitude with configuration L-Rect-270.

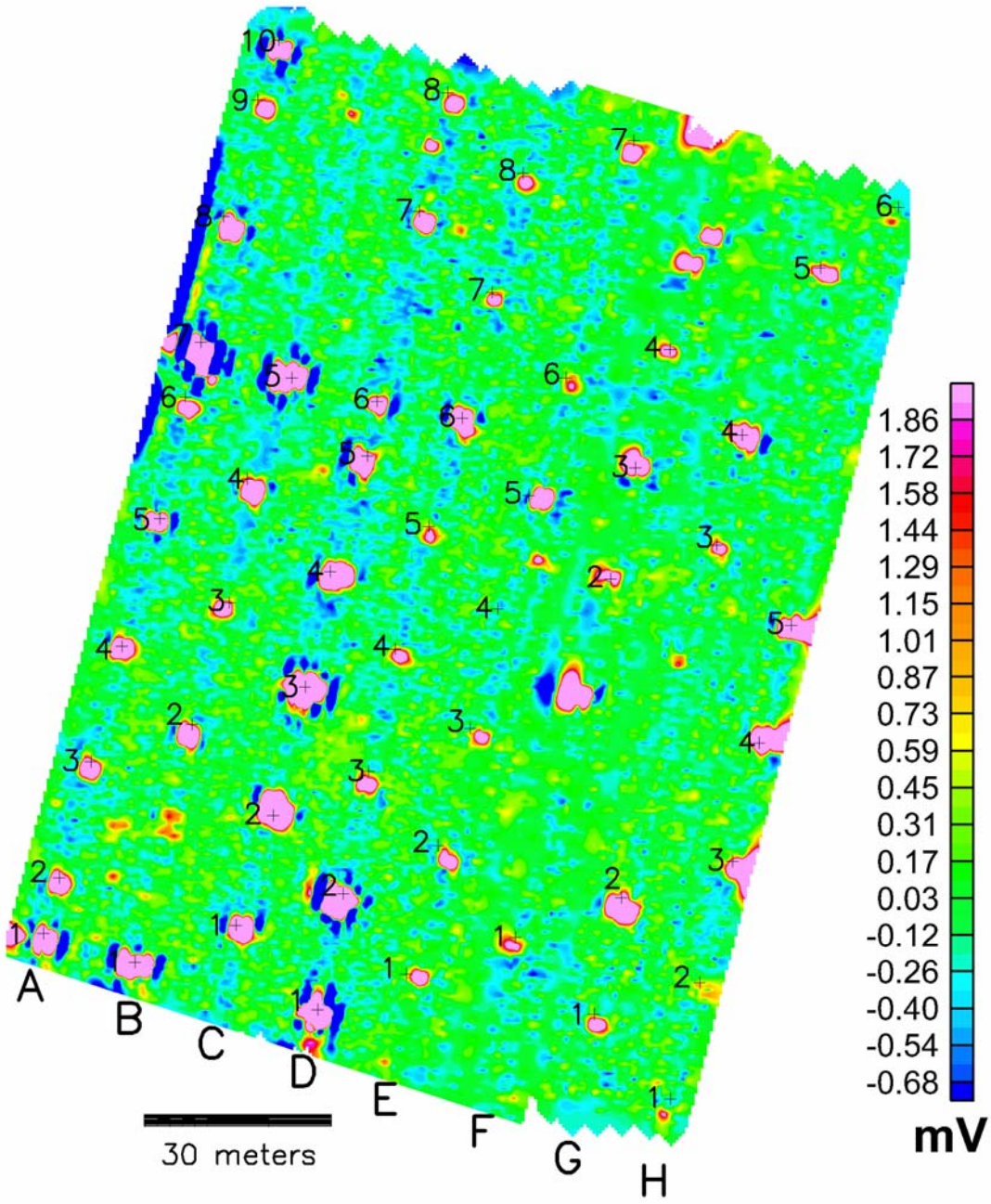

Figure 19. Results from ground-based EM61, bottom coil, BBR Test Grid, for comparison with airborne results.

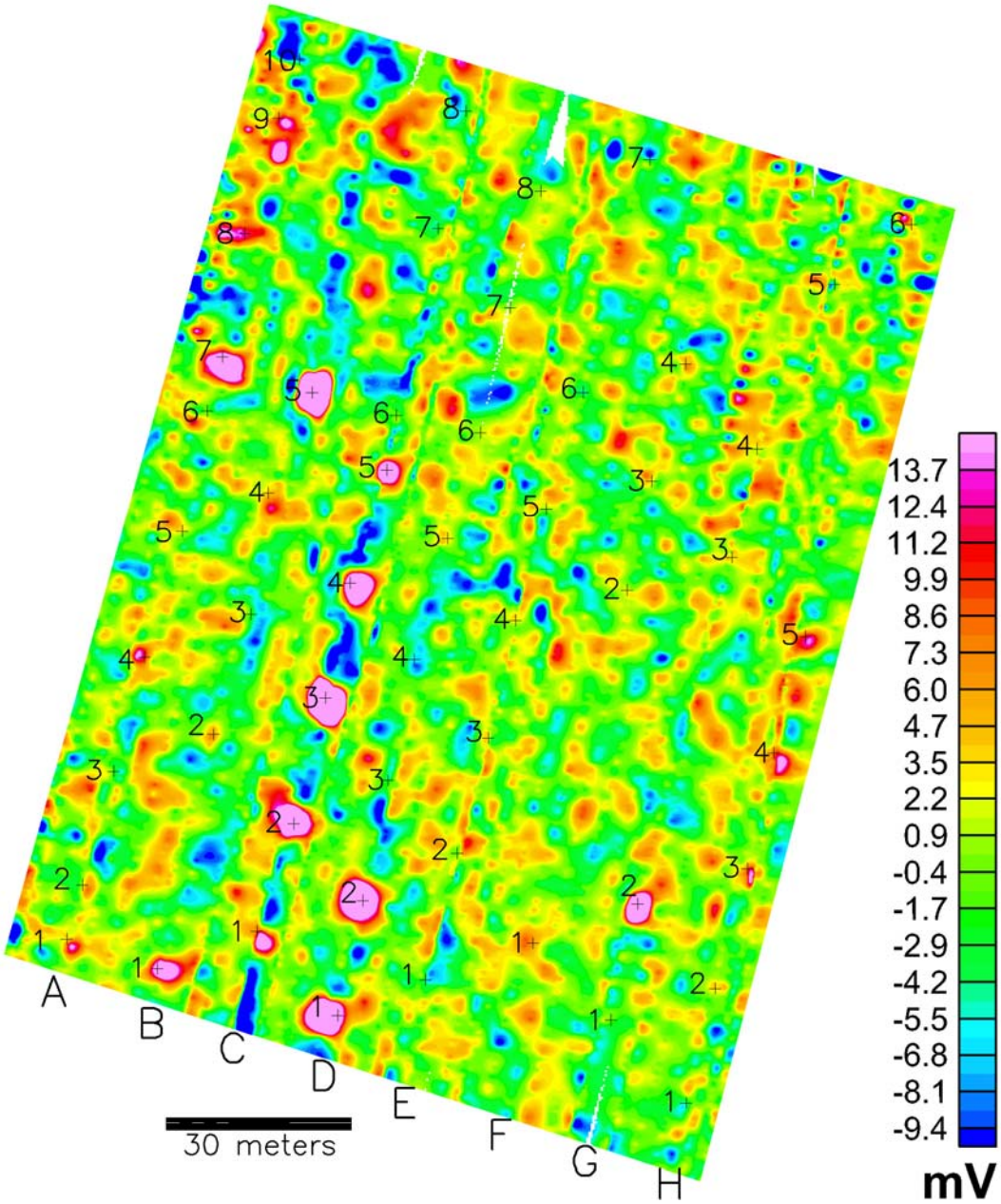

Figure 20. Results from EM-61AB-based airborne proof-of-concept system, BBR Test Grid, outer coil receiver.

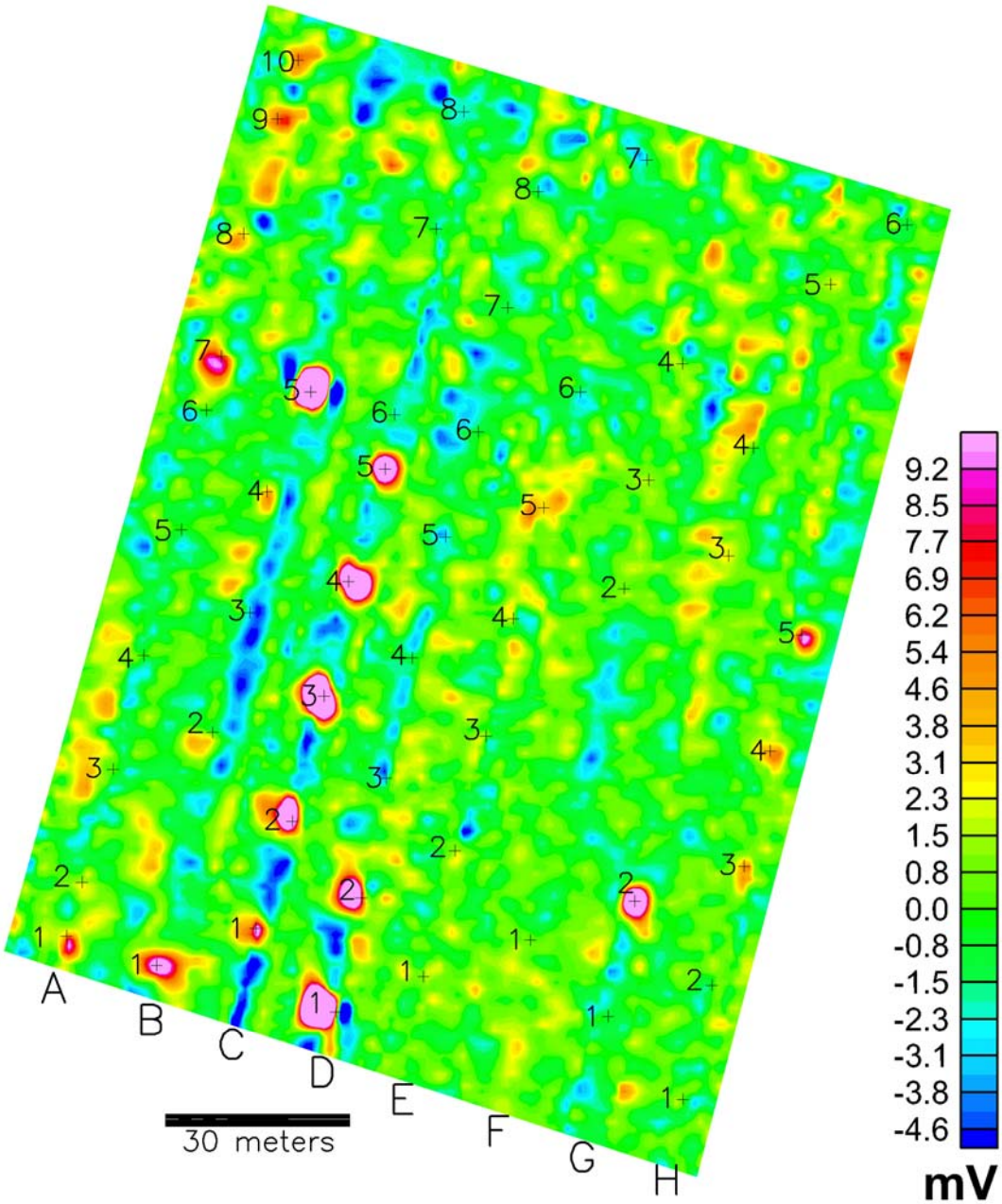

Figure 21. Results from EM-61AB-based airborne proof-of-concept system, BBR Test Grid, horizontal difference (outer coil minus scaled inner coil).

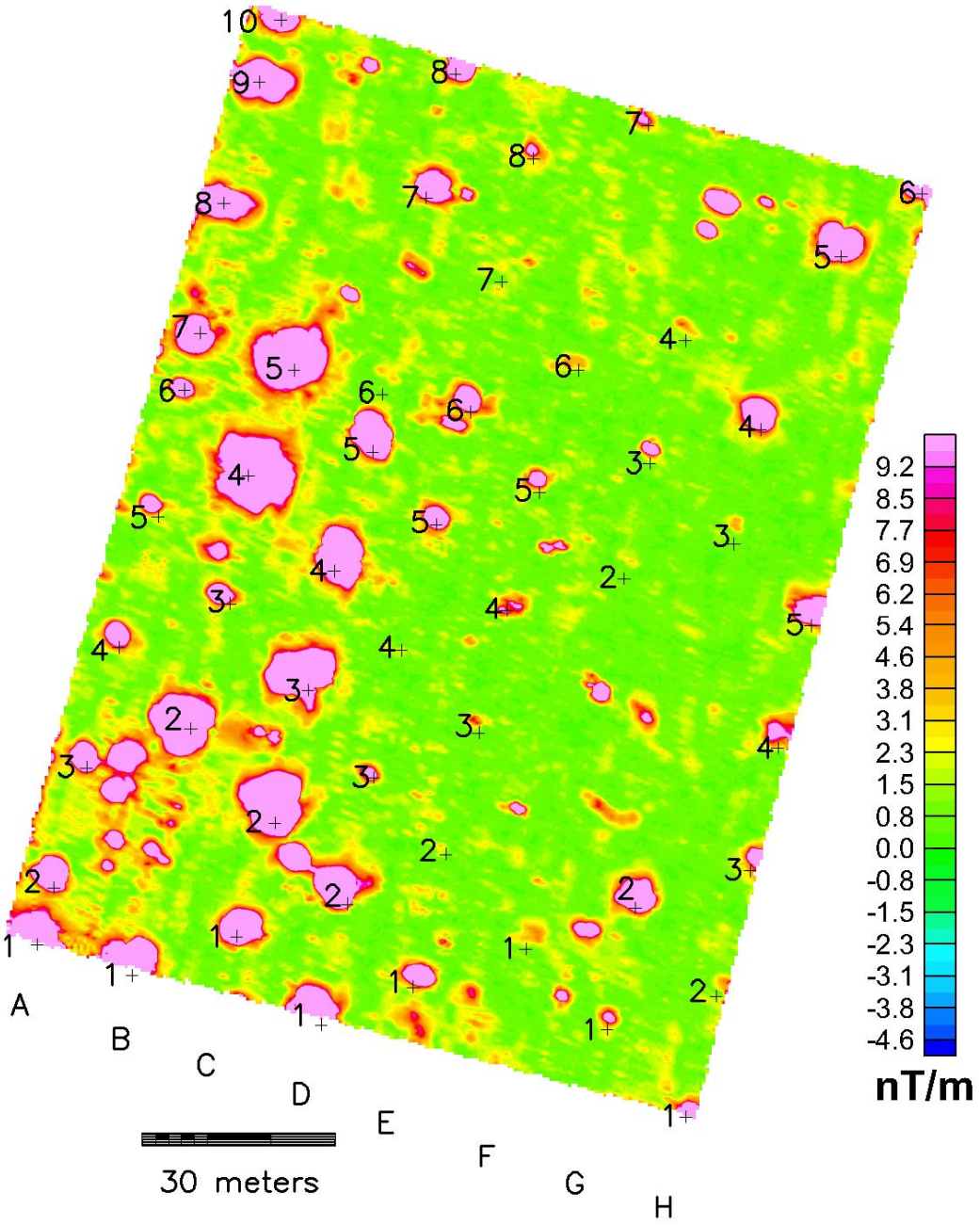

Figure 22. Analytic signal derived from ground-based magnetometer bottom sensor (G858), BBR Test Grid.

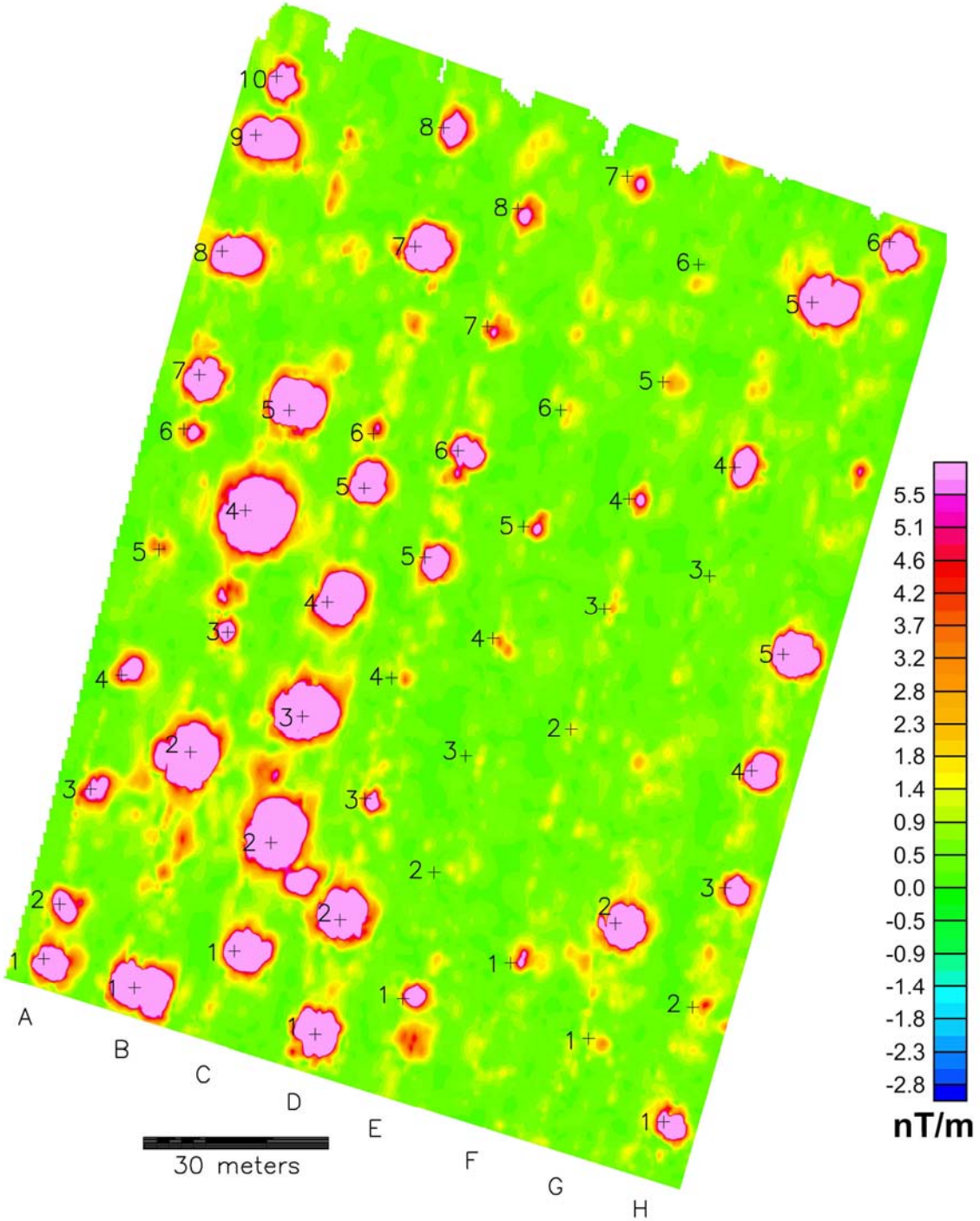

Figure 23. Analytic signal map derived from airborne (ORAGS-Arrowhead) magnetic data, BBR Test Site, September 2002, for comparison with EM results.

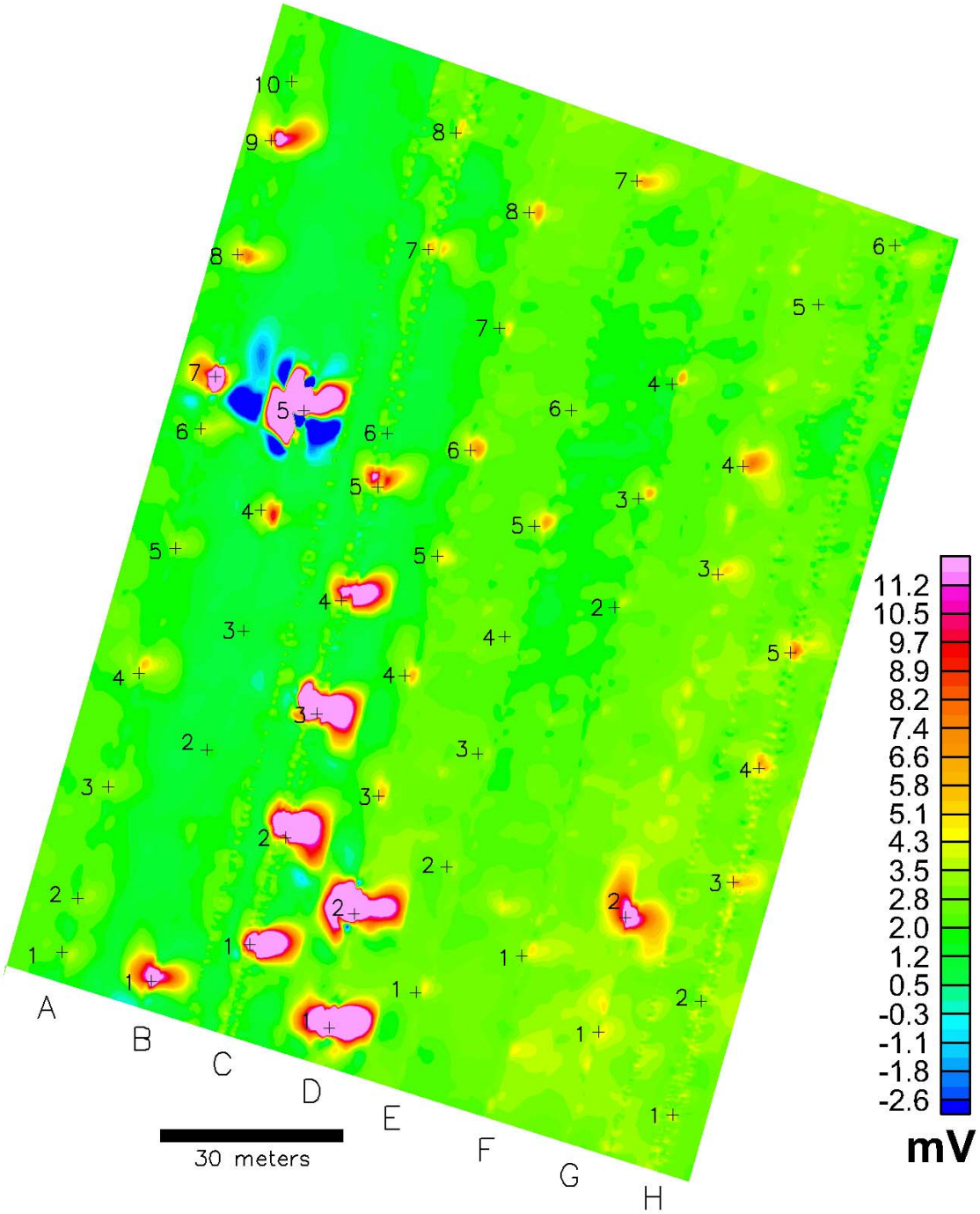

Figure 24. ORAGS-TEM results for 90 Hz base frequency small coil data, BBR Test Site. Data acquired at 1.0-1.5 m altitude.

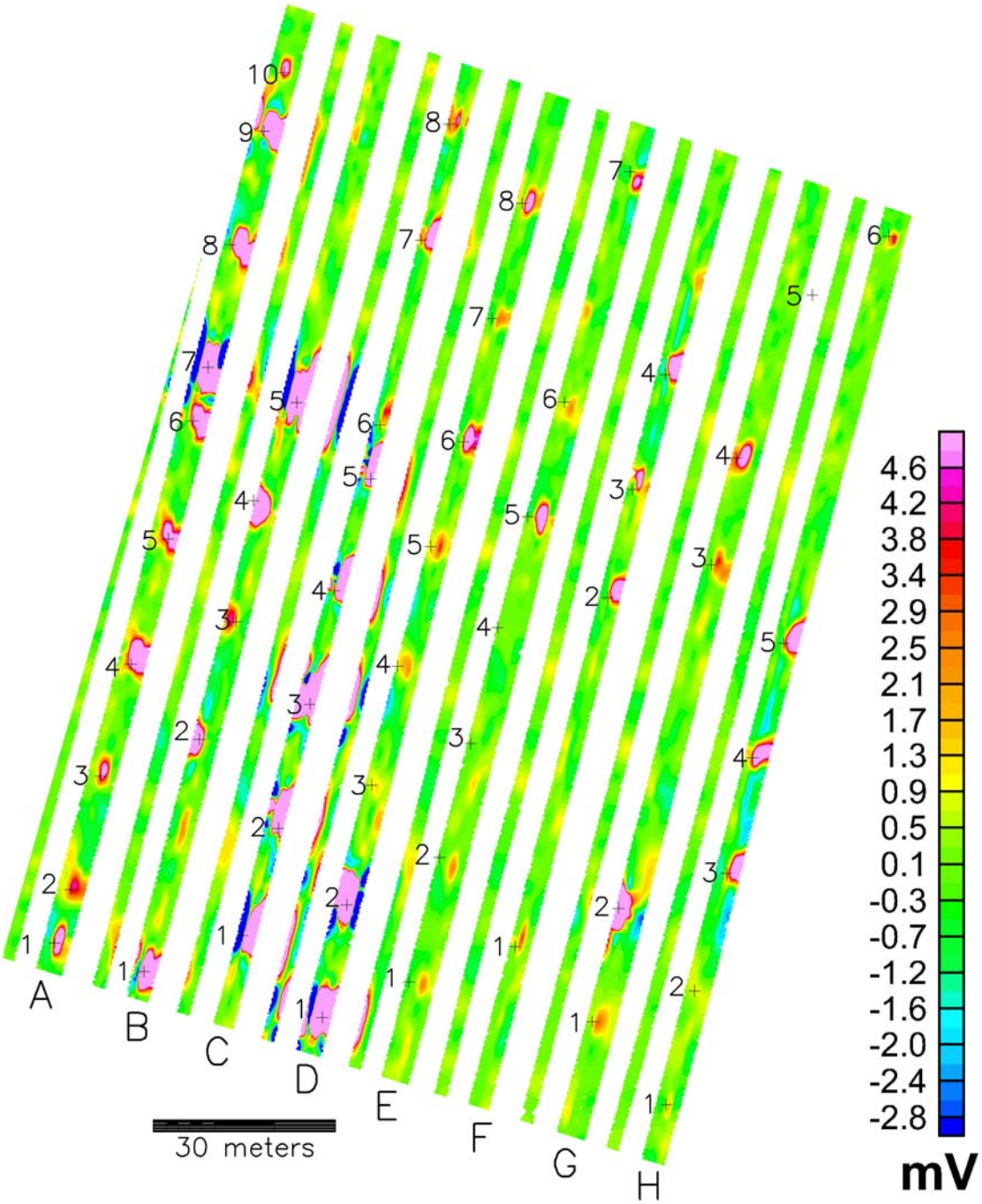

Figure 25. Results for ORAGS-TEM small coil vertical gradient configuration, BBR Test Site. Data acquired at 270 Hz base frequency and 1.0-1.5 m altitude.

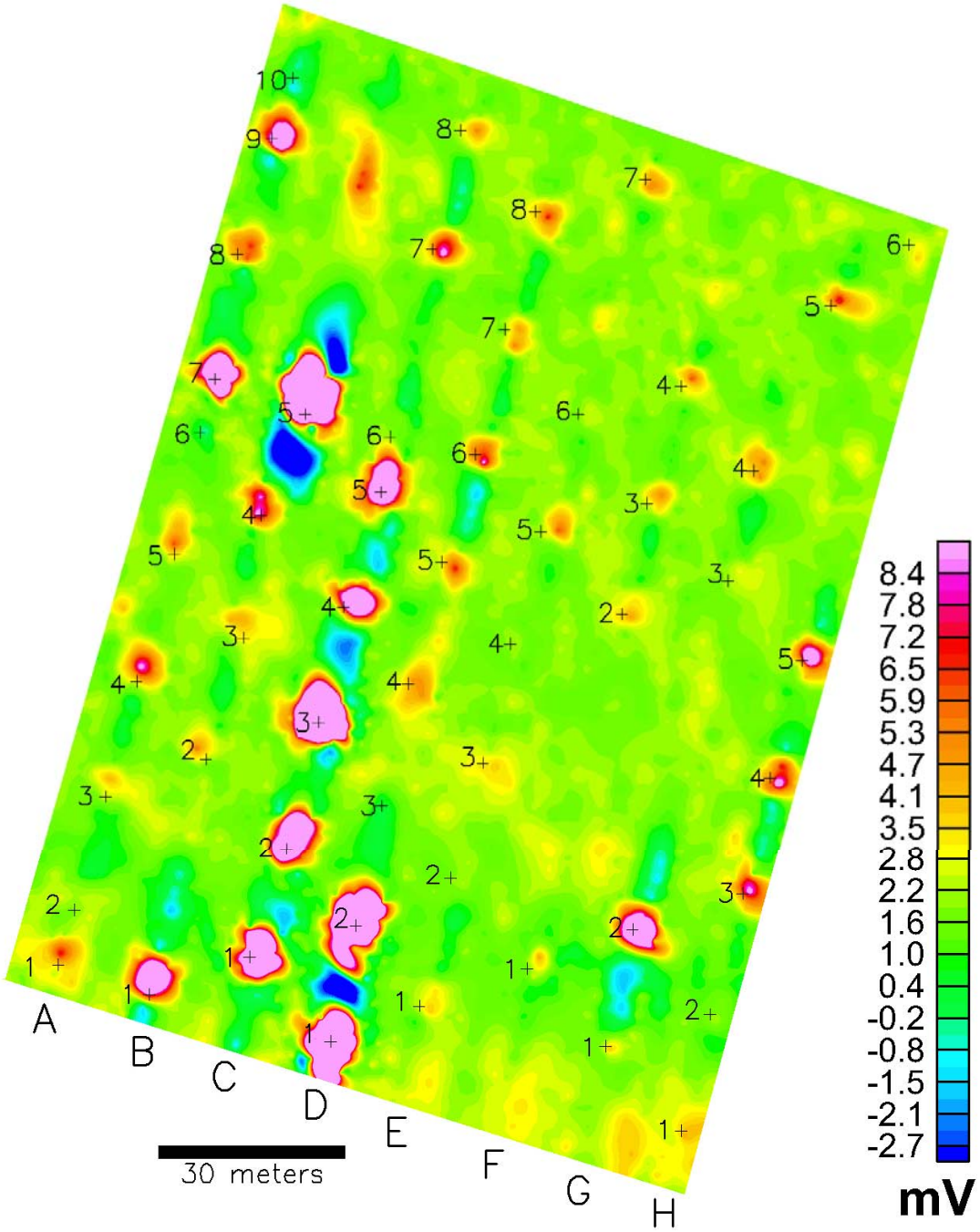

Figure 26. Results for ORAGS-TEM, lobed symmetric transmitter configuration, large loop receivers, BBR Test Site. Data acquired at 270 Hz base frequency and 1.0-1.5 m altitude.

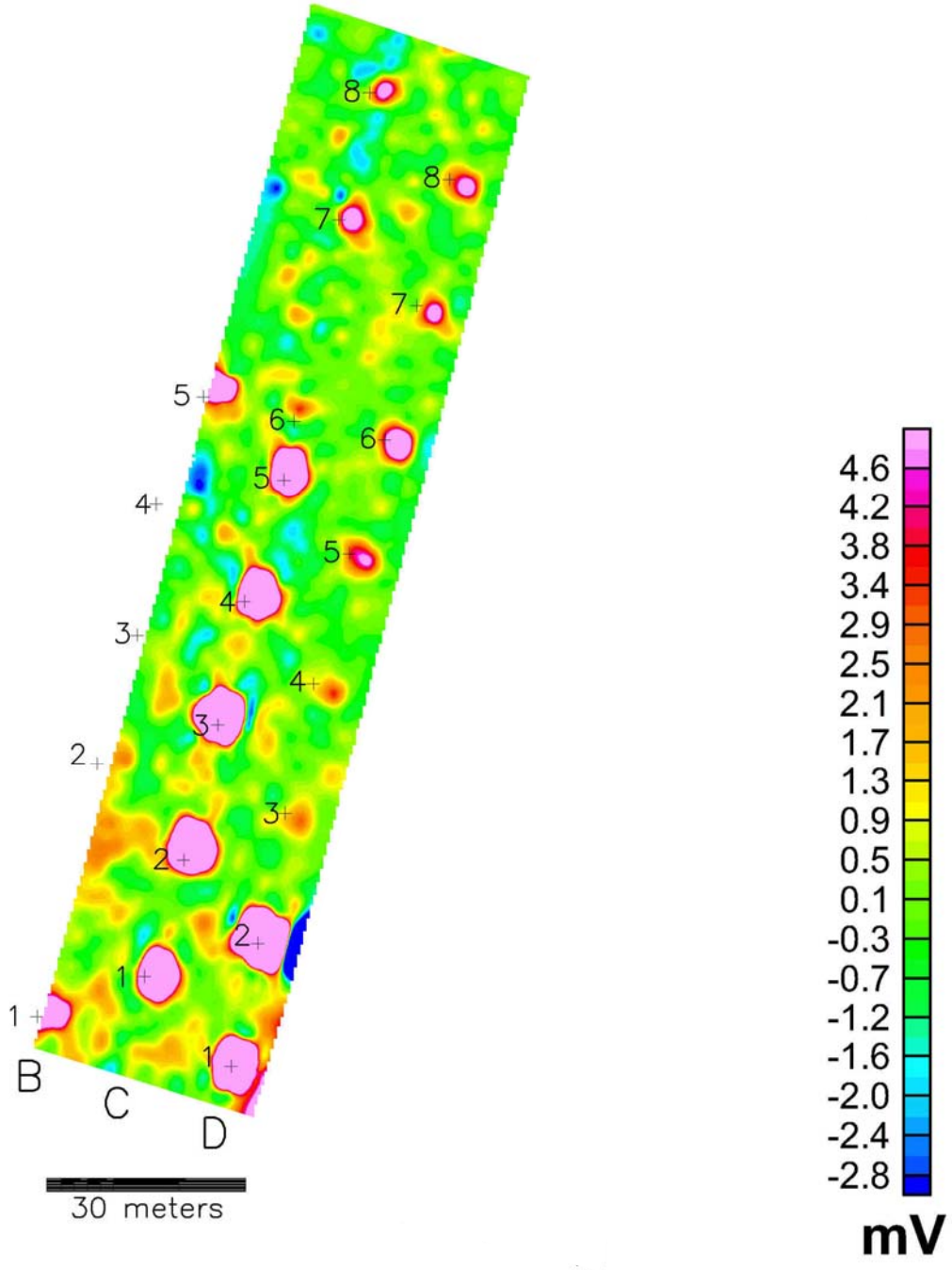

Figure 27. Results for anti-symmetric lobed transmitter configuration with large loop receivers, BBR Test Site. Data acquired at 270 Hz base frequency and 1.0-1.5 m altitude.

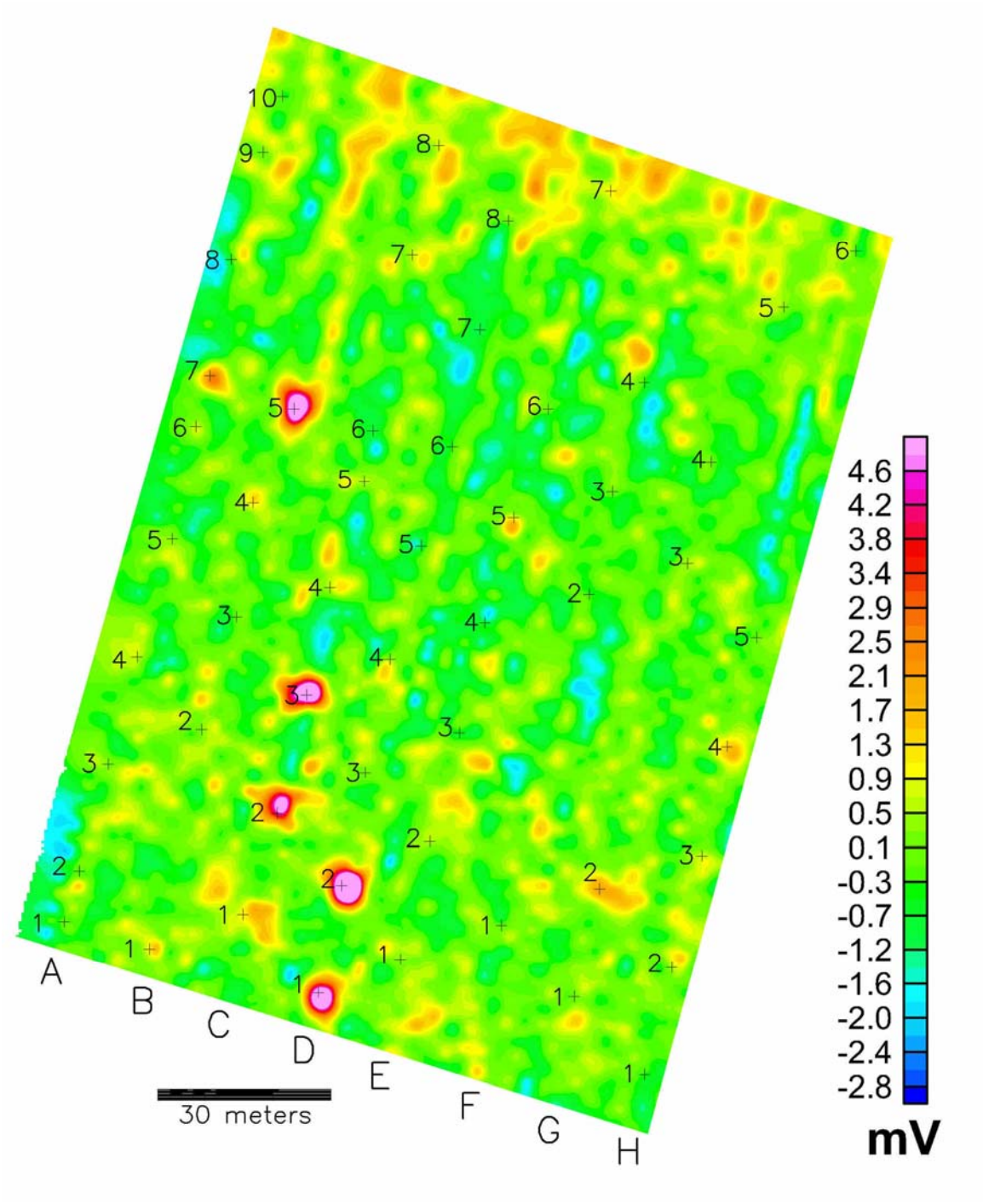

Figure 28. Results for large loop receiver, 270 Hz base frequency, and standard rectangular transmitter at 3 m nominal altitude.

4.3.1.2 Signal/Noise Comparison to Other Systems from BBR Test Site Data

Figure 29 shows a composite of profiles acquired along Line C of the BBR Test Site. A signal-to-noise (SNR) assessment was done to compare the performance of the different system configurations that were tested. Background noise was quantified by the first standard deviation from filtered, leveled measurements of the first time gate in an area where no UXO were buried, and the UXO signal was taken as the anomaly peak minus the background for the first time gate. SNR results are tabulated in Table 10. The SNRs are not corrected to a constant target-to-receiver vertical offset, nor was an effort made to find the best SNR for a given target (typically achieved when the receiver passes directly over the target). A line was identified that passed over or near each of the items buried in Line C, and the SNR was computed for the response to each of the eight targets along the line. The SNRs shown in Table 10 should be considered as typical, in contrast to the best case SNRs, in the form of amplitude factors, given in Table 11. Table 11 shows that the IS-Rect-270 (small isolation-mounted receivers, with the large rectangular transmitter at 270 Hz base frequency) had the best overall performance of those configurations tested, for items in Line C. Comparison of Figures 17-27 indicates that this configuration is among the best overall.

The best helicopter EM configuration shows higher SNRs in comparison with the ground EM-61 by a factor of 6.2 times for the M-38 practice bomb and 2.7 for the 250 lb bombs. For smaller UXO, helicopter SNRs were comparable for the best helicopter data (typically the isolated small coil receiver data) and the differential EM-61 responses.

Table 10. Calculated SNR for Items in Line C of the BBR Test Site

Item	C1	C2	C3	C4	C5	C6	C7	C8	Average SNR
Description (following Table 8)	100 lb bomb fragments	250 lb bomb simulant	250 lb bomb simulant	100 lb bomb intact	100 lb bomb fragments	2.75 in rocket nose section	155 mm round	105 mm round	
Ground EM-61 Differential	55	90	406	56	64	10	26	10	89.6
Arrowhead Magnetic System	48	288	500	115	56	4	100	24	141.9
L-Rect-270	91	134	368	109	86	9	20	11	103.5
L-Rect-270-Diff	43	57	193	57	50	2	14	7	52.9
L-Alob-270	52	75	149	55	34	5	7	2	47.4
S-Rect-270	80	98	333	48	42	2	13	4	77.5
S-Rect-270-Diff	46	42	192	19	19	1.5	8	2	41.2
IS-Rect-270	**295**	247	**652**	**219**	**171**	10	33	7	204.3
IS-Rect-270-Diff	**342**	209	472	**231**	94	**11**	26	1	173.3
S-Rect-90	13	31	175	11	10	2	5	2	31.1

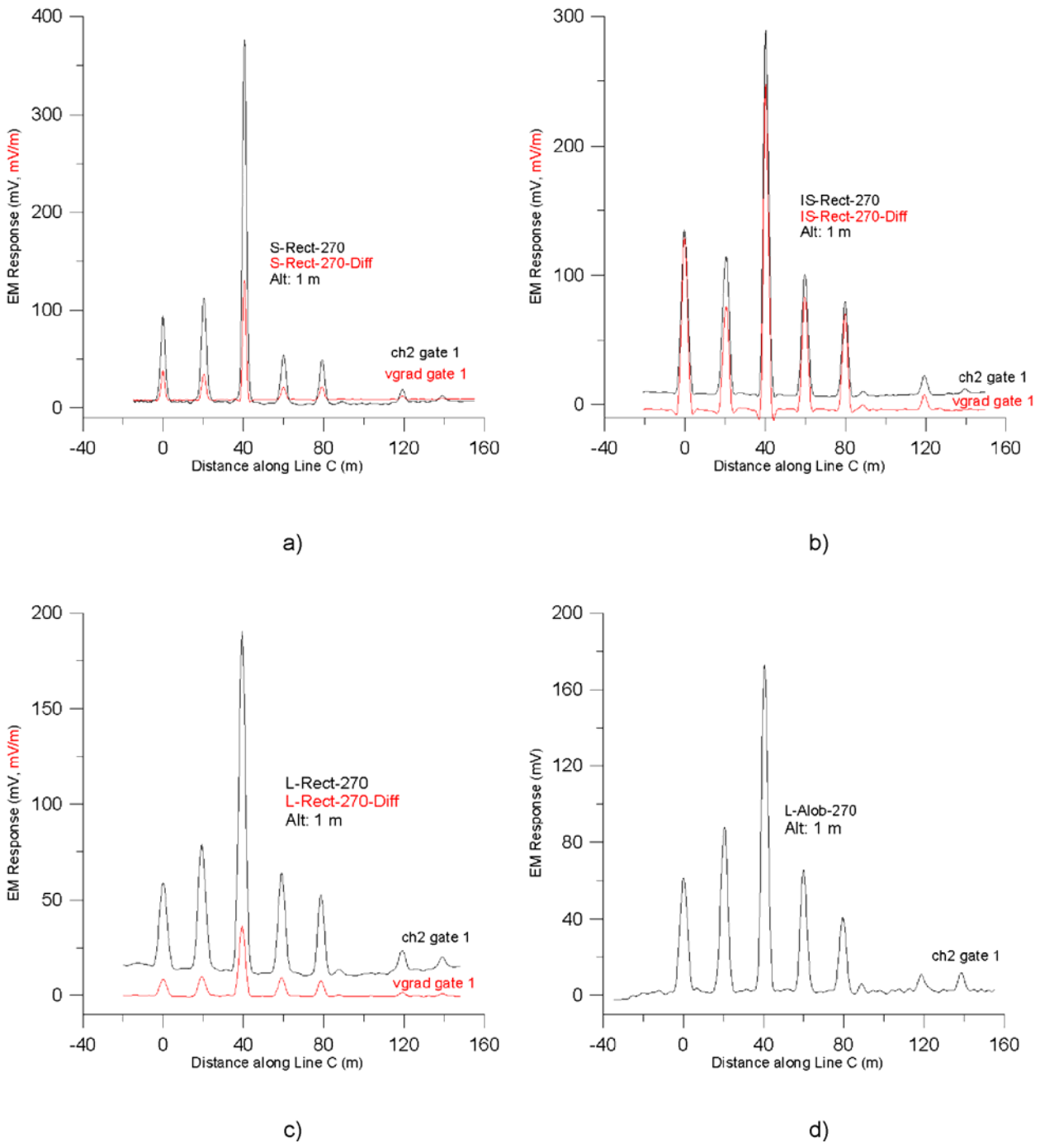

Figure 29. Profiles for selected configurations and acquisition systems over Line C of the BBR Test Grid. a) Configurations S-Rect-270 and S-Rect-270-Diff; b) Configurations IS-Rect-270 and IS-Rect-270-Diff; c) Configurations L-Rect-270 and L-Rect-270-Diff; d) Configuration L-Alob-270. Figure continued on next page.

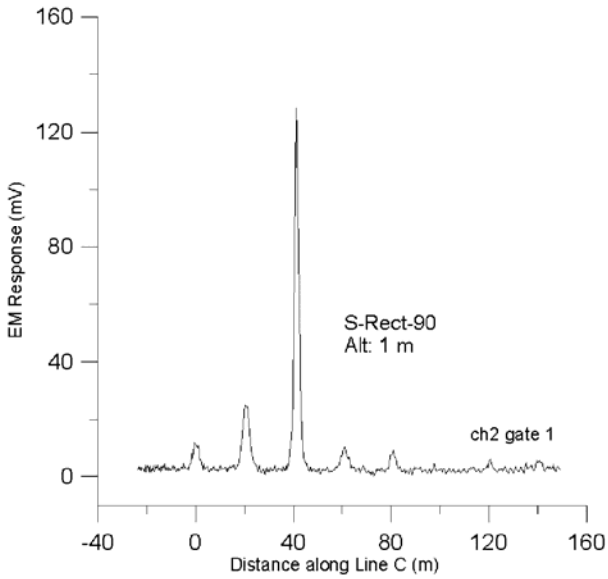

e)

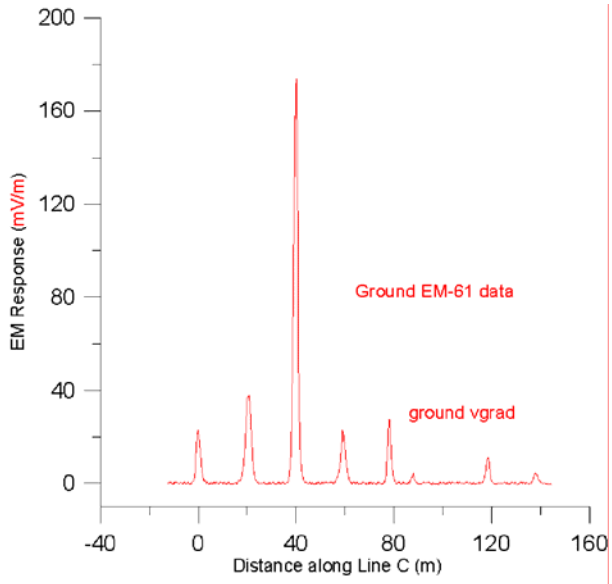

f)

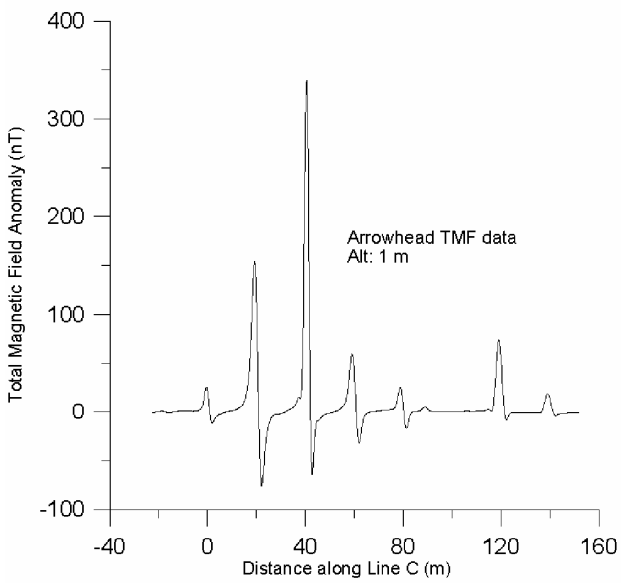

g)

Figure 29 (cont). Profiles for selected configurations and acquisition systems over Line C of the BBR Test Grid. e) Configuration S-Rect-90; f) Ground-based EM-61, top minus bottom coil; g) Total magnetic field data acquired with the ORAGS-Arrowhead system.

4.3.1.3 Altitude and Signal/Noise Assessment for Specific Ordnance Types

4.3.1.3.1 Signal/Noise Ratio Estimation Method

In this section, we describe the methodology used to estimate SNRs as a function of sensor-to-target vertical offset from the BBR test site dataset for various system configurations and EM targets. Data were acquired at sensor heights ranging from 0.5 m to over 3 m, and targets were buried at depths ranging from 0 to 1.3 m.

Data for each EM configuration were baselined by removal of long-wavelength features, which appeared to be geological in origin. The data as recorded comprised "target" anomalies arising from isolated conductors overlaid on a response arising from EM induction in the soil. This "ground response" was strongly altitude-dependent, so that small variations in sensor height generated significant anomalies, particularly at early delay times. These ground responses were strong enough to complicate gridding of the data. Fortunately, the target anomalies and of the ground responses displayed distinct length scales, with the target responses exhibiting sharp, narrow anomalies, in contrast to the long scale length of the ground response anomalies. Preparation of the gridded anomaly maps shown in this paper was therefore preceded by a long-wavelength anomaly suppression procedure for each receiver component and delay time. In the first step of this procedure, anomaly peaks were located within the time series. These anomalies were then removed by interpolating a straight line through the neighborhood of each peak. The interpolated time series was low-pass filtered to yield a smoothed estimate of the long-wavelength features, which was subtracted from the original time series to approximately remove long-wavelength anomalies from the data. This procedure proved highly effective for the Badlands data set.

The filtered data were then divided by the standard deviations of those data, as observed along representative "clean" low-level passes over portions of the test area that did not contain seeded targets, to yield SNR estimates at each sample location for all profiles and for all data bins. Noise levels in the "clean passes" were undoubtedly exaggerated by ground and contaminant response during this procedure, but it was desirable to perform these low-altitude estimates to capture the level of vibrational noise present at these heights. It was observed that low-altitude noise levels were lower by as much as a factor of two at the eastern end of the test grid as compared to the western end, but to keep the SNR estimates conservative, the standard deviations used for SNR estimation were obtained at the noisier western end. The long-wavelength-removal method occasionally underestimates peak response amplitudes when the width of the anomaly above the detection threshold is large enough to "leak" into the smoothed long-wavelength estimate. Also, because the amplitude of the surrounding ground response has been subtracted from the target anomaly's amplitude by this long-wavelength removal procedure, the SNRs of weak anomalies are typically under-reported in areas of more conductive soil. For some coil configurations and (small) target types in this dataset, SNRs computed after application of this tool can be underestimated by a factor of two or more, rendering such SNRs moderately to highly conservative.

Peak SNR values were "picked" from profile plots and correlated with specific targets at known

depths and locations. These peak SNR values were plotted, for each EM configuration and target type, on log-log axes versus sensor-target distance, as shown in Figure 30 for a 250 lb bomb target at 270 Hz base frequency.

"Bounding lines" representing maximal observed values of SNR for a given EM configuration and target type were estimated as power-law relationships of the form $SNR_{peak}=A \times H^B$, where A is an Amplitude Scaling factor and B is an exponent. In most cases, different B values are required for different height ranges to represent the variation in response in those ranges. These bounding lines are indicated in Figure 30 for a 250 lb bomb target, as measured by the system configuration incorporating small receiver coils, isolation-mounted at 4m from the helicopter centerline, with the large 3 m X 12 m transmitter operating at 270 Hz (IS-Rect-270 configuration). The A and B values for each EM configuration, height range and target type are listed in Table 11.

As indicated above, SNR estimates derived in this manner are based on signal amplitudes following long-wavelength removal, this being the critical measure of the sensitivity of the system to isolated conductive targets. The estimated system sensitivity, particularly to small targets, is thus conservative, with SNR estimates being under-reported by as much as a factor of two in some cases.

In Figure 30, the strong SNR values for the 250 lb bomb target type permitted estimation of the SNR variation over a considerable height range. This clearly highlights the break between SNR falloff at heights smaller than or comparable to the smallest transmitter dimension of 3 m (proportional to ht^{-4}) and in the 4-5 m range (proportional to ht^{-6}). In future testing, it would be desirable to obtain SNR estimates at intermediate sensor-target distances as well as at larger distances in order to "fill in" the gap between the two height ranges and extend the observations to the point where SNR approaches unity.

It should be reiterated that the "bounding lines" represent the "best" SNR performance observed for a particular data bin (Bin 1), a given base frequency (270 Hz), and a given combination of target type and system configuration. This "best performance" represents the case where the transmitter-target-receiver coupling is maximized. Descriptors for these 250 lb bomb stimulant data are therefore Exp=-4 with an Amplitude Factor of 15000 at low altitudes, and Exp=-6 with an Amplitude Factor of 90000 at high altitudes. Note that for large-loop receivers (not shown on Figure 30), the exponent was found to be approximately -2 at low altitudes, where the dimensions of both the transmitter and receiver loops are larger than the sensor-to-target height.

The next section describes the variation of SNR vs. height, as estimated using the boundary line method and the Signal/Noise Descriptors defined above, for a variety of targets, system configurations, and base frequencies.

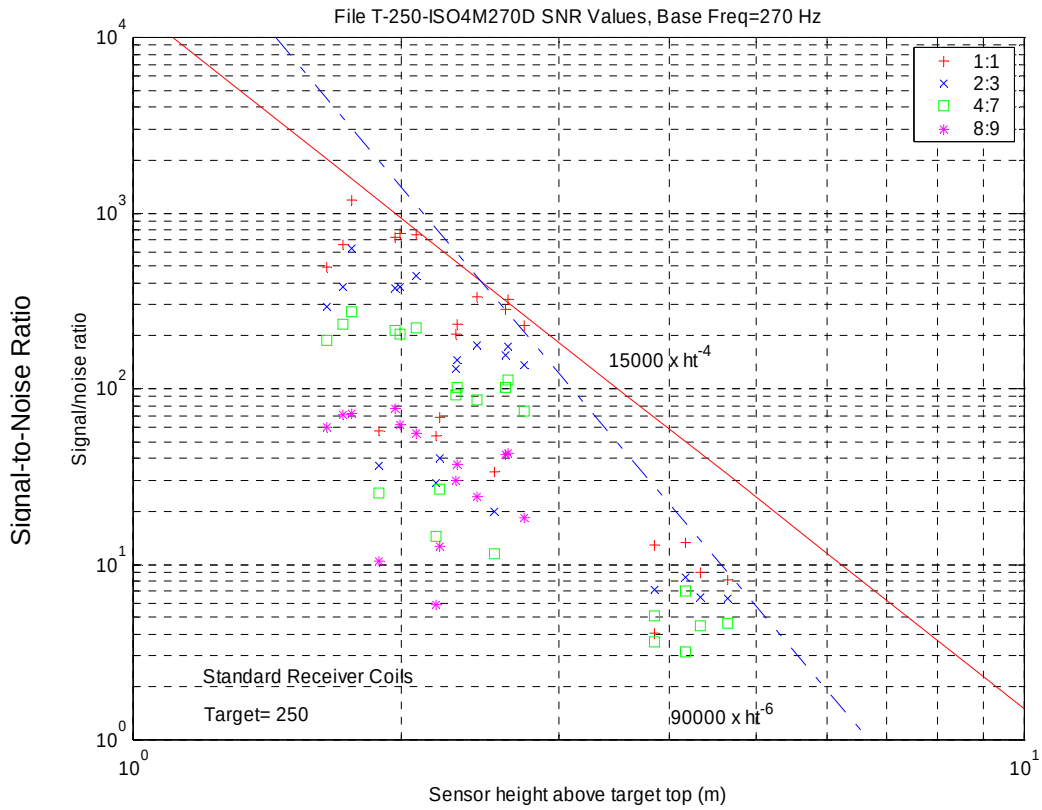

Figure 30. Signal/Noise estimates vs. sensor-to-target height for the 250 lb bombs (inert and simulants) located on the BBR Test Grid during the 2002 field trials for Bin 1 responses of the 270 Hz, isolation-mounted standard receiver coil configuration (IS-Rect-270). The legend lists the EM samples in each bin, starting with Bin 1 (red cross symbol), which comprises samples from 1 to 1 (i.e. only the first sample). Bin 2 comprises samples 2 to 3, and so on. Sample 1 begins at the end of the transmitter ramp and is 93 microseconds long.

Table 11. Signal/Noise Descriptors for Various ORAGS-EM Configurations at BBR02 Test Grid

Configuration ID	**Exp**	**Amplitude factors for specified targets**											
		250	M-38	155	105	2.75	81mm	61mm	60mm	Stove Pipe	Al Sheet	Nail	Al Rod
IS-Rect-90 (low)	-4	10000	5500	550	290	270				600			
IS-Rect-270 (low)	-4	15000	5500	650	420		115	115	70	5000	700	22	
IS-Rect-270 (low)	-4	5000	1250	250	170	110				1500			
S-Rect-90 (low)	-4	5300	1250	270	165								
S-Rect-270 (low)	-4	8500	2750	750	240	190	92	72		1950		44	
IS-Rect-270 (high)	-6	90000	33000										
S-Rect-270 (high)	-6	75000	24000	6000									
IS-Rect-270-Diff (low)	-5	20000	7000	800	530	270	150		35	7000			
S-Rect-270-Diff (low)	-5	16000	3000	750	220	85	160			1000			
L-Rect-90 (high)	-4	3800	980	110	70					650			
L-Rect-270 (high)	-4	5000	1400	250	100	55	55	24	15	1450		5	
L-Rect-270 (low)	-2*	650	320	90	35	30	21	16	11	320		4.5	
L-Rect-270-Diff	-3	1100	320	80	35	44	36			950		14	
L-Rect-270 (high)	-4	4800	1150	210	120	45	55			15	560		
L-Slob-270 (high)	-4	4200	1200	130	95	40	60	18	12	1000			20
L-Slob-270 (low)	-2*	950	300	45	33	25	25	9	10	230			10
L-Alob-270 (high)	-4	8000	2200	350	230	400							
L-Alob-270 (low)	-2*	1420	600	75	53	48		25					

*Power-law falloff exponents of –2 were indicated on inspection of these records when flying at low altitude with large loops. The ratio of loop dimension to target distance is large for these measurements, resulting in a low order falloff

4.3.1.3.2 SNR variation with height

In Table 11, the descriptors for each boundary line (defined in the previous section) are given as the height exponent (column 2) and an amplitude coefficient for each target type (columns 3-14). These descriptors are listed for the transmitter-receiver configurations and base frequencies indicated by the "Configuration ID" shown in column 1 and defined in the previous section. The expression for the boundary line pertaining to a particular target and height range is constructed by extracting the height exponent *E* from column 2 and the amplitude coefficient *A* for the particular target and configuration ID. For a target-to-sensor height of *h*, the boundary line expression is then

$$SNR_{\max} = A \cdot h^{E}$$

For example, for the Iso4m90 configuration, the descriptors are *A*=5500 and *E*=-4, so the bounding line for the M-38 at a target-to-sensor height of 1.5m is described by

$$\begin{aligned} SNR_{\max} &= 5500 \cdot h^{-4} \\ &= 5500 \cdot 1.5^{-4} \\ &= 1086 \end{aligned}$$

This value describes the best SNR expected (usually found in the shortest time bin) for the specified target-to-sensor height, system configuration, and target type.

Table 12 indicates the estimated maximum SNR values for two selected target-to-sensor vertical distances: 1.5 and 4 m. The maximum for a selected vertical distance is identified as the top edge of a cloud of SNR measurements on log-log coordinates. The SNR_{max} estimate of 1086 computed in the example above may be found in the first row and fourth column of this table, corresponding to the M-38 target at 1.5 m below the sensor for the Iso4m90 configuration. The practical detection threshold for profile data should occur for SNR values on the order of 3; below this level, the false positives rate climb rapidly. We shall consider items with SNR larger than 3 to be "detectable". Note that spatial correlation effects in map presentations further reduce the detection threshold for such presentations. If further improvements in system noise are obtained, SNR's will be increased, bringing more targets above the detection threshold for a given EM configuration and height.

The lower height represents the case where the system is flown over near-surface targets, with a sensor to target distance of 1.5 m. Zero values of SNR in this case indicate that values of A and B were not determined for the combination of EM configuration and target type indicated. The upper height of 4 m represents the case where targets are deeply buried or the system altitude is relatively high due to vegetation or other obstructions.

Due to the build-up of uncertainties in the estimation of these SNR values, differences of 10% or less in SNR between different EM configurations for a given target should not be given much weight, but differences of 50% or more are considered to be significant, particularly for large values of SNR. At low altitude/shallow depth, most ordnance targets appear to be detectable. The most sensitive configurations, ranked by SNR values for strong targets at the 1.5 m target-to-sensor height were as follows:

- IS-Rect-270 and IS-Rect-270-Diff, followed by
- S-Rect-270-Diff,
- IS-Rect-90,
- S-Rect-270 and S-Rect-90,
- IS-Rect-270-3m,
- L-Alob-270,
- L-Slob-270,
- L-Rect-270,
- L-Rect-270-Diff

Only the larger ordnance targets, such as 250 lb bombs and M-38s, were typically detectable at the 4m target-sensor vertical distance. The order of sensitivity in this case was different, due to the lower attenuation rate of the LL relative to the small-coil receivers in this height range:

- L-Alob-270,
- IS-Rect-270,
- L-Rect-270,
- L-Rect-270-Dual,
- S-Rect-270,
- L-Slob-270, and
- L-Rect-90

Based on these observations, it appears that the most sensitive configuration for measurements in the 1-3 m sensor-target distance range tested at BBR used vibration-isolated small-coil receivers. The distance between the small-coil array and the helicopter CL was a significant factor-the coils mounted at 3 m from CL were substantially less sensitive than the coils mounted at 4 m from CL. This effect appears to be due to clipping of the earliest time bins by the acquisition system, caused by the increased helicopter anomaly at the 3m position. Later time bins were not affected.

The anti-symmetric lobed transmitter configuration was substantially more sensitive (Table 11) than the best rectangular-transmitter large-loop receiver configuration over the full altitude range, and was also substantially more sensitive than the symmetric lobed transmitter.

Table 12. Signal-to-Noise Estimates for 1.5 and 4 m Sensor-Target Distance

Maximum Target SNR (frac) for Target-Sensor Distance= 1.5 m

Config ID	Exp't	Target ID									
		250	M38	155	105	2.75	81mm	61mm	60mm	Stove Pipe	Nail
IS-Rect-90(low)	-4	1975	1086	109	57	53	0	0.0	0.0	118.5	0.0
IS-Rect-270 (low)	-4	2963	1086	128	83	0	23	22.7	13.8	987.7	4.3
IS-Rect-270-3m (low)	-4	988	247	49	34	22	0	0.0	0.0	296.3	0.0
S-Rect-90 (low)	-4	1047	247	53	33	0	0	0.0	0.0	0.0	0.0
S-Rect-270 (low)	-4	1679	543	148	47	38	18	14.2	0.0	385.2	8.7
L-Rect-270 (low)	-2	289	142	40	16	13	9	7.1	4.9	142.2	2.0
L-Slob-270 (low)	-2	422	133	20	15	11	11	4.0	4.4	102.2	0.0
L-Alob-270 (low)	-2	631	267	33	24	21	0	11.1	0.0	0.0	0.0
IS-Rect-270-Diff	-5	2634	922	105	70	36	20	0.0	4.6	921.8	0.0
S-Rect-270-Diff	-5	2107	395	99	29	11	21	0.0	0.0	131.7	0.0
L-Rect-270-Diff	-3	326	95	24	10	13	11	0.0	0.0	281.5	4.1

Maximum Target SNR (frac) for Target-Sensor Distance= 4 m

Config ID	Exp't	Target ID									
		250	M38	155	105	2.75	81mm	61mm	60mm	Stove Pipe	Nail
IS-Rect-270 (high)	-6	22.0	8.1	0.0	0.0	0.0	0.0	0.0	0.0	0.0	0.0
S-Rect-270 (high)	-6	18.3	5.9	1.5	0.0	0.0	0.0	0.0	0.0	0.0	0.0
L-Rect-90 (high)	-4	14.8	3.8	0.4	0.3	0.0	0.0	0.0	0.0	2.5	0.0
L-Rect-270 (high)	-4	19.5	5.5	1.0	0.4	0.2	0.2	0.1	0.1	5.7	0.0
L-Rect-270-Dual (high)	-4	18.8	4.5	0.8	0.5	0.2	0.2	0.0	0.0	0.1	0.0
L-Slob-270 (high)	-4	16.4	4.7	0.5	0.4	0.2	0.2	0.1	0.0	3.9	0.0
L-Alob-270 (high)	-4	31.3	8.6	1.4	0.9	1.6	0.0	0.0	0.0	0.0	0.0

4.3.1.4 Summary of Data Analysis from BBR Test Site

We make the following summary observations regarding detection and SNR from the test site configuration tests:

1) The large loop and small loop configurations have similar response at the test site. The small loop receiver produced higher SNR than the large loop receiver at target-receiver distances below 2 m. At intermediate target-receiver distances (2-3 m), the performance of the two receiver coil configurations were comparable. For target-receiver distances above 4 m, the large loop receivers appear to be favored. The small loop may be better suited for detecting the smallest targets, whereas the large loops have reduced risk of spatial aliasing, due to their intrinsic spatial averaging, and they are simpler, lighter, and require no special mounting techniques.
2) Performance of the most effective configurations of the ORAGS-TEM system at the 1.0-1.5 m altitude is comparable to the performance of the ORAGS airborne magnetic systems. Comparison of Figures 17 and 18 with the ORAGS-Arrowhead result in Figure 23 indicate that the ORAGS-TEM performed similar to the ORAGS-Arrowhead. This is validated by the SNR assessment summarized in Table 10 for the IS-Rect-270 and L-Rect-270 configurations.
3) The performance of all ORAGS-TEM small loop and large loop configurations is considerably better than the previous ORAGS-EMP (EM-61AB) surveys. Noise levels are much lower, and smaller targets appear above the noise floor. The signal-to-noise ratio (SNR) approaches and occasionally exceeds that of the airborne magnetometer system, and at the lowest altitudes, exceeds the performance of the ground-based EM61 for many targets, as shown in Table 10.
4) Gradients provided somewhat greater sensitivity at low altitudes with the small receiver loops (Figure 25). They produced mixed results with the large receiver coils (not shown here). EM gradient data can be used in conjunction with single loop data as a depth discriminator because gradient response decays faster with burial depth than single loop response. Shallow UXO may give strong gradient and single loop responses whereas more deeply buried objects may appear only on the single loop maps.

The principal SNR results indicate that:

1. At low altitudes, the small coils, when isolation-mounted, yielded almost twice the SNR of the rigidly-mounted small coils, and 4-6 times the SNR of the best large-loop configurations. For the isolated vs. rigid-mounted small-coil comparison, the twofold improvement is entirely due to a decrease in noise. The small coils generate a ~3x stronger but narrower anomaly than do the large loops for targets tracking directly beneath the center of the coil, and the isolation-mounted small coils display ~1.5x lower noise than does the large loop.
2. At relatively high altitude (4 m sensor-target) the best large-loop receiver configuration yielded substantially higher SNR than did any of the small-coil configurations.
3. The anti-symmetric lobed-transmitter, large-loop receiver configuration yielded higher SNR than did the other large-loop receiver configurations.
4. The best vertical difference mode (isolated small-coil array at 4 m from helicopter centerline) was comparable to the best small-loop mode at a sensor-target distance of 1.5 m, but degraded much more rapidly with height than did any of the other configurations.
5. For bombs, the best helicopter SNRs exceeded the SNR from the ground EM-61 system. For smaller ordnance, helicopter SNR was comparable to or lower than ground EM SNR.

The improvement in low-altitude small-coil SNR, compared to the results of earlier shakedown tests, was initially surprising. This improvement is attributed to two factors: the isolation mounting of the small coils and their location at increased distance from the transmitter cable. When the isolation mounts were removed but the small coils were left at 4 m from the helicopter CL, the SNR values at low altitude dropped but remained much higher than the large-loop receiver results. This meshes well with ground test results, which indicated that signal levels from the small coils were higher than those from the large loops, particularly at low altitudes, provided that the small receiver coils tracked within half a meter of the target and that the receiver coils were spatially separated from the transmitter coil. Thus, the strength of the small-coil configuration is that it yields higher signal levels when the coil passes directly over the target, while its weaknesses are that the coils are more vulnerable to noise generation arising from coil vibration and therefore require vibration isolation, and that they must be located away from the transmitter cable.

The strengths of the large-loop receiver configuration are that its footprint is larger and its sensitivity does not drop as rapidly with respect to height as does the small-coil configuration. The 3-4 m target-sensor distance is the approximate crossover range. Thus, if large objects are sought in areas where the sensor coils cannot be flown at ground clearances of less than 2 to 4 m (depending on target depth below surface), the large loop configuration may be preferable unless further improvements are achieved in isolation-mounting of small-coil receivers and a denser array of small-coil receivers is used. Fortunately, it will not be necessary to select one method over the other prior to construction of the final system, due to the ease with which large-loop receivers may be mounted on the booms.

Finally, <u>at the present state of development,</u> vertical difference results are useful for detection of surface objects and discrimination of surface objects from deeper ones, provided that low survey altitudes can be maintained. Maps generated from the difference results did have other

advantages, particularly in cluttered zones where their increased lateral resolution is an asset, so further development of this approach would be desirable to accommodate similar situations. These benefits must be weighed against the operational compromises (reduced number of lateral receiver locations and hence reduced coverage rate, lower survey altitude envelope) associated with vertical gradient measurements during survey planning.

4.3.2 Comparison of Gridded Data at Bombing Target 1

Data were acquired along north-south transects at Bombing Target 1 using the rectangular transmitter with the small coil receivers and the large coil receivers. The data acquired with the large coil system were acquired at 3 m line spacing. The results for two time gates are shown in Figures 31 and 32. For comparison, the result for an equivalent area acquired with the ORAGS Arrowhead magnetometer system is shown in Figure 33. A smaller area was covered with the small coils because the footprint of this system required that a nominal line spacing of 1m be used for the two-channel system that we used. Both channels were used to obtain vertical gradient measurements on the starboard side of the helicopter. The small coil result is shown in Figure 34. In Figure 35, we compare the vertical gradient result with the single coil result for small loop receivers at Bombing Target 1.

Note that neither the large coil nor small coil receivers were operated in their optimal configuration at Bombing Target 1. Based on the SNR comparisons for different receiver, altitude and base frequency configurations listed in Tables 11 and 12, a further factor of between 1.5 and 2 in SNR (depending on height) would have been obtained using the anti-symmetric large loop transmitter, and slightly smaller improvements would be expected for the small loop receiving coil when fitted with vibration isolators. The expected improvement is mainly due to the increased sensitivity of the anti-symmetric large-loop configuration and the isolated small-coil receivers compared to the configurations used at Bombing Target 1.

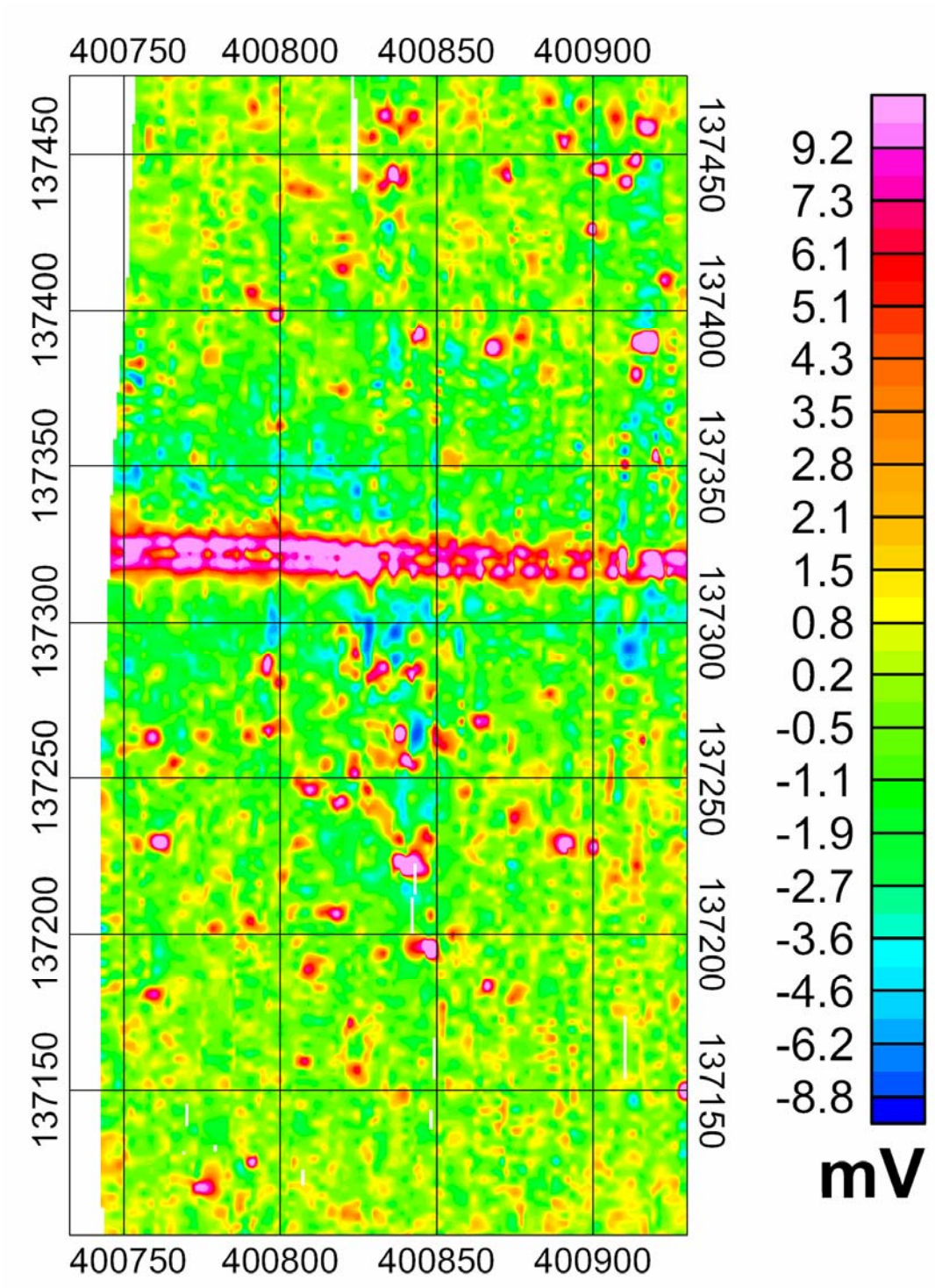

Figure 31. ORAGS-TEM results for Bombing Target 1 – large loop, time gate 1 (ending at 93 μs). Coordinates are UTM Zone 13 N, NAD83 meters.

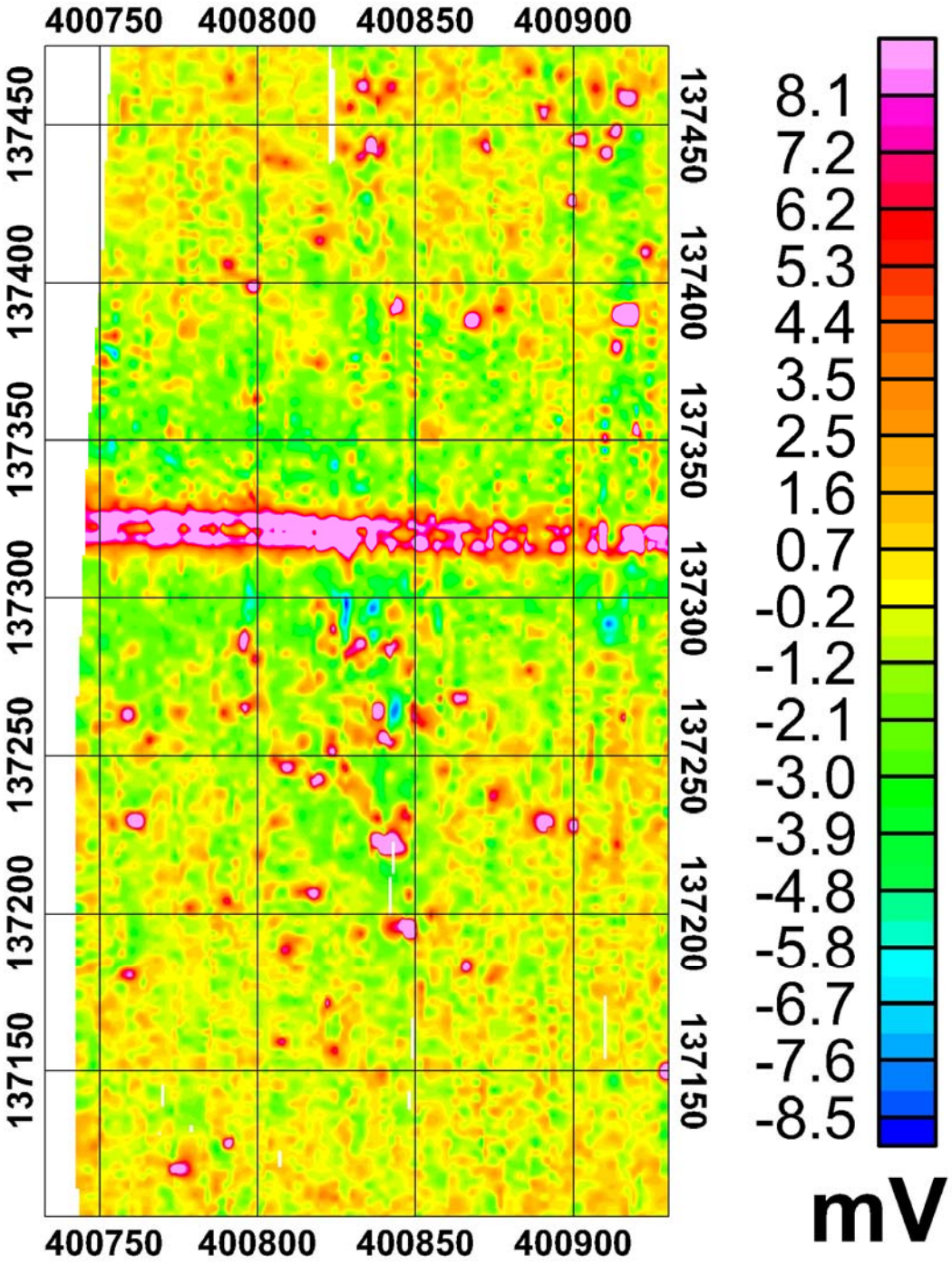

Figure 32. Results from Bombing Target 1 for the ORAGS-TEM system, large loop receiver, time gate 2 (93-186 μs). Coordinates are UTM Zone 13 N, NAD83 meters.

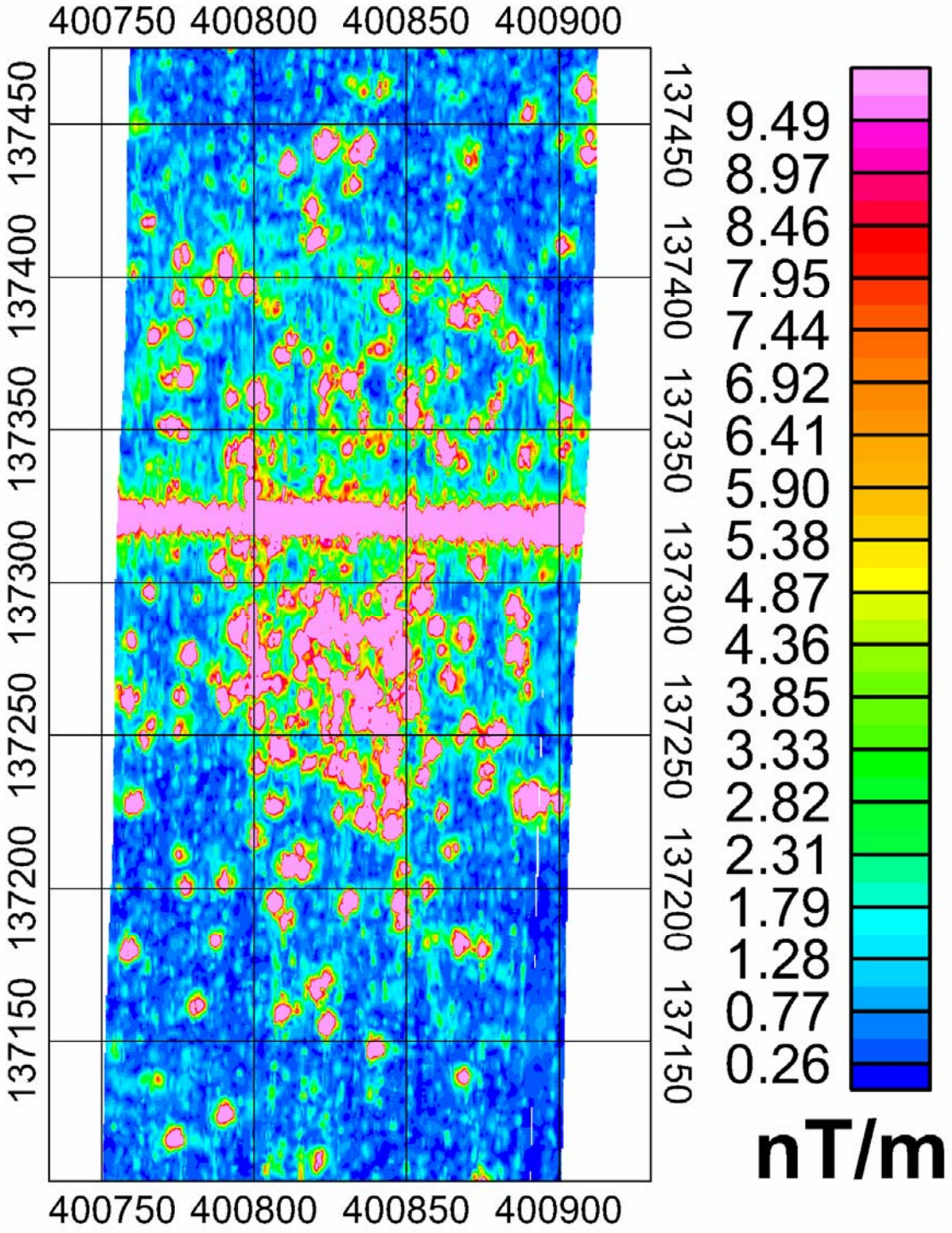

Figure 33. Analytic signal map of Bombing Target 1, derived from ORAGS-Arrowhead airborne magnetic data. Coordinates are UTM Zone 13 N, NAD83 meters.

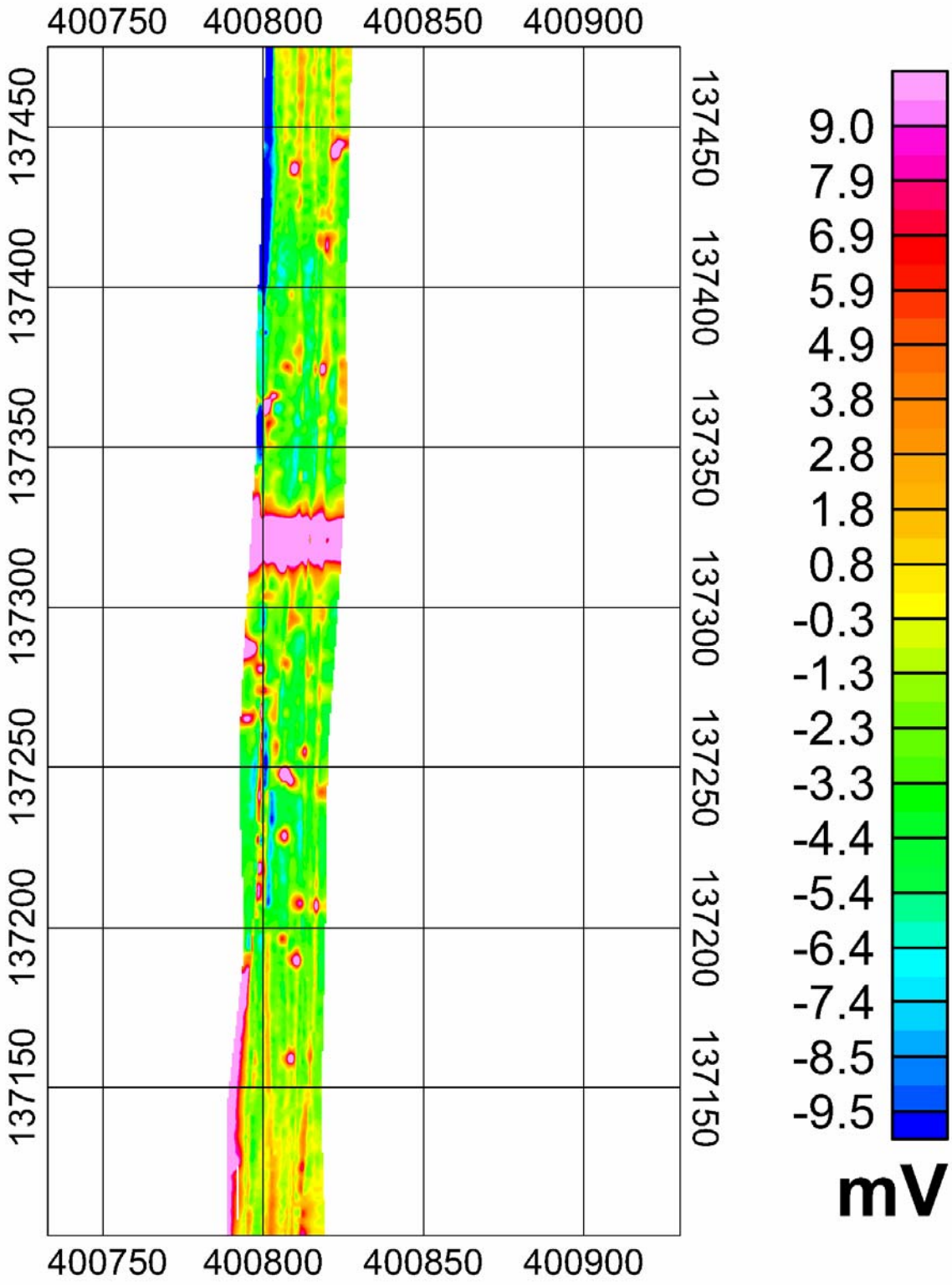

Figure 34. ORAGS-TEM results for BBR Bombing Target 1 small coil receiver, first time gate. Coordinates are UTM Zone 13 N, NAD83 meters.

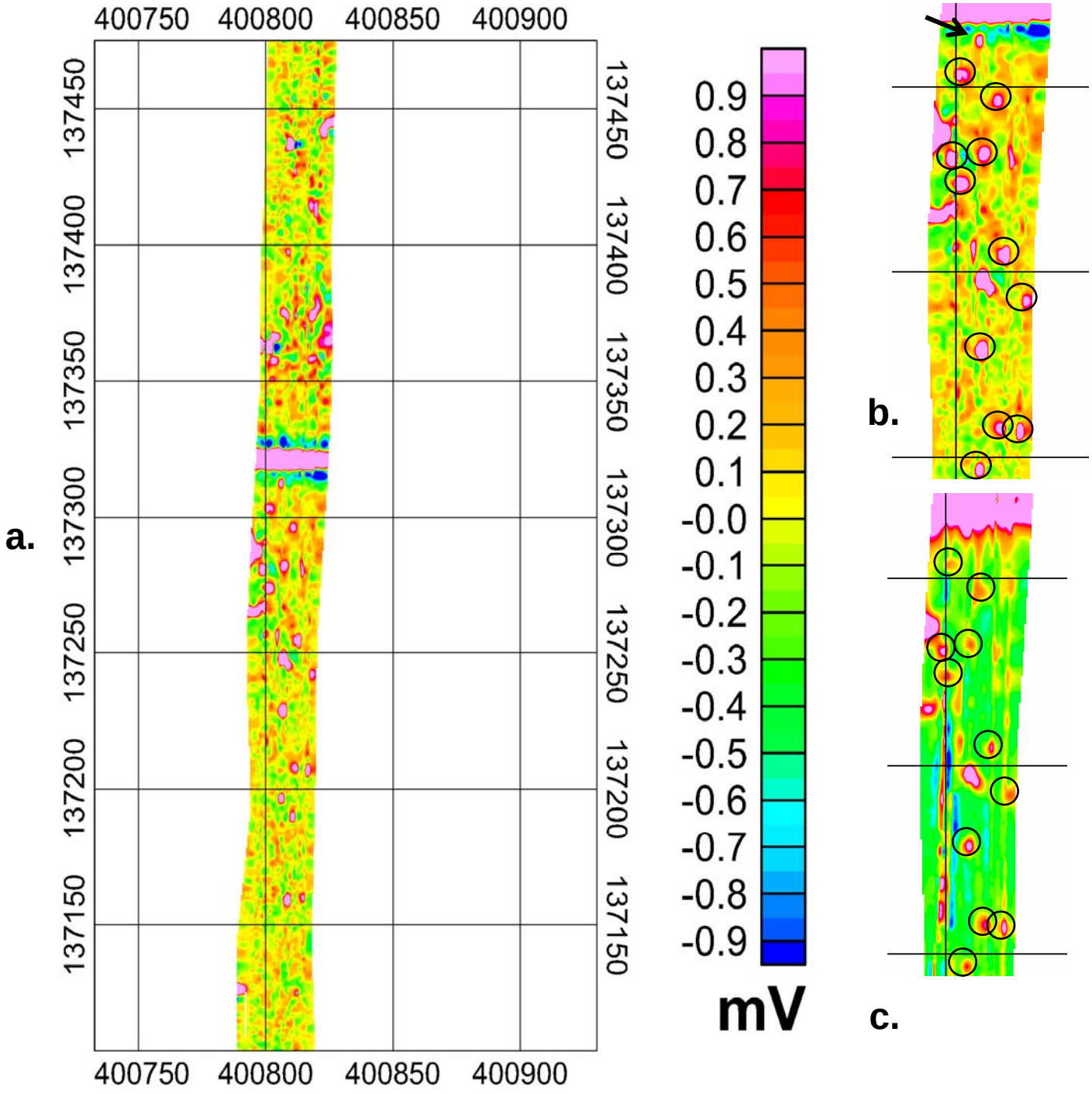

Figure 35. Vertical gradient small coil result from Bombing Target 1; a) shows the entire area surveyed; b) highlights in the vertical gradient data, and c) shows the equivalent anomalies in the single coil (vertical component) data. Coordinates are UTM Zone 13 N, NAD83 meters.

4.3.2.1 Comparison of EM and Magnetic Anomaly Picks, Bombing Target 1

Data acquired over Bombing Target 1 provide the basis for an initial comparison of the detection capabilities of the airborne EM system with the ORAGS-Arrowhead magnetometer system. In the magnetic analytic signal map (Figure 33), the berm of the target yields a magnetic anomaly in the northern half of the map area. The barbed wire fence produces a strong anomaly across the center of the target. Visual inspection indicates a strong correlation between the magnetic anomalies in Figure 33 and the large receiver coil EM anomalies in Figures 31 and 32, and small coil anomalies in Figures 34, and 35. It is noteworthy that the fence produces a double peak in the EM data and a slightly narrower single peak in the magnetic data. The target berm does not produce an EM anomaly, in contrast with the magnetic response.

Figure 36 shows anomalies that have been picked from the magnetic and EM data sets. All anomalies along the fence line at 137325N have been excluded. Magnetic anomalies are shown as red circles, and EM anomalies are represented by blue triangles. In both cases, symbol size is proportional to the log of the signal amplitude. A threshold of 5 nT/m was used for the magnetic data, and a threshold of 1.5 mV was used for picking the EM data.

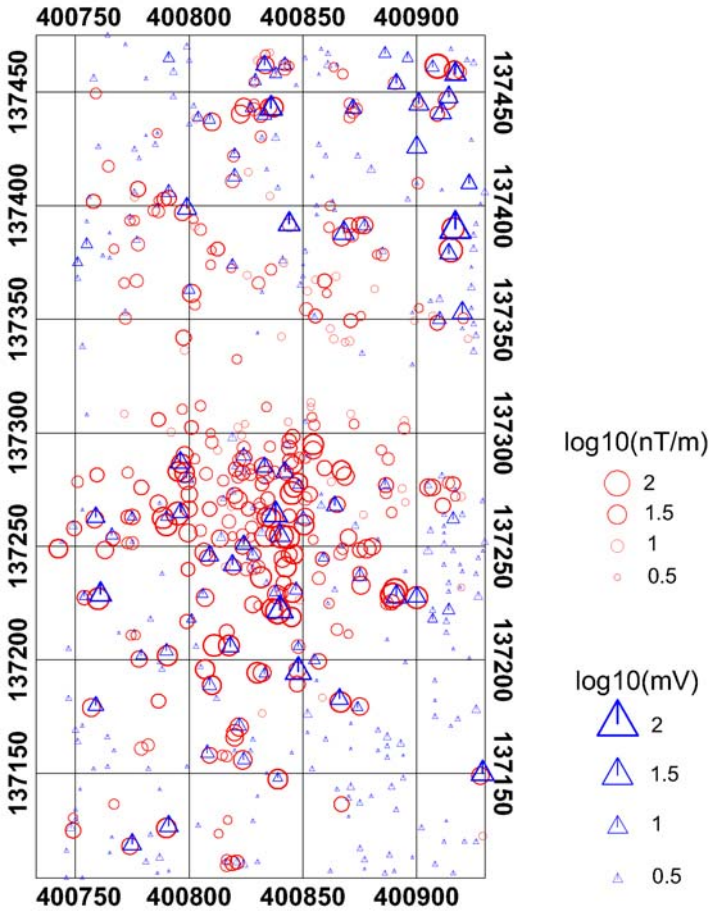

Figure 36. Comparison of anomaly picks from ORAGS-TEM system and ORAGS-Arrowhead system, Bombing Target 1, BBR. Coordinates are UTM Zone 13 N, NAD83 meters.

The selected thresholds generated 324 picks from the magnetic data set and 319 picks from the ORAGS-TEM data set. Each magnetic analytic signal anomaly was manually inspected for nearby EM anomalies. Almost all of the selected magnetic and TEM anomalies were within 2.5 m of one another, but a small percentage (<2%) were between 2.5 and 3 m. In the event the analytic signal anomaly was near more than one EM anomaly and had similar magnitude, the nearest was chosen. If one of the EM anomalies was distinctly larger, it was chosen, even though it might be further away than some of the smaller EM anomalies. Using this approach, 118 of the magnetic picks correspond with EM picks. 206 magnetic anomalies do not have corresponding EM anomalies, and 201 EM anomalies do not have corresponding magnetic anomalies. Figure 37 shows the percentage of EM anomalies in each of the five classes that have corresponding magnetic anomalies. The vertical bars show the range of analytic signal anomalies corresponding to a given EM anomaly class. Although the highest analytic signal in a class increases with an increase in EM anomaly magnitude, all EM classes contain low amplitude analytic signals. All but one of 29 EM anomalies above 10 mV have corresponding magnetic anomalies, but in the lowest EM noise category (1.5-2 mV), only 12 of 113 EM anomalies have clearly correlated magnetic anomalies. A sharp break occurs at about 3 mV, above which over 70% of EM anomalies have corresponding magnetic anomalies.

Under optimal circumstances, a validation exercise would have been conducted to compare the performance of the EM and magnetometer systems at this site. This might be premature, in that the ORAGS-TEM system has not yet been optimized for production surveying. In particular, these data required an extreme amount of interleaving, due to having only two receiving channels. Previous magnetic surveying demonstrated that altitude irregularities associated with such interleaving reduces data quality as well as production rates. We believe that it is critical that validation be conducted once the final system is constructed with a full complement of receivers.

In lieu of validation, we provide a more descriptive assessment of the results. Data from test sites indicate that intact M-38 ordnance will typically generate analytic signal anomalies with magnitudes of 13 nT/m or larger for the survey height range used in this survey. 161 of 206 magnetic anomalies at Bombing Target 1 above this 13 nT/m threshold (78%) have corresponding EM anomalies (Figure 37), and thus could represent intact M-38s. If we assume that the M-38s are at depths shallower than or similar to those at which the test objects were placed, and therefore that the 13 nT/m is a reasonable cutoff for the magnetic response for M-38s, we can conclude that most of the magnetic anomalies that weren't detected by the EM system are likely to be associated with fragments or other items that are not of concern. Exceptions may be related to altitude perturbations (in one data set or the other), unfavorable orientations for EM coupling, false magnetic positives, or burial depth. The 13 nT/m threshold is reasonable because the test M-38s were placed at depths that were consistent with measured depths at BBR. Small EM anomalies that don't have corresponding magnetic anomalies are likely to be associated with noise. Alternatively, they may be caused by non-ferrous metallic objects.

Figures 38 and 39 show a weak positive correlation between the strength of an EM anomaly and a magnetic anomaly. However, there is a large variance in the correlation such that a large magnetic anomaly does not always correspond to a large EM anomaly. The scatter in the EM

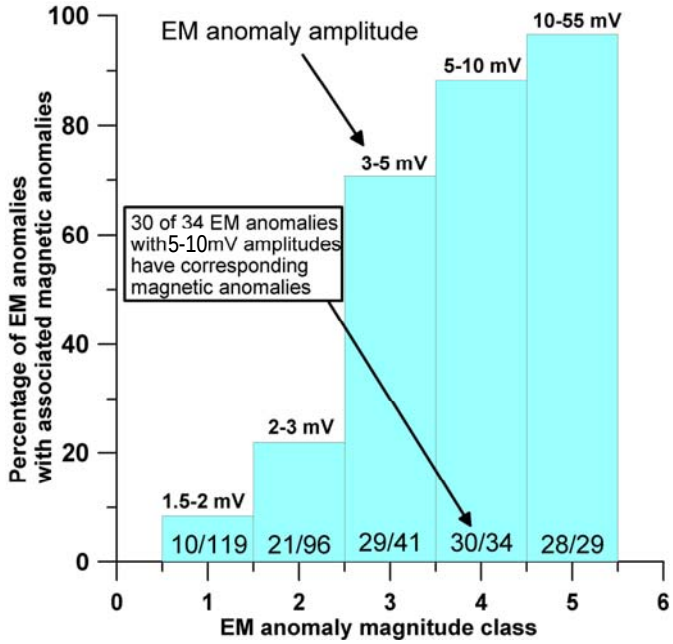

Figure 37. Bar graph showing the number of EM anomalies in a given class that have corresponding magnetic anomalies.

amplitude vs. magnetic amplitude in Figure 38 is presumably due to effects such as: 1) noise; 2) altitude variations; 3) target orientation; or 4) target shape. Even in altitude-corrected data (if we could make such a correction), we would anticipate a large amount of scatter. Correction for altitude might provide opportunities for discrimination (e.g. inversion), using both magnetic and EM data sets. We anticipate that this would be more complex than the analysis based on the EM data alone, described in the next section, and would build from work in progress by other researchers (e.g. joint inversion evaluation at the University of British Columbia). Such integration of EM and magnetic data sets could be used to improve the down-selection of anomalies that have a high probability of association with UXO, as opposed to other types of metallic debris.

The results presented here, while very encouraging, do not represent the performance of the optimal *known* system configuration for an airborne EM system, as noted earlier in this report. Data were also collected with the small coil receiver configuration over a small portion of Bombing Target 1 and were assessed for performance. However, the size of the small coil survey area was too small for a suitable comparison with magnetic results. Similarly, results from a lobed transmitter (Beard et al., 2003) have about twice the SNR of the large rectangular transmitter, but this configuration was not flown at Bombing Target 1. Furthermore, additional system improvements are anticipated that will further enhance the capabilities of the ORAGS-TEM system for detecting UXO.

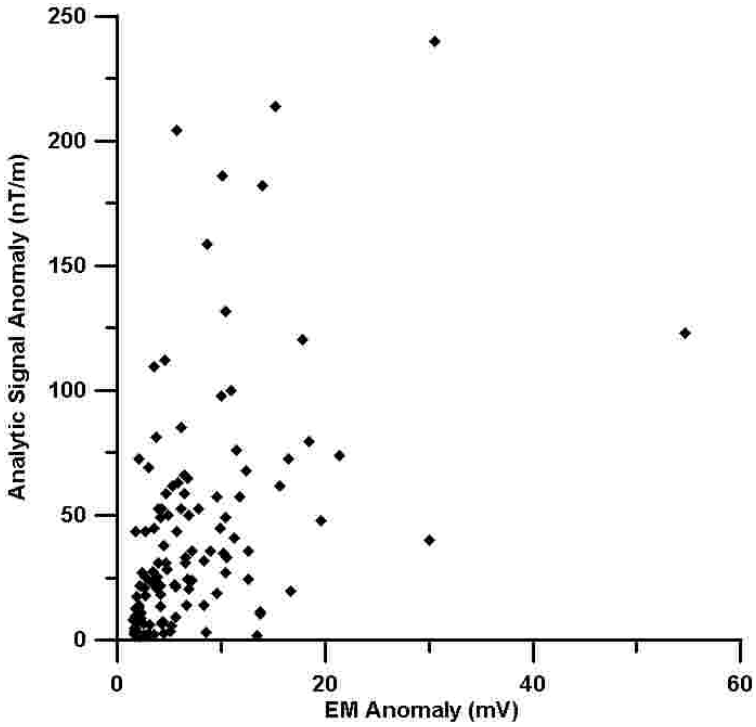

Figure 38. Scatter plot of EM and magnetic anomalies at Bombing Target 1.

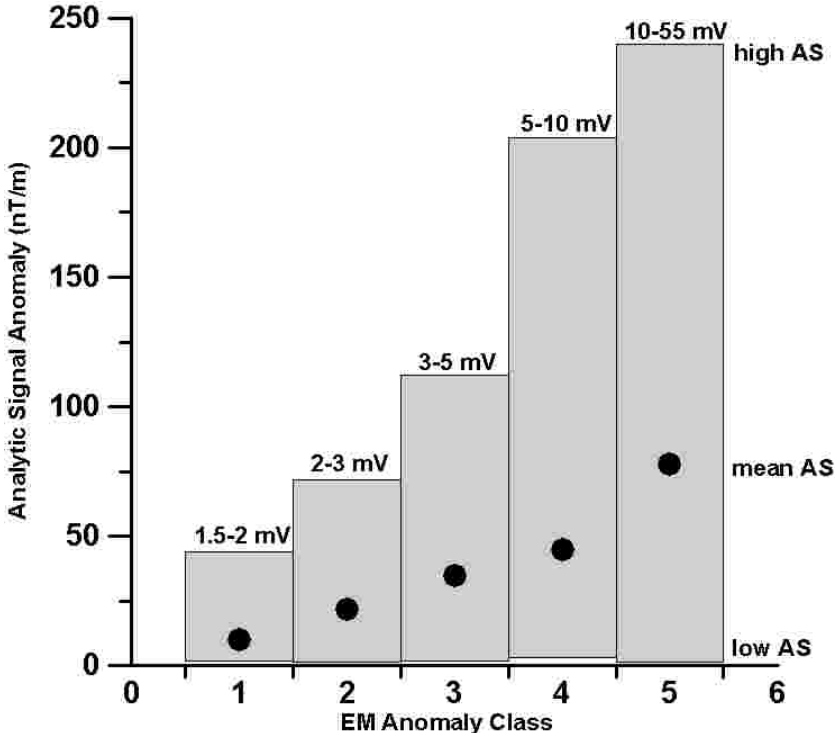

Figure 39. Scatter and mean of analytic signal anomalies according to EM anomaly class, arranged by EM anomaly amplitude.

4.3.2.2 Advantages of Processing Schemes that Use the Full Transient Response

The TEM maps over the Test Grid and Bombing Target 1 presented in earlier sections were prepared using a single "time bin" of transient response data. This approach is optimal for the "detection" problem, in which the locations of all EM targets are sought. Since signal levels tend to be highest at the beginning of the transient, using the earliest "good" data from the transient is a reasonable practice, provided that "geological" responses can be stripped out of the data prior to plotting, as was done for these maps.

There is, however, substantially more information present in transient data than the earliest-time amplitude. The decay characteristics for a particular target provide opportunities for discrimination of that target from objects possessing a similar early-time response but different decay behavior. For example, thin sheets of scrap from M-38 100 lb practice bombs would be expected to display much faster decays than intact 155 mm projectiles, owing to the thick walls and substantial volume of the projectile. The degree to which a particular TEM measurement can distinguish between the decay characteristics of two targets depends on the SNR at the beginning and the end of the off-time, the size of the initial measurement delay time, the sampling density (and type of sampling) of the transient during the off-time, and the length of the off-time relative to the exponential "time constant" of the object. Elongated objects will also typically display somewhat different late-time time constants for different target orientations relative to the TEM sensor.

Electromagnetic sensors intended for UXO detection and characterization are usually designed to maximize signal levels from highly conductive, compact objects, while reducing or minimizing responses due to conductive ground or soil magnetization effects. Where such effects are present, it should be possible to model these conditions (Billings et al., 2001) and thereby remove them from the total response. This discussion focuses on the response of the UXO target itself.

Exponential Decomposition

It is well known (e.g. Holladay, 1981, Chen and Macnae, 1998) that the observed transient response of an isolated target, measured in magnetic field B, the time derivative of magnetic field dB/dt, or output voltage V, can be decomposed into a weighted sum of pole responses:

$$B(t) \cong \sum_j R_j e^{-t/\tau_j}$$

$$\frac{dB}{dt}(t) \cong \sum_j \frac{-R_j e^{-t/\tau_j}}{\tau_j}$$

$$V(t) = A_{eff} \frac{dB}{dt}$$

$$\cong \sum_j Q_j e^{-t/\tau_j}$$

The relationship between the weights R_j and Q_j, for effective receiver coil area A_{eff} and time constants τ_j, using MKS units throughout is:

$$R_j = \frac{-Q_j \tau_j}{A_{eff}}$$

These expressions indicate that weights and time constants derived from the decomposition of voltage data can be used to estimate magnetic field response, and vice versa.

Estimation of B from dB/dt data

The magnetic field response B(t) can also be estimated as $B_{int}(t)$ by integration of dB/dt or voltage data from the end of the off-time T_{off} backward in time to t, followed by correction for $B(T_{off})$, the portion of the B field transient cut off at T_{off}. This is easily shown as follows:

$$\begin{aligned} B_{\text{int}}(t) &= -\int_t^{T_{off}} \frac{dB(\zeta)}{d\zeta} d\zeta, \quad where\ T_{off} \succ t \\ &\cong -\int_t^{T_{off}} \sum_j \frac{-R_j e^{-\zeta/\tau_j}}{\tau_j} d\zeta \\ &\cong \sum_j R_j e^{-t/\tau_j} - \sum_j R_j e^{-T_{off}/\tau_j} \\ &\cong B(t) - B(T_{off}) \end{aligned}$$

$$B(t) \cong B_{\text{int}}(t) - B(T_{off})$$

Estimation of Decay Parameters

The estimation of decay parameters (time constants and weights) from off-time data using these decompositions is a notoriously difficult numerical problem. When measurement error is present, it becomes especially difficult to distinguish time constants having similar values. Fortunately, the electrical engineering community has developed tools for estimating stable and accurate results from noisy data. The technique used here is known as the Matrix Pencil Method, or MPM (Hua and Sarkar, 1991), and was discussed in relation to TEM time constant estimation by Chen and Macnae (1998).

MPM works by factorizing data into "signal" and "noise" components using Singular Value Decomposition (SVD) subspace techniques, and estimating the decay parameters τ_j from the "signal" component only. Weight values R_j or Q_j are then determined by a separate SVD-based operation. A key advantage of the MPM over most other methods is that it estimates the minimum number of time constants and weighting coefficients consistent with the data for a given data noise level.

Synthetic Data Example

Consider a square, non-magnetic plate with edge dimension L_p, thickness t_p, and conductivity σ_p, excited by the ORAGS-TEM system geometry at 90 Hz base frequency. dB/dt (expressed in mV) and B (in nT) transients for this model are shown in Figure 40. The late-time response of such a plate decays with time constant $\tau_p \sim \mu_0 \sigma_p t_p L_p/10$, where μ_0 is the permeability of free space. Using values of L_p=0.45 m and conductance $\sigma_p t_p$ = 68,000 S yields a time constant at late time of 3.8 ms, considerably longer than the 2.6 ms off-time of the 90 Hz waveform.

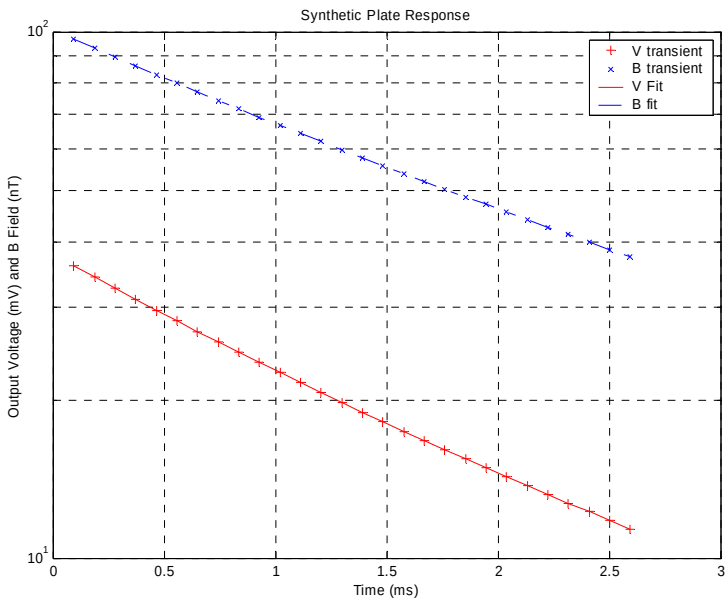

Figure 40. Log-linear plot of plate model response in mV (+) and nT (x), with corresponding approximate responses estimated by during MPM exponential decomposition fitting process (solid and dashed lines). Two time constants were estimated by the Matrix Pencil Method for this example, τ_1=3.2 and τ_2=1.2 ms, approximating the two strongest eigencurrent modes in the plate model. The dominant time constant estimated from observed field data over an aluminum plate having the same characteristics as this model was 3.1 ms.

Field Examples

Data from system trials flown over a previously established test grid at the Badlands Bombing Range (Beard et al, 2004) were used to estimate the dominant apparent time constants for a number of UXO and non-UXO targets. The items located on the test grid are indicated schematically in Figure 12. Early-time ORAGS-TEM responses are shown in gridded form for the 90 Hz base frequency dataset in Figure 24.

Figure 41 shows the high SNR values observed for the larger intact ordnance items and for the scrap pits at A7, B5, C1, C5, D1 and D2. Further description of the BBR test grid and ORAGS-TEM data acquisition are given in Beard et al (2004), but a brief description is in order here.

Compact targets located on the BBR test grid included intact 155 mm and 105 mm projectiles. Such objects are known to have long late-stage time constants, in the tens of ms. Disrupted and open-geometry targets included "scrap" consisting of broken and flattened 100 lb practice bombs (M-38s), 60 mm illumination shells, and various "cultural" objects, including a 1m long, thin-walled stovepipe. These objects typically displayed short time constants of less than 1 ms. An intermediate class, which included intact M-38s as well as 250 lb bomb simulants, comprises thin-walled targets with closed geometries. These were observed to have time constants between the two extremes, in the 1 to 3 ms range. Sample transients and corresponding dominant time constants for M-38 scrap pits at locations A7, B5, C5 and D2 are shown in Figure 41.

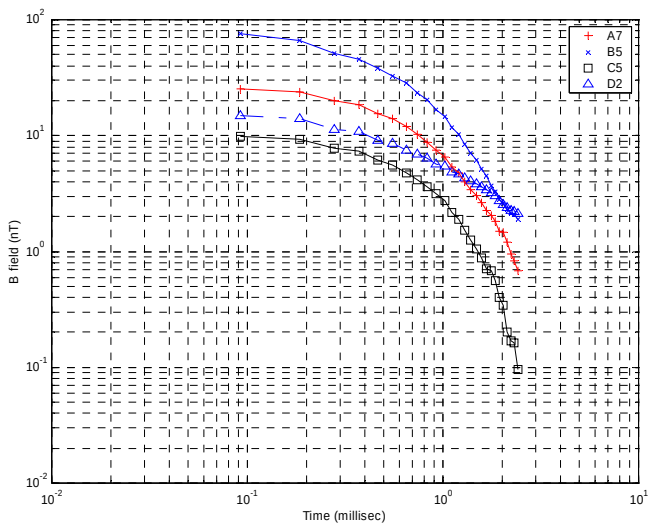

Item	Time Constant (ms)
Scrap A7	0.64
Scrap B5	0.37
Scrap C5	0.58
Scrap D2	1.33

Figure 41: B-field transients and estimated dominant time constants for M-38 scrap pits.

The transient shapes and corresponding time constants illustrate the consistency of the responses observed for Scrap Pits A7, B5 and C5. Scrap Pit D2 (triangular symbols) yielded substantially different results: with a time constant approximately double that of the other scrap pit anomalies, it may be that one or more of the scrap items in D2 retained significant physical integrity relative to those in the other pits.

Transient responses for two 250 lb bomb simulants (B4 and C3) and one M38 100 lb practice bomb (C4) are shown in Figure 42. The 250 lb simulants display similar time constant estimates, although their response amplitudes vary due to sensor-target coupling differences. The M-38 (labeled "100 lb") displays a shorter time constant and smaller amplitude.

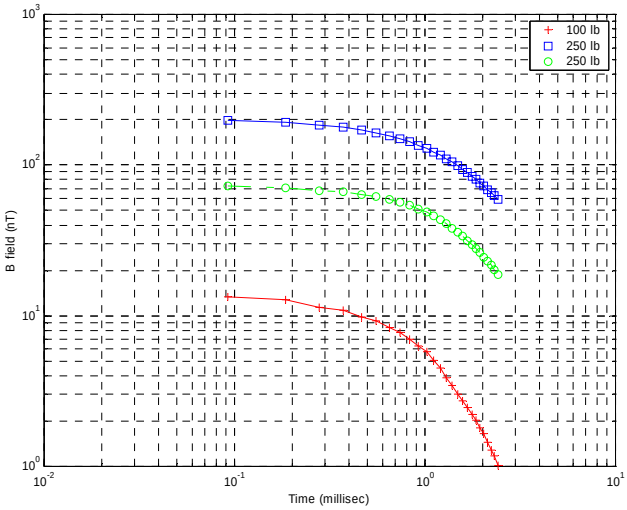

Item	Time Constant (ms)
250 lb Simulant #1	1.84
250 lb Simulant #2	1.95
100 lb Practice Bomb	1.03

Figure 42: B-field transients and time constant estimates for 250 lb simulants and 100 lb practice bomb.

As a final example, consider the response of a 155 mm artillery projectile (item C7), shown in Figure 43. Late-time time constants for a 155 mm projectile would be expected to be in excess of 30 ms. Given the relatively short off-time window available for this airborne measurement, the apparent time constant was expected to be an underestimate of the true value, and to exhibit substantial uncertainty. This was borne out by the observed data: in this case, the apparent time constant was estimated to be 8 ms.

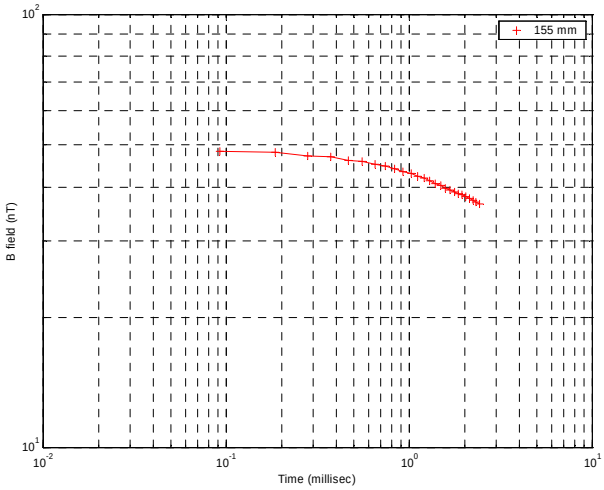

Figure 43: B-field transient response for 155 mm projectile, yielding a time constant estimate of 8 ms.

Item	Time Constant (ms)
155mm Projectile	8

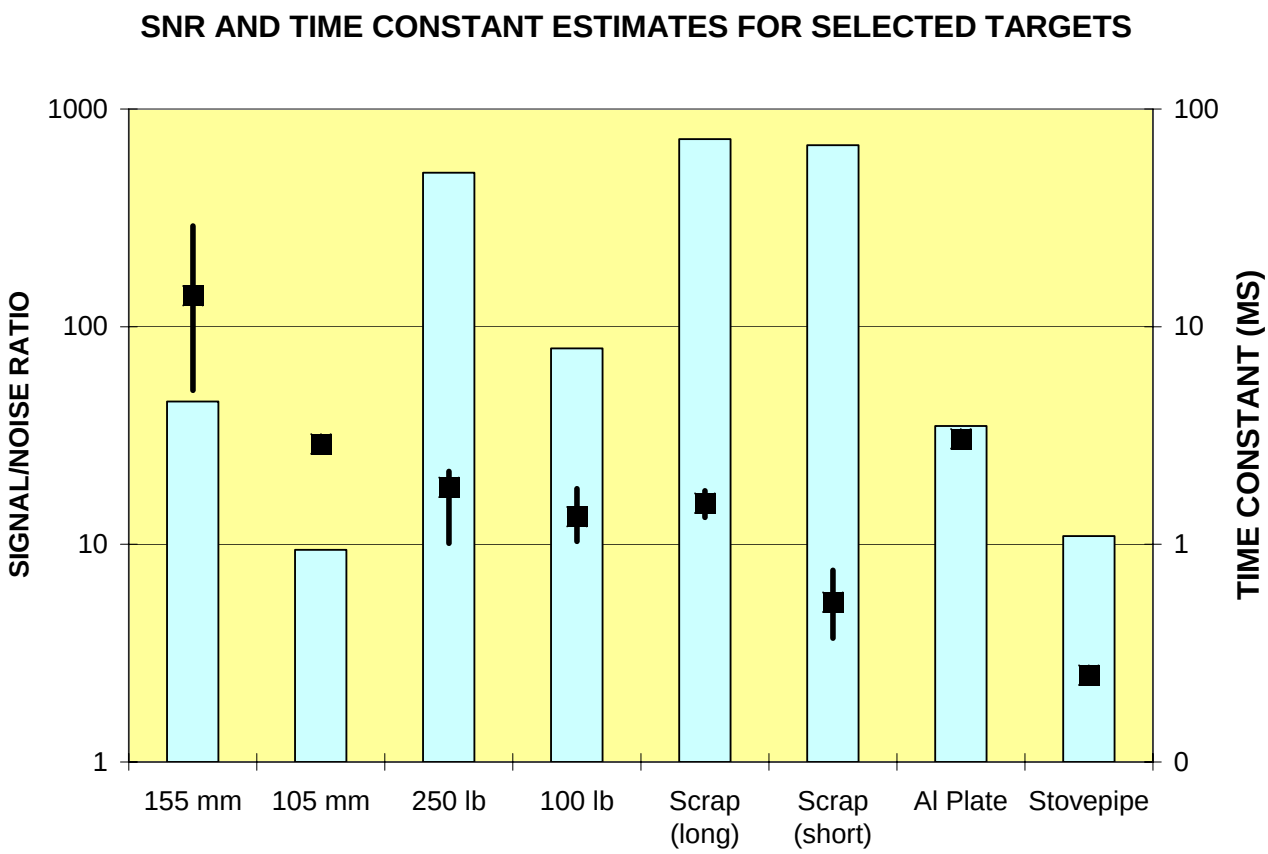

Figure 44: Time constants and SNR values for selected objects on BBR test grid. Left axis represents observed Signal/Noise Ratio (blue bars), while right axis represents estimated time constant (square symbols ■ with error bars).

Discussion

The survey flights that provided this dataset were primarily focused on UXO detection, not discrimination. As a result, the survey methodology was not optimal for discrimination purposes. Despite the relatively high base frequency of 90 Hz, estimated time constants varied over a wide range, including values considerably longer than the 2.7 ms off-time.

A summary plot of SNR and time constant estimates obtained for some of the items on the BBR test grid is shown in Figure 44. The large time constant estimates (from 5 to 30 ms) for the 155 mm projectile also exhibited a large amount of scatter, consistent with the expectation that long time constant estimates should be subject to increased uncertainty. Much less scatter was observed for time constants comparable to or smaller than the off-time interval of 2.8 ms, again consistent with expectations. Despite the limitations of this dataset, the summary diagram indicates discrimination of at least three classes of target. The first consisted of targets with short time constants of less than 1 ms (100 lb bomb fragments), the second, of targets with intermediate time constants in the 1 to 3 ms range (250 lb simulants and 100 lb practice bombs, plus atypical scrap), and the third, of targets with time constants greater than 3 ms (155 mm and 105 mm projectiles). The use of additional selection criteria, such as response amplitude and/or vertical gradient information, should augment the discrimination potential of this approach.

5.0 Conclusions

The primary goal of this project was to evaluate parameters critical to the design of an airborne electromagnetic system capable of detecting a variety of buried ordnance. The basic design of the system is analogous to the previously developed helicopter magnetic systems developed through the ESTCP program (Doll et al., 2003); that is, we sought a frame mounted, multiple sensor design that would permit a helicopter to fly within a few meters of UXO-contaminated terrain, and thus attain a high level of detection and positional accuracy. The results presented in this report show that we have achieved this goal. In the BBR field tests, we were able to establish the base frequencies for the system—90 Hz and 270 Hz—that allowed the highest signal-to-noise ratio for the given system. Using these frequencies, we were able to combine different transmitter configurations, receiver types and positions to find the combinations that gave the highest SNR. We demonstrated that, under good field conditions, the helicopter EM system is capable of producing data of a quality that approached or exceeded ground-based EM survey results and ORAGS-Arrowhead airborne survey results. At a one-meter survey altitude we were able to detect objects as small as 60 mm mortar rounds, a level of detection equivalent to that of the ORAGS helicopter total field magnetic systems.

The sensitivity of the ORAGS-TEM system proved to be well in excess of the proof-of-concept EM-61AB system (Doll et al., in press). At the BBR test site, the EM-61AB was able to detect 155 mm and 105 mm rounds, but failed to detect 81 mm shells and smaller items. At the lowest survey altitude over the same test site, the ORAGS-TEM system reliably detected both the 81 mm and the 60 mm mortar rounds. To achieve this degree of resolution was not a straightforward process; the BBR field tests produced excellent results because of lessons learned from results of prior shakedown flights in Ontario, Massachusetts, and New Mexico (Beard et al., 2002a, 2002b).

The electromagnetic response of ordnance is more complicated than its magnetic response, and the falloff in response with increasing altitude does not follow the $1/R^3$ decay of magnetic fields in the presence of compact bodies where R is the source-receiver distance and 3 is the decay exponent. As shown in Table 11, the decay exponent can vary from 2 to 6 according to the transmitter-receiver configuration and the survey height. Below 1.5 m survey height, we found that vertical gradient receivers usually produced superior signal-to-noise than single loop receivers. However, because the decay of the vertical gradient field is more extreme than that of the single loop, single loop receivers were as good as or superior to vertical gradient receivers above 1.5 m. Decay exponents greater than 3 imply more rapid field decay than would be found in magnetic data, therefore magnetic systems such as the ORAGS-Arrowhead may have an advantage over EM systems where survey altitudes exceed a few meters. As shown in Figures 36 and 37, there are about three times more magnetic anomalies above the noise floor at Bombing Target 1 than EM anomalies, although we reiterate that the EM system used in this comparison has lower SNR than other configurations that were tested at the BBR Test Site. Because a fence runs through the middle of the target area, and a raised circular berm defining the target, a portion of the survey was conducted at heights of more than 3 m. At this altitude, the EM response of many small items falls below the noise threshold, whereas small magnetic signals can still be detected. There is a weak positive correlation between the size of the

magnetic anomaly and the magnitude of a corresponding EM anomaly.

A system to detect small UXO would use a different base frequency than one designed to discriminate the type of target. Low base frequencies produce excellent EM response and a longer decay time over large targets, but in moving systems give poor SNR over smaller targets because too few transmission cycles occur to define the target. High base frequencies produce better SNR for smaller targets, but the decay time may be too short to define the time constant of the target. We found that with a 270 Hz base we could detect 60 mm mortars, but estimates of the time constants associated with these and with larger targets were inconsistent because the time between transmissions was too short to get an adequate decay curve. At 90 Hz base frequency, the SNR of the 60 mm mortars decreased, but time constant estimation for larger ordnance was more consistent. At 90 Hz, thick-shelled objects such as 155 mm rounds produced consistently larger time constants than smaller, thin-shelled items. An understanding of this behavior is helpful in setting acquisition parameters for a particular survey.

A number of different factors contributed to the success of the ORAGS-TEM system. Incremental improvements in system electronics, especially suppression of early time noise and faster transmitter turnoff, contributed to enhanced SNR. Vibration isolation improved small coil receiver data. Careful analysis of power spectra at different base frequencies enabled us to find those frequencies that gave the highest SNR for ordnance anomalies. Experiments with transmitter and receiver geometries and styles, including vertical gradient receivers also improved data quality. We should emphasize that, besides these project-specific considerations, the success of this project relied in large part on the cumulative knowledge obtained in development of airborne magnetic systems for UXO detection.

In its current configurations, the ORAGS-TEM is a two-channel system. This was adequate for comparing one configuration with another, but is inefficient for “production” surveys because the swath width is small and requires interleaving and precise positioning in order to fully survey a site. Similar magnetic system tests have demonstrated that interleaving and variations from one flight pass to the next results in a degrading of data quality. The cost for expanding from a two-channel to an eight-channel system is quite small, as it will only require construction of more receiver channels in the existing console, as well as additional new coils and preamplifiers. The BBR demonstration provided a thorough evaluation of several system configurations and comparison with previous airborne magnetic and electromagnetic systems, but did not exploit the strengths of electromagnetic systems in environments where magnetic systems fall short. It is therefore appropriate to follow this project with a demonstration of a “production” 8-channel system at a site where geologic conditions are unsuitable for magnetometer-based systems, as a demonstration of the value of the ORAGS-TEM system in future UXO remediation efforts.

6.0 Cost Assessment

6.1 Cost Reporting

Cost information associated with the demonstration of all airborne technology, as well as associated activities, were closely tracked and documented before, during, and after the demonstration to provide a basis for determination of the operational costs associated with this technology. It is important to note that the costs for airborne demonstrations and surveys are very much dependent on the character, size, and conditions at each site; ordnance objectives of the survey (e.g. flight altitude); type of survey conducted (e.g. high-density or transects); and technology employed for the survey (e.g. total field magnetic, time domain electromagnetic induction) so that a universal formula cannot be fully developed. The following table contains the cost elements that were tracked and documented for this demonstration. These costs include both operational and capital costs associated with system design and construction; salary and travel costs for support staff; subcontract costs associated with helicopter services, support personnel, and leased equipment; costs associated with the processing, analysis, comparison, and interpretation of airborne results generated by this demonstration.

Notes for Table 13, Cost Assessment Table

[1]Includes all overhead and organization burden, fees, and associated taxes
[2]No costs were incurred for the establishment of Calibration Sites in Albuquerque, NM and Pine Ridge, SD. Existing sites established under previous survey projects were used for system testing and development
[3]These costs were included in related airborne magnetic survey projects occurring in conjunction with EM system testing and development (leveraged cost)
[4]Capital costs associated with many airborne system components and related equipment were acquired under other projects (e.g. development of airborne magnetic system) and are not included in the cost of this project (leveraged cost)

Table 13: Cost Assessment Table

Cost Category	Sub Category	Details	Quantity	Cost[1] (in dollars)
Pre-Survey (Start-up)	Site Characterization	Site inspection		
		Toronto, ON	0 days	$0
		Hyannis, MA (includes hotel and per diem; airfare covered in corresponding Camp Wellfleet survey project)	1 day	$1,969
		Albuquerque, NM (includes hotel and per diem; airfare covered in corresponding Laguna/Isleta survey projects)	1 day	$1,869
		Pine Ridge, SD (includes hotel and per diem; airfare covered in corresponding Laguna/Isleta survey projects)	1 day	$1,869
		Mission Plan preparation & logistics (majority of effort covered under corresponding Camp Wellfleet, Laguna/Isleta, and BBR survey projects)	10 days	$17,690
		Calibration Site development (includes pre-seed and post-seed ground-based surveys) at the following sites:		
		Toronto, ON	2 days	$6,618
		Hyannis, MA	2 days	$6,618
		Albuquerque, NM	0 days[2]	$0
		Pine Ridge, SD	0 days[2]	$0

Cost Category	Sub Category	Details	Quantity	Cost[1] (in dollars)
Pre-Survey (cont'd)	Mobilization	Equipment/personnel transport (includes travel):		
		Toronto, ON	2 days	$7,698
		Hyannis, MA	0 days[3]	$0
		Albuquerque, NM	0 days[3]	$0
		Pine Ridge, SD	0 days[3]	$0
		Helicopter/personnel transport (includes travel):		
		Toronto, ON	0 days[3]	$0
		Hyannis, MA	0 days[3]	$0
		Albuquerque, NM	0 days[3]	$0
		Pine Ridge, SD	0 days[3]	$0
		Unpacking and system installation:		
		Toronto, ON	1 day	$4,559
		Hyannis, MA	1 day	$4,559
		Albuquerque, NM	1 day	$4,559
		Pine Ridge, SD	1 day	$4,559
		System testing & calibration:		
		Toronto, ON	1 day	$6,309
		Hyannis, MA	1 day	$6,309
		Albuquerque, NM	1 day	$6,572
		Pine Ridge, SD	1 day	$6,747
Pre-survey subtotal				**$88,504**

System Development & Capital Equipment[4]	Advisory panel	9 persons, 2 meetings	1 each	$19,000
	Conceptualization & modeling	ORNL, USAERDC, Temple	1 lot	$175,754
	Design and construction (not including hardware)	Prototype and final systems	1 lot	$220,560
	Testing and assessment	Final system	1 lot	$50,000
	EM transmitter and receivers	$12,000 total cost	1 each	$12,000
	GPS	$15,500 total cost	1 each	$0
	Booms and mounting hardware	$16,500 total cost	1 set	$16,500
	Navigation system	$5,200 total cost	1 each	$0
	Laser altimeter	$7,300 total cost	1 each	$0
	Data management console	$31,200 total cost	1 each	$31,200
	GPS base station	$15,600 total cost	1 each	$0
	PCs for data processing & analysis	$3,450 total cost	2 each	$0
Cost Category	**Sub Category**	**Details**	**Quantity**	**Cost[1] (in dollars)**
System Development	Shipping cases	$2,375 total cost	3 each	$2,375
	Trailer	$3,600 total cost	1 each	$0

(cont'd)				
Capital subtotal				**$527,389**
Operating Costs (includes Toronto, Hyannis, Albuquerque, and Pine Ridge)	Equipment Rental	GPS equipment	1 each	$165
	Data acquisition	Helicopter time, including pilot and engineer labor	28 days (53.6 hours airtime)	$12,211
	Operator labor		23 days	$4,900
	Data processing	Geophysicist	28 days	$43,120
	Field support/management	Engineer/Senior Geophysicist	28 days	$49,532
	Hotel, per diem, rental car	Survey team	28 days	$15,107
	Airport Landing Fees		28 days	$700
	Data analysis and interpretation	2 Geophysicists	54 days	$178,686
	Project management		36 days	$63,684
	Reporting and documentation		18 days	$59,562
Operating cost subtotal				**$427,667**
		Disassembly from helicopter, packing, and loading for transport:		
		Toronto, ON	1 day	$4,559
		Hyannis, MA	1 day	$4,559
		Albuquerque, NM	1 day	$4,559

Post-Survey	Demobilization	Pine Ridge, SD Equipment/personnel transport (includes travel): Toronto, ON Hyannis, MA Albuquerque, NM Pine Ridge, SD Helicopter/personnel transport (includes travel): Toronto, ON Hyannis, MA Albuquerque, NM Pine Ridge, SD	1 day 2 days 0 days[3] 0 days[3] 0 days[3] 0 days[3] 0 days[3] 0 days[3] 0 days[3]	$4,559 $7,698 $0 $0 $0 $0 $0 $0 $0
Post-survey subtotal				**$25,934**
Indirect environmental activity costs	Environmental and Safety Training[3]	8-hour HAZWOPR (includes the course cost)	0 days[3]	$0
Miscellaneous	Department of Energy Federal Acquisition Cost (FAC)	3% of project total; Congressionally-mandated charge for administering the Work-for-Others (WFO) program		$32,085
Total costs				**$1,101,579**

7.0 Implementation Issues

7.1 Environmental Checklist

In order to operate, each system must have Federal Aviation Administration approval (STC certificate). The required testing and evaluation performed in Toronto before mobilization to New Mexico has been completed. The report associated with this "shakedown" testing is being prepared under separate cover. In addition, ground crews are required to complete the 40-hour HAZWOPR course and to maintain their annual 8-hour refreshers for operation at most UXO sites.

7.2 Other Regulatory Issues

There are no additional regulatory requirements for operation at the BBR site.

7.3 End-User Issues

The primary stakeholders for UXO issues at BBR are the members of the Oglala Sioux Tribe, other residents of the Indian Reservation, and State of South Dakota regulatory authorities. ORNL is currently supporting UXO activities at other sites with the ORAGS-Arrowhead magnetometer system. Airborne UXO surveys are being designed to accommodate the limitations and needs of each site. USAESCH has assisted in efforts to commercialize the existing technology and this has led to shared operation with one contractor for engineering evaluation/cost analysis (EE/CA) activities. As new systems are developed and proven, they will enter into the same cycle of application and commercialization.

8.0 References

Andrews, A.M., E. Rosen, and I. Chappel, 2001, Review of unexploded ordnance detection demonstrations at the Badlands Bombing Range, Institute for Defense Analysis Document D-2615, December 2001, 22p.

Barrow, B. and H.H. Nelson, 2003, Comparison of EMI measurements on large projectiles and on exploded projectile fragments: Extended abstract, *Proceedings of 2003 SAGEEP Symposium*, San Antonio, 1399-1405, on CD.

Beard, L.P., W.E. Doll, T.J. Gamey, J.S. Holladay, J.L.C. Lee, and D.T. Bell, 2002, Field tests of an experimental helicopter time-domain electromagnetic system for unexploded ordnance detection, Geophysics 69, 664-673, on CD.

Beard, L.P., W.E. Doll, T.J. Gamey, J.S. Holladay, and J.L.C. Lee, 2003, Aspects of system design for airborne electromagnetic detection of unexploded ordnance: Extended abstract, *Proceedings of 2003 SAGEEP Symposium*, San Antonio, 1445-1454, on CD.

Beard, L.P., W.E. Doll, T.J. Gamey, J.S. Holladay, J.L.C. Lee, and D.T. Bell, 2002a, A helicopter electromagnetic system for UXO mapping: Extended abstract, *Proceedings of 2002 UXO/Countermine Forum*, Orlando, FL, September 3-6, 2002 on CD.

Beard, L. P., W.E. Doll, T.J. Gamey, and J.S. Holladay, 2002b. A helicopter-borne electromagnetic system for detection and mapping of unexploded ordnance, *Abstract in AMEREM2002 Conference Proceedings*, Annapolis, Maryland, June 2-7, 2002.

Becker, A, H.F. Morrison, and T. Pandit, 2003, Bandwidth requirements for metal detectors, Paper Z-99, *Proceedings of 65'th EAGE Conference*, Stavanger, Norway.

Billings, S.D., Pasion, L.R., Oldenburg, D.W., and J. Foley, 2001, The influence of magnetic viscosity on electromagnetic sensors, Proc. UXO Forum 2001.

Chen, J. and J.C. Macnae, 1998, Automatic estimation of EM parameters in tau-domain, Exploration Geophysics 29, 170-174.

Doll, W.E., J.E. Nyquist, L.P. Beard, and T.J. Gamey, 2000, Airborne geophysical surveying for hazardous waste site characterization on the Oak Ridge Reservation, Tennessee, Geophysics 65, 1372-1387.

Doll, W.E., T.J. Gamey, and J.S. Holladay, 2001, Current Research into Airborne UXO Detection, *Proceedings of the Symposium on the Application of Geophysics to Engineering and Environmental Problems*, Denver, CO, available on CD-ROM, 10 pgs.

Doll, W.E., T.J. Gamey, L.P. Beard, D.T. Bell, J.S. Holladay, J.E. Nyquist, and J. Llopis, 2002, Development and Evaluation of a Second-Generation Airborne Electromagnetic System for Detection of Unexploded Ordnance, Extended Abstract, *Proceedings of the 2002 Symposium on the Application of Geophysics to Environmental and Engineering Problems*, 9pp., available on CD-ROM.

Doll, W.E., T.J. Gamey, L.P. Beard, D.T. Bell, and J.S. Holladay, 2003, Recent Advances in Airborne Survey Technology Yield Performance Approaching Ground-Based Surveys, *The Leading Edge*, Society of Exploration Geophysicists, p. 420-425, v. 22, n. 5, May 2003.

Doll, W.E., T.J. Gamey, J.S. Holladay, and J.L.C. Lee, *in press*, Viability of an Airborne Electromagnetic System for Mapping of Shallow Buried Metal, Accepted for publication in *Near-Surface Geophysics: volume 2, Applications and Case Histories*, D.K. Butler (Ed.), Society of Exploration Geophysicists, Tulsa, OK.

Doll, W.E., P. Hamlett, J. Smyre, D.T. Bell, J.E. Nyquist, T.J. Gamey, and J.S. Holladay, 1999,

A Field Evaluation of Airborne Techniques for Detection of Unexploded Ordnance, *Proceedings of the Symposium on the Application of Geophysics to Engineering and Environmental Problems*, 1999, p. 773-782.

Gamey, T.J., W.E. Doll, A. Duffy, and D.S. Millhouse, 2000a, Evaluation of Improved Airborne Techniques for Detection of UXO, *Proceedings of the Symposium on the Application of Geophysics to Engineering and Environmental Problems*, p. 57-66.

Gamey, T.J., R. Mahler, 1999, A Comparison of Towed and Mounted Helicopter Magnetometer Systems for UXO detection, *Proceedings of the Symposium on the Application of Geophysics to Engineering and Environmental Problems*, March 1999, pp. 783-792.

Gamey, T.J., 1994, UXO Detection from a Helicopter Platform, *Proceedings of UXO Detection and Range Remediation Conference*, May 1994, pp163-168.

Holladay, J.S., 1981, YVESFT and CHANNEL, A subroutine package for stable transformation of sparse frequency domain electromagnetic data to the time domain, Research in Applied Geophysics, No. 17, Geophys. Lab., Dept. of Physics, University of Toronto

Holladay, J.S., W.E. Doll, L.P. Beard, J.L.C. Lee, T.J. Gamey, and D.T. Bell, UXO Time-Constant Estimation from Helicopter-Borne TEM Data, Extended abstract, *Proceedings of the 2004 Symposium on the Application of Geophysics to Environmental and Engineering Problems*, Colorado Springs, 2004.

Holladay, J.S., J.L.C. Lee, W.E. Doll, L.P. Beard, T.J. Gamey, and D.T. Bell, Moving Beyond Detection: Airborne Transient EM Data Analysis for Discriminating of UXO Targets by the ORAGS-TEM System, UXO Forum, St. Louis, MO, March 9-12, 2004.

Hua, Yingbo and T.K. Sarkar, 1991, On SVD for Estimating Generalized Eigenvalues of Singular Matrix Pencil in Noise, IEEE Trans. Sign. Proc. 39, 892-900.

McDonald, J.R., H.H. Nelson, J. Neece, R. Robertson, and R.A. Jeffries, 1998, MTADS Unexploded Ordnance Operations at the Badlands Bombing Range, Pine Ridge Reservation Cuny Table, South Dakota, July 1997, NRL Report NRL/PU/6110-98-353.

McDonald, J.R., H.H. Nelson, 1999, MTADS Live Site Demonstration at Pueblo of Laguna, N.M., August 1998, NRL Report NRL/PU/6110-00-398.

McNeill, J.D. and M. Bosnar, 1996, Application of Time Domain Electromagnetic Techniques to UXO Detection, Proceedings of UXO Forum, March 1996, pp.34-42

ORNL, 2004, Final Report on 2002 Airborne Geophysical Survey at Badlands Bombing Range, South Dakota, Final Project Report to ESTCP, submitted July 2004.

9.0 Points of Contact

Name	Organization		Project Role
Gary K. Jacobs	ORNL		Division Director
David Bell	ORNL		Project Manager
Bill Doll	ORNL		Technical Manager
Les Beard	ORNL		Operations Manager
Jeff Gamey	ORNL		Geophysicist
Scott Millhouse	USAESCH		Project Lead
Emma Featherman-Sam	Oglala Sioux Tribe		Director, BBR Project
Dan Munro	National Helicopters		Helicopter Contractor President

Appendix A: Data Storage and Archiving Procedures

General
Digital data are on the CD accompanying this report. Included are: (1) readme files, (2) a copy of the final report in *.DOC format, (3) digital copies of maps shown in the report in TIF format, (4) ASCII files of grids shown in the report, and (5) geophysical data files in ASCII format.

Geophysical Data
The data included with this report is ASCII text and conforms to the format described in the "EM_Data_Readme.txt" file on the CD-ROM provided. Files are named according to area surveyed and the EM system configuration used: Coordinates are South Dakota CS 83, NAD83 (Continental US).

ASCII data files have the suffix FDF and consist of 34 columns: timestamp, gps_time, latitude, longitude, laser_altimeter, system_voltage, system_current, transmitter_temperature, console_temperature, ADU_azimuth, ADU_pitch, ADU_roll, Reference_On, Manual_Fiducial, channel_1_gate_1, …., channel_1_gate_10, channel_2_gate_1, …, channel_2_gate_10.

Accompanying each FDF file is an SDF file. The SDF file describes attributes of the particular transmitter-receiver configuration used.

SDF file entries are as follows:
Word 1: NRecFull, the number of samples in a full waveform
Word 2: NInChan, the number of high-precision data streams (sig or ref)
Word 3: NHarms, the number of harmonics real-time processed by the system (5)
Word 4: NBins, the number of data bins real-time processed by the system (10)
Word 5: NDec, the decimation factor used in the real-time filtering
Word 6: Mode, flag = 0 for FD or 1 for TD output
Word 7: Relay_On: 1 if relay connects channel 1 to Reference
Word 8: NDead, number of samples (including filter delay of 34) between sync and first good bin
Word (8+1 to 8+NHarms): Harmonic numbers for FD output harmonics
THEN
Word (8+NHarms+1 to 8+NHarms +NBins): Bin sizes in samples for output TD data

Images
Geophysical anomaly maps are provided as image files in TIF formats. The TIF images have been saved at 200dpi at the scale labeled on each map. These files are named according to the area surveyed and the EM system configuration.